Cover Page

# Universiteit Leiden

# Advanced *in vitro* models for studying drug induced toxicity

Sreenivasa ramaiahgari

Cover: Designed by Sreenivasa Ramaiahgari. 96-well microplate on Nikon imager. Immunofluorescent images of 3D cultures: Top panel - HepG2 spheroids: β-catenin (left) and MRP2 (right) staining; Actin stained kidney proximal tubules (left) and MCF-7 (Breast cancer cell) spheroid (right) stained for actin and nuclei (blue).

# Advanced *in vitro* models for studying drug induced toxicity

Proefschrift

ter verkrijging van
de graad van Doctor aan de Universiteit Leiden,
op gezag van Rector Magnificus prof.mr. C.J.J.M. Stolker,
volgens besluit van het College voor Promoties
te verdedigen op Woensdag 4 June 2014
klokke 11.15 uur

door

**Sreenivasa Chakravarthy Ramaiahgari**

geboren te Pulivendula, India
in 1981

**PROMOTIECOMMISSIE**

Promotor:            Prof. Dr. B. van de Water        Universiteit Leiden

Co-promotor:         Dr. L.S. Price                   Universiteit Leiden

Overige leden:       Prof. Dr. J. Kleinjans           Universiteit Maastricht
                     Prof. Dr. G.M.M. Groothuis       Universiteit Groningen
                     Prof. Dr. P.H. van der Graaf      Universiteit Leiden
                     Prof. Dr. J. Kuiper              Universiteit Leiden

*To my sister*

# TABLE OF CONTENTS

# CHAPTER 1

## GENERAL INTRODUCTION AND SCOPE OF THIS THESIS

Sreenivasa C. Ramaiahgari, Bob van de Water, Joost van Delft and Leo S. Price

# INTRODUCTION

Driven by the emergence of new diseases, increased drug resistance and an unmet need for therapies for existing diseases, there is an ever-increasing demand for new medicines. The remarkable advances in science and technology have supported the discovery of new chemical entities but the pharmaceutical industry is struggling to translate this into approved drugs for the clinic. Considering the enormous investments associated with the development of a new drug, attrition at later stages of drug development or after release into the market is a major concern for pharmaceutical companies, not to mention patients. Toxicity is the major reason for drug attrition with 40% of new chemical entities failing after pre-clinical safety studies in animals and 89% before they enter clinical trails [1], with hepatotoxicity and cardiotoxicity being the main reasons followed by nephrotoxicity, neurotoxicity and gastro-intestinal toxicity [2]. It is therefore important to efficiently screen new chemical entities for their adverse effects, excluding toxic drugs at an earlier stage, and selecting the most promising drug candidates for further development.

Predicting safety of a chemical entity at the preclinical stage has remained a major challenge. Recent years have seen an increase in attrition rates - even after rigorous testing in both *in vitro* and *in vivo* test models. This is partly due to poor prediction of human-specific responses in these models. The drug metabolism of animals differs from those of humans and may not accurately predict a human specific stress response. For example nifedipine, a calcium channel blocker, is metabolized by CYP3A4 in humans but not in rats [3] [4]. Human derived cell lines might offer an advantage in drug screening at the pre-clinical stage; currently primary human hepatocytes are considered as the gold standard [5] for toxicity testing but they too lose liver cell properties within hours after *in vitro* culture and show a high donor specific variability in gene expression [6, 7]. In addition to primary cells, immortalized cell lines and hepatocarcinoma cell lines can be used.  These cells have either undergone mutations or lost a majority of liver specific functions under non-physiological culture conditions. The unnaturally high rate of proliferation of these cell lines also compromises their suitability for testing. Therefore there is a lack of *in vitro* models that can stably maintain human liver specific functions. To address this, development of a physiologically relevant human organotypic *in vitro* model is essential for safety assessment. In such models hepatocytes should remain differentiated and acquire many of the growth and metabolism characteristics of functional liver, thereby offering a promising tool to improve *in vitro* testing by both reducing and complementing pre-clinical animal testing.

**Drug discovery and development**

Drug discovery and development is a precarious process taking up to 12-16 years with costs exceeding $1.8 Billion and increasing every year [8, 9]. The process of drug development is mainly divided into the discovery phase, clinical development phase and approval phases. In the early discovery phase once a druggable target is selected for a disease compounds are screened with a battery of *in vitro* and *in vivo* tests to identify hits [10]. Later, the identified hits or lead compounds go through a series of tests to characterize the pharmacokinetic and toxicological properties of the drug. Successful lead candidates are further optimized and rigorously tested in both *in vitro* and *in vivo* models before they are tested in humans. Accurate screening of safe druggable targets plays a key role in the success of the drug.

After a thorough investigation at the discovery phase, drug candidates are selected for human clinical trials by filing an application with regulatory agencies. Both EMEA and FDA have a similar evaluation process with preclinical testing followed by a clinical development phase [11]. On approval, phase I clinical studies are conducted, in which the compound is tested in about 20 to 80 volunteers looking mainly at pharmacokinetics and pharmacodynamics of the drug to evaluate a safe dosing range. In phase II, effectiveness of the drug is analyzed in about 100 to 300 patients with a disease condition that is intended for treatment and studying any side effects caused by the drug. After a positive evaluation the drug candidate is ready for phase III testing on a large number of patients (100 – 3000) to further evaluate safety and efficacy of the drug candidate [12]. Different populations are analyzed at this stage to find dosage, drug reactions, and drug-drug interactions [12]. After successful clinical trials and approval by regulatory authorities the drug is released into the market.

Even after this conscientious drug development process there are several drug withdrawals from the market due to adverse drug reactions. When we look from the early discovery phase 40% of the drugs are withdrawn due to toxicity after animal testing [1]. Between 1997-2005, forty-five of the approved drugs had black box warnings with 10 related to hepatotoxicity and 16 drugs were withdrawn out of which 5 (31%) were due to hepatotoxicity [13, 14]. In another survey on post-marketed drug withdrawals between 1998 to 2008 liver toxicity was the major reason for drug withdrawal [2]. After liver toxicity renal injury is the second most leading cause of drug attrition [15]. 25% of the marketed drugs with potential nephrotoxicity warnings lead to acute kidney injury increasing mortality and morbidity in patients [15, 16]. Development of advanced alternative methods to identify the liver and kidney organ toxicities may therefore aid in decreasing drug attrition.

**The liver: a major organ for drug metabolism and a main target for drug-induced toxicity.**

The liver is the major organ involved in drug metabolism and disposition. Liver parenchymal cells (hepatocytes) carry out this function and possess the majority of the enzymes involved in metabolism, which are housed in smooth endoplasmic reticulum. Of all cell types in the body, hepatocytes have the most extensive network of smooth endoplasmic reticulum. The expression of the xenobiotic metabolizing enzymes is a coordinately regulated and controlled mechanism. Drug metabolism by Phase I enzymes involves catalysis of the drug either by oxidation, reduction and hydrolysis steps leading a water-soluble or toxic reactive metabolites, which are further, modified by phase II enzymes for excretion. Phase II enzymes are mainly involved in conjugation steps, where a charged group is added to make a reactive metabolite less toxic to hepatocytes either by glucuronidation, sulphation, acetylation, methylation. Phase I and II steps render drugs into less toxic water soluble molecules that could be excreted through various routes, either blood, bile or renal elimination.

Approximately 70% of drugs are eliminated by CYP450 metabolism [17]. CYP450 metabolism can also lead to toxic reactive metabolites, which can cause hepatocellular necrosis [18]. These enzymes can also convert certain chemicals to carcinogenic metabolites; electrophilic metabolites produced by the CYP450 enzymes may bind to nucleophilic cellular components such as DNA leading to mutations and cancer in humans [19]. Some drugs have the ability to induce or reduce the expression levels of CYP450 enzymes, which can be detrimental to patients who are on multiple medications, as the co-administered drug may change the pharmacokinetics of a second drug leading to adverse drug reactions [20, 21]. It is estimated that out of two million serious adverse drug reactions that occur per year in United States, 26% of them are caused due to such drug-drug interactions, [17, 22] emphasizing a need for creating a complete safety profile of all the drugs. Positive evaluation of hepatotoxic drugs may decrease the incidence of liver toxicity and therefore drug attrition and huge costs involved with it.
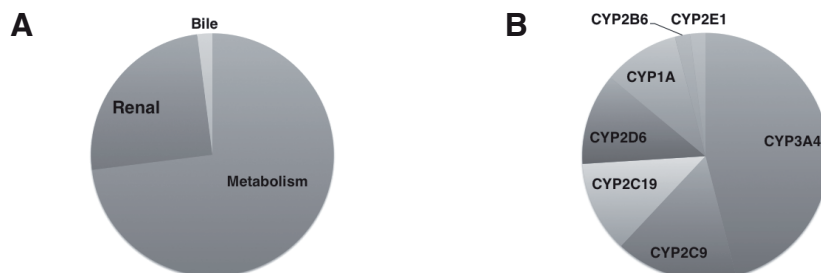


**Figure 1.** Process of metabolism and excretion of 200 drugs prescribed in 2002 (A) and CYP450 enzymes associated in their metabolism (B) (adapted from Wienkers *et al* (2005) ([17]).

**Renal drug clearance and toxicity**

After the liver, the kidneys play a major role in the clearance of drugs [17]. The primary functions of the kidney are filtration, secretion, reabsorption of body fluids, but importantly, excretion of drugs and drug metabolites. When the filtrates or drug metabolites reach the nephron, the functional unit of the kidney, they are highly concentrated to up to 100–fold in the tubular regions of the nephron [23, 24], making the kidney vulnerable to toxic injury leading to acute renal failure or loss of kidney function. In a study of patients admitted to intensive care due to kidney failure, 19% were caused by drug-induced toxicity [23, 25].

Proximal tubular epithelial cells in the nephron have the highest level of transporters compared to any other segment in the nephron playing a major role in reabsorption [26, 27]. These are the first cells that are exposed to the glomerular filtrate containing high levels of toxins, which makes them susceptible to toxic injury causing mitochondrial dysfunction, increased oxidative stress and decreased excretion leading to kidney injury [24, 28, 29]. Upon injury by a nephrotoxic agent proximal tubule cells die either by apoptosis or necrosis [30]. Nephrotoxic drugs have either a direct toxic effect on various segments of the nephron or they induce inflammation of the renal interstitium leading to acute renal failure. Many antibiotics, chemotherapeutics and immunosuppressant's induce direct injury to the tubules [31]. The intact tight junction complex, which is essential for proper reabsorption, may also be disrupted causing a leaky epithelium ultimately leading to proximal tubular disruption [31, 32].

**Renal Inflammation in nephrotoxicity**

Several nephrotoxic compounds induce an inflammatory response, which can aggravate renal injury. At the early stages of injury morphological and functional changes in tubular epithelium and vascular endothelial cells are observed [33]. This leads to infiltration of leukocytes to the injured site where renal tubular epithelial cells produce inflammatory cytokines TNFα, IL-6, IL-1β and TGF-β [34, 35] which induce an inflammatory cascade and can enhance cytotoxicity.

Nephrotoxic drugs such as cisplatin can increase the expression of various pro-inflammatory cytokines and chemokines, with TNFα being identified as a key factor in enhancing the inflammatory response. Inhibition of cisplatin-induced TNFα production led to downregulation of other cytokines and decreased renal injury [36-38]. Several mechanisms have been proposed for cisplatin-induced TNFα production, involving ERK and p38 MAPK mediated activation, [37, 39] imbalance in NF-κB and JNK/c-Jun signaling [40]. Therefore, inflammation plays a major role in the pathophysiology of kidney injury, which needs to be thoroughly investigated during early phases of drug discovery. Nephrotoxicity is mainly detected at late stages of

drug development with only 2% of attrition at preclinical testing and 19% during clinical trials [41]. Besides the current conventional end points, use of advanced screening methods such as live cell imaging for early apoptotic events [42] might help in identifying safe compounds thereby decreasing attrition rates due to nephrotoxicity.

**Pre-clinical safety testing: where do we stand?**

With a high incidence of drug-induced organ toxicity it is very important to make an accurate estimation of pharmacokinetic and pharmacodynamics properties of a new chemical entity during pre-clinical assessment. Currently various *in vivo* and *in vitro* studies are performed to validate the safety of chemical entities and their targeted use for a human disease, mainly relying on animal models for long-term effects of the drug. But only 50% of the chemicals that caused hepatotoxicity in clinical developmental phases had concordance with toxicity in animal models [43]. This may be attributed to species difference, interbred lab animals, disease state vs. healthy animals, genetic and environmental difference that exist in human population [14]. This emphasizes a need for efficient models that could accurately predict the safety profile of the compounds. Human cell based models offer several advantages in terms of relevance to humans and increased throughput compared to animal models. Current standard *in vitro* models used for screening assays include hepatocytes for liver toxicity, renal proximal tubule epithelial cells for nephrotoxicity, vascular endothelial cells for vascular toxicity, neuronal and glial cells for neurotoxicity, cardiomyocytes for cardiotoxicity, skeletal myocytes for rhabdomyolysis [44].

| | Sensitivity | Specificity |
|---|---|---|
| DNA synthesis | 10 | 92 |
| Protein synthesis | 4 | 97 |
| Glutathione depletion | 19 | 85 |
| Superoxide induction | 1 | 97 |
| Caspase-3 induction | 5 | 95 |
| Membrane integrity | 2 | 99 |
| Cell viability | 10 | 92 |
| Cell viability or GSH or DNA synthesis | 25 | 83 |
| Regulatory animal toxicity tests | 52 | N/A |

**Table 1.** Percentage predictivity of *in vitro* toxicity assays and regulatory animal studies for 611 compounds with hepatotoxicity warnings as described by Xu *et al* in [14].

However, *in vitro* models fail to preserve organ specific functions in an artificial environment and are not reliable for making accurate predictions. For example, *in vitro* testing on hepatic cell lines measuring various indicators of cell stress and toxicity

did not improve predictivity compared to animal studies alone [14, 45]. All the *in vitro* tests combined together had only half the sensitivity to that of regulatory animal testing (as shown in table 1, sensitivity and specificity of 611 hepatotoxic compounds tested [14]).

The main focus of this thesis work is to explore improved *in vitro* models and methods for organ toxicity, with a principal focus on *in vitro* liver toxicity, which will be discussed in detail.

**Predicting drug induced liver injury (DILI) at preclinical stages**

There are several possible reasons for poor prediction of human toxicity in pre-clinical studies. The current methods used to assess toxicity at the preclinical level were introduced in 1970's and have not kept pace with technological developments [46]. Furthermore, test models may not give a toxic response due to loss of organ specific cell functionality or there is a difference in the mechanism of drug metabolism between humans and the cells/tissues of the model. The implementation of improved toxicological approaches and exploring the mechanistic toxicity on human-relevant test models may improve the early safety prediction.

Preclinical hepatotoxicity assessment is done in a tiered approach. In the tier 1 studies normal animal models (rodent and non-rodent) are exposed with multiple doses and durations of the drug at much higher levels than those used in clinical studies to estimate the 'dose-limiting toxicity' or no effect level (NOEL) and no adverse effect level (NOAEL) [47]. Various parameters are measured to evaluate toxicity and identify the safety level of the drug that could be administered in the clinical phases. If hepatotoxicity was found to be the limiting factor, then various *in vitro* screening assays, including covalent binding assays are considered to indicate specific toxicity issues and their potential severity [48, 49]. Though the main reason for poor prediction lies with a lack of physiological relevance of the models, human genetics and other underlying disease conditions might lead to idiosyncratic reactions, which are hard to identify at the pre-clinical and clinical phases. Of 28 compounds developed by Rhone-Poulenc Rorer (now a subsidiary of Sanofi-Aventis) between 1988 and 1994, 10 of them showed signs of liver toxicity in animal models; 7 of these compounds were tested in humans of which only 1 compound showed human liver toxicity [50]. There are many other studies, which show a lack of correlation with animal toxicity [51]. In this respect, human cell based models with a stable liver specific function could make an important contribution to predicting drug safety.

***in vitro* cell models for studying hepatotoxicity**

***Precision cut liver slices (PCLS)***: Tissue slices contain all the cell types and tis-

sue microenvironment [52], which may enable them to respond better to a chemical stimulus. Precision cut human liver slices have shown to retain drug metabolism enzymes [53-55] and they have been used for various drug metabolism and toxicity studies [56, 57]. Microarray transcriptomic studies on rat PCLS showed similar mechanistic gene expression profile as *in vivo* liver tissue [58]. Recently, proteomic analysis after compound exposure on mouse, rat and human PCLS was shown to demonstrate *in vivo* like responses [59]. Though the model is unique in its composition and similarity to *in vivo* liver responses, a rapid decline in liver specific functions [54] is a limitation for chronic drug exposure studies. Recent advances in slicing and cryo-preservation techniques were shown to maintain the viability of liver slices [52], which may help to overcome laborious extraction procedures for test samples and low-throughput.

***Primary hepatocytes (PHH):*** Primary hepatocytes isolated from human or animal tissue largely retain liver specific enzymes and are widely used for evaluating drug metabolism. Freshly isolated primary human hepatocytes are considered the 'gold standard' for *in vitro* drug assessment [5, 60]. Isolation of primary human hepatocytes is a complex process, which can lead to poor retention of liver enzyme activity [61]. Recent advances in cryopreservation techniques have helped to maintain the differentiated status of primary hepatocytes without any major loss of functions due to cryoinjury [62, 63]. But once cultured *in vitro*, primary hepatocytes rapidly lose their liver specific functions [5, 64]. Sandwich culturing of primary hepatocytes (between layers of collagen gel) has been shown to improve stability of expression of metabolic enzymes and support formation of bile canaliculi [65-68]. Although human primary hepatocytes are most promising for *in vitro* assessment in terms of physiological relevance, the limited availability of human donors, donor specific variability and cost have made this impractical for routine assessment [6, 61]. Primary hepatocytes from rat and mouse were also investigated and similar limitations were observed. Compared to rat hepatocytes, mouse hepatocytes are better in maintaining liver specific functions and discriminating carcinogens from non-carcinogens in a toxicogenomics study [69-71].

**Immortalized cell lines:** Cell immortalization either due to mutations in growth regulating genes or certain gene insertions provide a valuable and limitless source of material for studying the biological responses of the organs. Due to their unlimited growth, ease of availability and use they are convenient for high-throughput screening assays without large variation between experiments. Among the various immortalized cell lines available, Fa2N4 and HepG2 are 'first alternatives' after primary human hepatocytes [72] and the recently introduced HepaRG is a promising addition

with their high levels of metabolic enzymes [73].

***Fa2N4:*** Fa2N-4 cells are derived from primary human hepatocytes and immortalized with SV40 large T-antigen [60, 74, 75]. These cells were shown to posses various CYP450 enzymes and transporters [75] but at the same time they lack certain xenobiotic nuclear receptors like CAR and important drug transporters classes like OATPs [60, 76] which limits their use for assessing hepatotoxicity.

***HepaRG:*** HepaRG cell line is derived from female carcinoma patient. It is a bi-potent progenitor cell line, which differentiates into biliary and hepatocyte-like cells in the presence of DMSO [77-79]. Once differentiated in the presence of DMSO, HepaRG cells express high levels of metabolic enzymes, transporters and xenobiotic nuclear receptors [73, 80]. The culture of HepaRG cells in high concentration of DMSO in the medium has seen certain drawbacks such as increased cell death and LDH and AST enzymes levels [81]. Earlier observations in primary hepatocytes and our observations with HepG2 cells have shown that concentrations of DMSO at 0.1% or above can induce phase 1 and 2 enzyme expression [5, 6, 82]. Therefore high levels of DMSO might give an inappropriate estimation of enzyme induction. It was also observed that prototypical inducers of CYP3A4 like rifampin and phenobarbital did not induce CYP3A4 induction in HepaRG cells [73, 80]. Though promising with high levels of drug detoxifying enzymes, the media formulation and proprietary status of these cells may complicate their use for routine toxicological assessments.

***HepG2 cells:*** HepG2 is a well-differentiated hepato-carcinoma cell line. HepG2 cells are best characterized and are widely used for various toxicological and pharmacological studies [83-87]. They express various liver-specific enzymes and drug metabolizing enzymes [88]. HepG2 cells express functionally active p53 protein, which can activate the DNA damage response and induce apoptosis, making it a desirable model for toxicity studies, especially genotoxic studies [60, 89]. These cells also show the presence of active nuclear transcription factor E2-related factor-2 (Nrf2) system, which is essential for induction and the expression of various phase II drug metabolizing enzymes and transporters for detoxification [90].

HepG2 cells are widely used in various high-throughput studies [86, 91-95] including EPA's ToxCast™ and Tox21™ programs for predicting and prioritizing chemicals [95-98]. The cells were also used in the pharmaceutical industry for lead identification [99]. A recent study combining a toxicogenomics approach and Ames test demonstrated that HepG2 cells could accurately predict *in vivo* genotoxicity [100]. In a high content screening approach these cells showed 93% sensitivity in identifying hepatotoxic compounds [86]. Comparative toxicogenomics analysis be-

tween HepG2 and HepaRG showed that HepG2 cells are better in discriminating genotoxic compounds and non-genotoxic compounds than HepaRG [101]. Earlier studies also indicated that these cells had high sensitivity and specificity in identifying genotoxic compounds [94, 102, 103].

With several advantages in ease of use, availability and considerable biological responses, HepG2 cells could be an ideal replacement for primary hepatocytes. However, the major concern with HepG2 cells and other hepatocyte cell lines is the lack of metabolic competence compared to primary hepatocytes [7, 14] [104]. This may be partly due to their hepatocarcinoma origin and oncogenic transformation, but also because they have been passaged extensively, resulting in drift from the original hepatocyte genetic profile. Furthermore, the absence of an *in vivo* like environment in a tissue culture dish results in a dedifferentiated phenotype with inevitable loss of function. A high proliferation rate associated with immortalized cells is a major limitation in identifying compounds that inhibit cell growth and induce apoptosis.

**3D cell culture**

*In vivo*, hepatocytes are highly polarized with distinct basal-lateral sinusoids and apical canalicular domains [105] which are essential for proper functioning of the liver. This highly polarized morphology is lost when cells are cultured under non-physiological conditions [106]. Hepatocytes cultured in a 3D environment using bioreactors [107, 108], hanging drop methods [109], collagen sandwich cultures [110], micro-space cultures [111], micro-patterned systems [112], microfluidic perfusion systems [113, 114], collagen and Matrigel cultures [115, 116] and other synthetic biomaterials [68, 117] have shown to re-acquire tissue specific properties and possess many hallmarks of *in vivo* epithelial cells.

Besides an increased physiological relevance, 3D models could also support long-term culture of the micro-tissues [108, 118, 119], representing a new dimension in *in vitro* toxicity assessment for repeated drug exposure studies. Maintaining robust tissue-like properties and balancing this with a high-throughput methodology is a big challenge. Some of the current 3D platforms cannot offer flexibility for high-throughput toxicity studies. A preferred choice for high-throughput screening assays would be to grow micro-tissues in a 384 or 1536 well formats. Bioreactors or microfluidic devices might emulate a tissue-like environment with respect to gaseous exchange and flow of nutrients but the throughput may be challenging with these models requiring complex equipment. High content imaging is increasingly used for toxicological screening assays [86]. Such imaging based approaches are technically challenging to apply to 3D culture systems. Although these challenges will inevitably be resolved as the technology develops, the use of biochemical end-points for 3D cultures are more feasible for routine high-throughput assays.

**HepG2 cells in 3D culture**

HepG2 cells show a spheroid morphology when cultured in micro-space cultures [111], bioreactors [107], peptide gels [68] and Matrigel [119] with distinctive characteristics of polarized epithelial hepatocytes. The gene expression of metabolic enzymes is also higher in HepG2 spheroids cultured on micro-space cultures [111] or ECM gels, in contrast to low levels with conventional 2D cultures. Increased expression of CYP450 enzymes might offer a great improvement to safety assessment studies and studying drug-drug interactions where the activation of a xenobiotic response by one (not necessarily toxic) compound may increase the metabolism of a second compound into toxic intermediates [120]. The absence or impairment of CYP450 enzymes most likely accounts for the failure to identify some hepatotoxic compounds *in vitro*.

Some functional activities of polarized hepatocytes were also recapitulated in 3D cell culture models. The formation of bile canaliculi is an important feature that was shown in HepG2 cells cultured on peptide hydrogels [68] and even more prominently with Matrigel cultures in our lab as described in chapter 2. The restoration of excretory function is likely due to the improved morphological differentiation of the hepatocytes, in particular, the establishment of apical-basal polarity - but also the restored expression of transporters and other components of the excretory machinery. Many drugs disrupt excretion pathways, for example rifampicin inhibits activity of OATP1B3, a transporter essential for bile acid flow [121]. HepG2 3D culture models may therefore allow the evaluation of the effects of new chemical entities on transporter function at the *in vitro* screening stage.

Earlier reports have shown that HepG2 cells have higher gene expression associated with cell cycle regulation, DNA, RNA nucleotide metabolism, transcription, transport and signal transduction and lower transcription levels associated with cell death, lipid metabolism and xenobiotic metabolism. In this thesis, we demonstrate that in HepG2 spheroids, genes associated with cell cycle were strongly downregulated and most of the xenobiotic metabolism pathways and stress signaling pathways such as the Nrf2 system were highly upregulated. HepG2 cells were also known to be inherently lacking in important nuclear xenobiotic receptors, [122, 123] but were re-expressed in the differentiated HepG2 spheroids as described in chapter 2 of this thesis.

An improved metabolic competence in 3D HepG2 spheroids and a functional similarity to *in vivo* hepatocytes in a micro plate setup would be promising for high-throughput toxicity screening assays. The ability to maintain a functionally stable phenotype for an extended period is an important feature that would allow the study of chronic drug exposure. A thorough investigation on low-dose, long-term effects on the gene expression, metabolite formation and morphological perturbations

will provide more insight into the mechanisms of toxicity, and should be taken into consideration when validating and evaluating the potential of 3D cell culture systems as surrogates to human liver tissue or a replacement for animal models. Modern sensitive approaches such as toxicogenomics to identify the mechanistic information and high content screening (HCS) to identify subtle morphological and physiological changes that occur before cell death on 3D organotypic models will provide further detailed insight into the mechanisms of toxicity and will help identify biomarkers of liver injury.

**Toxicogenomics approaches in DILI**

The availability of complete genome sequences led to the successful evolution of functional genomics which helped to discern biological responses at a whole new level. Toxicogenomics, a combination of transcriptomic, proteomic and metabolomic analysis with conventional toxicology investigates the effects of compounds on over-all changes giving comprehensive mechanistic information on mode of action of a toxic response.

Transcriptomics analysis with microarray technology allow us to identify tens of thousands of genes that change upon xenobiotic exposure, allowing us to quick-ly interpret genes and stress signaling pathways associated with chemical toxicity. Also, recent advances in proteomic technologies either by two-dimensional gel elec-trophoresis 2-DE and gel-free LC-MS techniques are available for high-throughput protein analysis [124, 125]. Many toxicogenomic studies have been conducted to assess hepatotoxicity in rodent species, especially in rats, as it is a preferred choice due to ease of manipulation and breeding characteristics [126-132]. These studies have demonstrated that specific liver pathologies can be predicted by toxicogenomic approaches [133-137].

A repository of toxicogenomics data is available in public databases such as Gene Expression Omnibus (GEO) [138], Array Express [139], Comparative Toxicog-enomics Database (CTD) [140] or EDGE [141, 142], Chemical Effects in Biological Systems (CEBS) [129]. Additionally, the InnoMed PredTox consortium developed large-scale toxicogenomics databases, aimed at assessing the value of toxicog-enomics by combining the results with conventional readouts [143]. TG-GATES (Ge-nomics Assisted Toxicity Evaluation System) has a database of *in vivo* and *in vitro* gene expression profiles of liver and kidney upon exposure to 150 chemicals, mainly including drugs that are currently used for patients [144]. These databases will help us to perform a comparative analysis of prototypical compounds in various models.

Availability of large 'omics' data sets requires complex analysis algorithms to interpret the biological response. Availability of open source bioinformatics tools, like Bioconductor are helpful for data normalization of transcriptomics data. Several

commercial applications like ingenuity pathway analysis (IPA ®), Metacore™ (and other tools as discussed in [145]) are valuable for interpreting complex genomic data. These programs are built on a knowledge base developed from scientific literature databases on genes, proteins and chemicals providing relationships between changes in the gene expression to biological pathways.

Toxicogenomics aims to discern biological responses upon toxic insult and develop biomarkers that could predict a toxic outcome. The discovery of biomarker signatures will not only help in accurate prediction of toxicity, but also greatly reduces the use of animals for toxicity studies or may even replace animal testing if an *in vitro* model out-performs animal test models. A thorough comparative investigation of *in vitro* models with their *in vivo* counter parts may weigh the similarities between them. Kienhuis *et al* compared rat hepatocytes and rat *in vivo* gene expression profiles, which showed only a very minor overlap between the models, although the overlap increased with modification of the cell culture medium [146]. Additional improvement in the cell culture conditions - either media or using 3D cell culture models might further improve the predictive power of *in vitro* assays. *In vitro* toxicogenomics studies using human cell lines might be valuable to predict human specific responses; a number of studies from human derived hepatocytes - either primary or cell lines - are currently available [101, 147-151] and are promising. Our observations of gene expression profiles with diclofenac exposed *in vitro* 3D HepG2 cells showed a similar pathway profile to that of *in vivo* models. A number of stress signaling pathways that are not activated in 2D HepG2 cells were seen in 3D HepG2 cells which were in common with human liver slices exposed to diclofenac.

**High-content screening for studying drug induced organ toxicity**

High content imaging is a valuable methodology, which has the capacity to identify sensitive biological changes that are otherwise impossible with end point cytotoxicity assays. It will allow us to visualize dynamics of stress induced biological perturbations inside a cell in real time. Recent technical advances in fully automated microscopy stations and image data analysis methodologies have further improved the power to HCS for high-throughput screening assays.

Availability of various cell-permeable fluorescent molecular probes allowed us to study the kinetics of stress responses in real time. Automated measurements of live-cell apoptosis using Annexin-V, which binds to phosphotidyl-serine during early events of apoptosis is an efficient way to measure the kinetics of apoptosis upon compound exposure [152]. HCS has an advantage that multiple parameters can be measured. In a study to identify DILI compounds, primary human hepatocytes were challenged with 300 compounds measuring mitochondrial damage, oxidative stress and intracellular glutathione levels [153]. This analysis had a true-positive rate of 50-

60% and very low false-positive rate of 0-5%. In another study using HepG2 cells, four parameters were used; these measured intracellular calcium (Fluo-4AM), DNA content (Hoechst), mitochondrial membrane potential (TMRM) and plasma membrane permeability (TOTO3) and were compared with 7 conventional readouts that are used to assess toxicity. The high-content image analysis showed much higher sensitivity of 93% and specificity of 98 % compared to 25% and 90% of conventional assay readouts [86].

The application of toxicogenomics and high content screening in drug safety testing on human relevant *in vitro* models, may increase the predictive power of *in vitro* toxicity screening assays and provide sufficient functional data to reduce the reliance on animal models. The near *in vivo* properties of 3D cultures, their ease of use, low cost and availability suggest that these models offer great promise and are likely to play a significant part in animal-free toxicity testing in the future.

**Aim and outline of this thesis:**

Currently there is a dearth of *in vitro* models that could preserve the functional properties of a tissue for an extended period and offer compatibility to high-throughput screening assays. The key aim of this thesis is to develop an organotypic *in vitro* model for toxicity studies that can be used in pre-clinical drug safety testing and the *in vitro* study of liver biology. To this end we have developed a robust *in vitro* model, which show many hallmarks of *in vivo* hepatocytes, is applied in a 384-micro-well format and is compatible with standard medium- and high-throughput lab infrastructure for routine drug screening.

**Chapter 2** describes the development and validation of a 3D cell culture methodology, which enables HepG2 cells to reacquire lost functional hepatocytes properties. The cells differentiated and formed spheroids. Spheroids were analyzed for their polarized morphology, expression of functional differentiation markers, presence of functional activities of hepatocytes and their sensitivity to identify hepatotoxic compounds.

**Chapter 3** further characterizes the 3D HepG2 spheroid model and compares them to other *in vitro* liver models by analyzing gene transcription. Microarray analysis gene expression data was acquired during the differentiation process of HepG2 cells in 3D culture. Biologically significant pathways that are altered in differentiated 3D HepG2 cells compared to conventional 2D cultured HepG2 cells were thoroughly investigated. A detailed comparison of gene expression profiles was made between 3D HepG2 spheroids and other hepatocyte models (PHH and HepaRG) to human

liver. Common pathways between human liver and 3D HepG2 spheroids were high-lighted.

**Chapter 4** describes a comparative transcriptomic study between various *in vitro* and *in vivo* models in response to hepatotoxicant exposure. Gene expression pro-files from *in vitro* HepG2 spheroids, primary human hepatocytes, primary rat and mouse hepatocytes, human liver slices and *in vivo* rat and mouse models exposed with diclofenac were compared. Various stress-signaling pathways that are activated upon diclofenac exposure were analyzed.

**Chapter 5** describes a novel live-cell HCS assay for measuring nephrotoxicity. Tox-icity caused by nephrotoxic compounds was analyzed in real time on proximal tubu-lar kidney cells. The role of inflammation in conferring sensitivity to nephrotoxicants was investigated using the pro-inflammatory cytokine TNFα.

**Chapter 6** provides a summary and general discussion of the findings and implica-tions of the work in this thesis.

# REFERENCES

1    McKim, J. M., Jr. Building a tiered approach to in vitro predictive toxicity screening: a focus on assays with in vivo relevance. Comb Chem High Throughput Screen 13, 188-206 (2010).

2    MacDonald, J. S. & Robertson, R. T. Toxicity testing in the 21st century: a view from the pharmaceutical industry. Toxicol Sci 110, 40-46, doi:10.1093/toxsci/kfp088 (2009).

3    Patki, K. C., Von Moltke, L. L. & Greenblatt, D. J. In vitro metabolism of midazolam, triazolam, nifedipine, and testosterone by human liver microsomes and recombinant cytochromes p450: role of cyp3a4 and cyp3a5. Drug metabolism and disposition: the biological fate of chemicals 31, 938-944, doi:10.1124/dmd.31.7.938 (2003).

4    Martignoni, M., Groothuis, G. M. & de Kanter, R. Species differences between mouse, rat, dog, monkey and human CYP-mediated drug metabolism, inhibition and induction. Expert opinion on drug metabolism & toxicology 2, 875-894, doi:10.1517/17425255.2.6.875 (2006).

5    LeCluyse, E. L. Human hepatocyte culture systems for the in vitro evaluation of cytochrome P450 expression and regulation. European journal of pharmaceutical sciences : official journal of the European Federation for Pharmaceutical Sciences 13, 343-368 (2001).

6    LeCluyse, E. et al. Expression and regulation of cytochrome P450 enzymes in primary cultures of human hepatocytes. Journal of biochemical and molecular toxicology 14, 177-188 (2000).

7    Westerink, W. M. a. & Schoonen, W. G. E. J. Cytochrome P450 enzyme levels in HepG2 cells and cryopreserved primary human hepatocytes and their induction in HepG2 cells. Toxicology in vitro : an international journal published in association with BIBRA 21, 1581-1591, doi:10.1016/j.tiv.2007.05.014 (2007).

8    DiMasi, J. a., Hansen, R. W. & Grabowski, H. G. The price of innovation: new estimates of drug development costs. Journal of health economics 22, 151-185, doi:10.1016/s0167-6296(02)00126-1 (2003).

9    Paul, S. M. et al. How to improve R&D productivity: the pharmaceutical industry's grand challenge. Nat Rev Drug Discov 9, 203-214, doi:10.1038/nrd3078 (2010).

10   Hughes, J. P., Rees, S., Kalindjian, S. B. & Philpott, K. L. Principles of early drug discovery. Br J Pharmacol 162, 1239-1249, doi:10.1111/j.1476-5381.2010.01127.x (2011).

11   San Miguel, M. T. & Vargas, E. Drug evaluation and approval process in the European Union. Arthritis and rheumatism 55, 12-14, doi:10.1002/art.21712 (2006).

12   Meadows, M. The FDA's drug review process: ensuring drugs are safe and effective. FDA consumer 36, 19-24 (2002).

13   Lasser, K. E. et al. Timing of new black box warnings and withdrawals for prescription medications. JAMA : the journal of the American Medical Association 287, 2215-2220 (2002).

14   Xu, J. J., Diaz, D. & O'Brien, P. J. Applications of cytotoxicity assays and pre-lethal mechanistic assays for assessment of human hepatotoxicity potential. Chemico-biological interactions 150, 115-128, doi:10.1016/j.cbi.2004.09.011 (2004).

15   in Accelerating the Development of Biomarkers for Drug Safety: Workshop Summary  The National Academies Collection: Reports funded by National Institutes of Health   (2009).

16   Pannu, N. & Nadim, M. K. An overview of drug-induced acute kidney injury. Critical care medicine 36, S216-223, doi:10.1097/CCM.0b013e318168e375 (2008).

17   Wienkers, L. C. & Heath, T. G. Predicting in vivo drug interactions from in vitro drug discovery data. Nat Rev Drug Discov 4, 825-833, doi:10.1038/nrd1851 (2005).

18   Park, B. K., Pirmohamed, M. & Kitteringham, N. R. The role of cytochrome P450 enzymes in hepatic and extrahepatic human drug toxicity. Pharmacology & therapeutics 68, 385-424 (1995).

19   Gonzalez, F. J. Overview of experimental approaches for study of drug metabolism and drug-drug interactions. Adv Pharmacol 43, 255-277 (1997).

20   Saito, M., Hirata-Koizumi, M., Urano, T., Miyake, S. & Hasegawa, R. A literature search on pharmacokinetic drug interactions of statins and analysis of how such interactions are reflected in package inserts in Japan. Journal of clinical pharmacy and therapeutics 30, 21-37, doi:10.1111/j.1365-2710.2004.00605.x (2005).

21   Sproule, B. A., Naranjo, C. A., Brenmer, K. E. & Hassan, P. C. Selective serotonin reuptake inhibitors and CNS drug interactions. A critical review of the evidence. Clinical pharmacokinetics 33, 454-471 (1997).

22   Lazarou, J., Pomeranz, B. H. & Corey, P. N. Incidence of adverse drug reactions in hospitalized

patients: a meta-analysis of prospective studies. JAMA : the journal of the American Medical Association 279, 1200-1205 (1998).

23    Loghman-Adham, M., Kiu Weber, C. I., Ciorciaro, C., Mann, J. & Meier, M. Detection and management of nephrotoxicity during drug development. Expert opinion on drug safety 11, 581-596, doi:10.1517/14740338.2012.691964 (2012).

24    Naughton, C. A. Drug-induced nephrotoxicity. American family physician 78, 743-750 (2008).

25    Uchino, S. et al. Continuous renal replacement therapy: a worldwide practice survey. The beginning and ending supportive therapy for the kidney (B.E.S.T. kidney) investigators. Intensive care medicine 33, 1563-1570, doi:10.1007/s00134-007-0754-4 (2007).

26    Lee, A. Pharmacokinetics, bioavailability, (hpmpc). Metabolism Clinical And Experimental 24 (1996).

27    Schlatter, P., Gutmann, H. & Drewe, J. Primary porcine proximal tubular cells as a model for transepithelial drug transport in human kidney. European journal of pharmaceutical sciences : official journal of the European Federation for Pharmaceutical Sciences 28, 141-154, doi:10.1016/j.ejps.2006.01.009 (2006).

28    Zager, R. A. Pathogenetic mechanisms in nephrotoxic acute renal failure. Seminars in nephrology 17, 3-14 (1997).

29    Markowitz, G. S. & Perazella, M. A. Drug-induced renal failure: a focus on tubulointerstitial disease. Clinica chimica acta; international journal of clinical chemistry 351, 31-47, doi:10.1016/j.cccn.2004.09.005 (2005).

30    Nony, P. A. & Schnellmann, R. G. Mechanisms of renal cell repair and regeneration after acute renal failure. J Pharmacol Exp Ther 304, 905-912, doi:10.1124/jpet.102.035022 (2003).

31    Choudhury, D. & Ahmed, Z. Drug-associated renal dysfunction and injury. Nature clinical practice. Nephrology 2, 80-91, doi:10.1038/ncpneph0076 (2006).

32    Lameire, N., Van Biesen, W. & Vanholder, R. Acute renal failure. Lancet 365, 417-430, doi:10.1016/S0140-6736(05)17831-3 (2005).

33    Becker, E. L. Acute Renal Failure: Diagnosis and Management. Archives of internal Medicine 126, 168-169 (1970).

34    Daha, M. R. & van Kooten, C. Is the proximal tubular cell a proinflammatory cell? Nephrol Dial Transplant 15 Suppl 6, 41-43 (2000).

35    Bonventre, J. V. & Zuk, A. Ischemic acute renal failure: an inflammatory disease? Kidney Int 66, 480-485, doi:10.1111/j.1523-1755.2004.761_2.x (2004).

36    Ramesh, G. & Reeves, W. B. TNF-alpha mediates chemokine and cytokine expression and renal injury in cisplatin nephrotoxicity. The Journal of clinical investigation 110, 835-842, doi:10.1172/JCI15606 (2002).

37    Ramesh, G. & Brian Reeves, W. Cisplatin increases TNF-alpha mRNA stability in kidney proximal tubule cells. Renal failure 28, 583-592, doi:10.1080/08860220600843839 (2006).

38    Tsuruya, K. et al. Direct involvement of the receptor-mediated apoptotic pathways in cisplatin-induced renal tubular cell death. Kidney Int 63, 72-82, doi:10.1046/j.1523-1755.2003.00709.x (2003).

39    Dumitru, C. D. et al. TNF-alpha induction by LPS is regulated posttranscriptionally via a Tpl2/ERK-dependent pathway. Cell 103, 1071-1083 (2000).

40    Benedetti, G. et al. TNF-alpha-mediated NF-kappaB survival signaling impairment by cisplatin enhances JNK activation allowing synergistic apoptosis of renal proximal tubular cells. Biochemical pharmacology 85, 274-286, doi:10.1016/j.bcp.2012.10.012 (2013).

41    Izzedine, H., Harris, M. & Perazella, M. A. The nephrotoxic effects of HAART. Nature reviews. Nephrology 5, 563-573, doi:10.1038/nrneph.2009.142 (2009).

42    Benedetti, G. et al. A screen for apoptotic synergism between clinical relevant nephrotoxicant and the cytokine TNF-alpha. Toxicol In Vitro, doi:10.1016/j.tiv.2013.09.004 (2013).

43    Olson, H. et al. Concordance of the toxicity of pharmaceuticals in humans and in animals. Regulatory toxicology and pharmacology : RTP 32, 56-67, doi:10.1006/rtph.2000.1399 (2000).

44    P.Li, A. in vitro approaches to evaluate ADMET drug properties. Current topics in Medicinal Chemistry 4 (2004).

45    Lee, W. M. Drug-induced hepatotoxicity. The New England journal of medicine 349, 474-485, doi:10.1056/NEJMra021844 (2003).

46    Hartung, T. Look back in anger - what clinical studies tell us about preclinical work. Altex 30, 275-291 (2013).

47    FDA, C. f. D. E. a. R. C. Guidance for the industry: Estimating the maximum safe starting dose in initial clinical trials for therapeutics in adult healthy volunteers, <http://www.fda.gov/down-loads/Drugs/Guidances/UCM078932.pdf> (2005).

48    Kapeghian, J. C. & Traina, V. M. The role of experimental toxicology in safety evaluation: challenges facing the pharmaceutical industry. Medicinal research reviews 10, 271-280 (1990).

49    Dean, J. H. & Olson, H. M. The integration of investigative toxicology in the drug discovery process. Biology of the cell / under the auspices of the European Cell Biology Organization 77, 3-8 (1993).

50    Ballet, F. Hepatotoxicity in drug development: detection, significance and solutions. Journal of hepatology 26 Suppl 2, 26-36 (1997).

51    FDA, U. S. F. a. D. A. Nonclinical Assessment of Potential Hepatotoxicity in Man, 2000).

52    de Graaf, I. A. et al. Preparation and incubation of precision-cut liver and intestinal slices for application in drug metabolism and toxicity studies. Nat Protoc 5, 1540-1551, doi:10.1038/nprot.2010.111 (2010).

53    de Kanter, R. et al. A rapid and simple method for cryopreservation of human liver slices. Xenobiotica 28, 225-234, doi:10.1080/004982598239533 (1998).

54    Graaf, I. A., Groothuis, G. M. & Olinga, P. Precision-cut tissue slices as a tool to predict metabolism of novel drugs. Expert opinion on drug metabolism & toxicology 3, 879-898, doi:10.1517/17425255.3.6.879 (2007).

55    Vickers, A. E. & Fisher, R. L. Organ slices for the evaluation of human drug toxicity. Chemico-biological interactions 150, 87-96, doi:10.1016/j.cbi.2004.09.005 (2004).

56    Klassen, L. W. et al. An in vitro method of alcoholic liver injury using precision-cut liver slices from rats. Biochemical pharmacology 76, 426-436, doi:10.1016/j.bcp.2008.05.012 (2008).

57    Hadi, M. et al. Human precision-cut liver slices as an ex vivo model to study idiosyncratic drug-induced liver injury. Chemical research in toxicology 26, 710-720, doi:10.1021/tx300519p (2013).

58    Elferink, M. G. et al. Microarray analysis in rat liver slices correctly predicts in vivo hepatotoxicity. Toxicol Appl Pharmacol 229, 300-309, doi:10.1016/j.taap.2008.01.037 (2008).

59    van Swelm, R. P. et al. Proteomic profiling in incubation medium of mouse, rat and human precision-cut liver slices for biomarker detection regarding acute drug-induced liver injury. Journal of applied toxicology : JAT, doi:10.1002/jat.2917 (2013).

60    LeCluyse, E. L., Witek, R. P., Andersen, M. E. & Powers, M. J. Organotypic liver culture models: meeting current challenges in toxicity testing. Critical reviews in toxicology 42, 501-548, doi:10.3109/10408444.2012.682115 (2012).

61    Pless, G., Sauer, I. M. & Rauen, U. Improvement of the cold storage of isolated human hepatocytes. Cell transplantation 21, 23-37, doi:10.3727/096368911X580509 (2012).

62    Li, A. P. Evaluation of drug metabolism, drug-drug interactions, and in vitro hepatotoxicity with cryopreserved human hepatocytes. Methods Mol Biol 640, 281-294, doi:10.1007/978-1-60761-688-7_15 (2010).

63    McGinnity, D. F., Soars, M. G., Urbanowicz, R. A. & Riley, R. J. Evaluation of fresh and cryopreserved hepatocytes as in vitro drug metabolism tools for the prediction of metabolic clearance. Drug metabolism and disposition: the biological fate of chemicals 32, 1247-1253, doi:10.1124/dmd.104.000026 (2004).

64    Wilkening, S. & Bader, A. Influence of culture time on the expression of drug-metabolizing enzymes in primary human hepatocytes and hepatoma cell line HepG2. Journal of biochemical and molecular toxicology 17, 207-213, doi:10.1002/jbt.10085 (2003).

65    LeCluyse, E. L., Fix, J. A., Audus, K. L. & Hochman, J. H. Regeneration and maintenance of bile canalicular networks in collagen-sandwiched hepatocytes. Toxicol In Vitro 14, 117-132 (2000).

66    LeCluyse, E. L., Ahlgren-Beckendorf, J. A., Carroll, K., Parkinson, A. & Johnson, J. Regulation of glutathione S-transferase enzymes in primary cultures of rat hepatocytes maintained under various matrix configurations. Toxicol In Vitro 14, 101-115 (2000).

67    LeCluyse, E. L., Audus, K. L. & Hochman, J. H. Formation of extensive canalicular networks by rat hepatocytes cultured in collagen-sandwich configuration. Am J Physiol 266, C1764-1774 (1994).

68    Malinen, M. M., Palokangas, H., Yliperttula, M. & Urtti, A. Peptide Nanofiber Hydrogel Induces Formation of Bile Canaliculi Structures in Three-Dimensional Hepatic Cell Culture. Tissue Eng Part A, doi:10.1089/ten.TEA.2012.0046 (2012).

69      Mathijs, K. et al. Discrimination for genotoxic and nongenotoxic carcinogens by gene expression profiling in primary mouse hepatocytes improves with exposure time. Toxicol Sci 112, 374-384, doi:10.1093/toxsci/kfp229 (2009).

70      Mathijs, K. et al. Gene expression profiling in primary mouse hepatocytes discriminates true from false-positive genotoxic compounds. Mutagenesis 25, 561-568, doi:10.1093/mutage/geq040 (2010).

71      Mathijs, K. et al. Assessing the metabolic competence of sandwich-cultured mouse primary hepatocytes. Drug metabolism and disposition: the biological fate of chemicals 37, 1305-1311, doi:10.1124/dmd.108.025775 (2009).

72      Szabo, M., Veres, Z., Baranyai, Z., Jakab, F. & Jemnitz, K. Comparison of human hepatoma HepaRG cells with human and rat hepatocytes in uptake transport assays in order to predict a risk of drug induced hepatotoxicity. PLoS One 8, e59432, doi:10.1371/journal.pone.0059432 (2013).

73      Aninat, C. et al. Expression of cytochromes P450, conjugating enzymes and nuclear receptors in human hepatoma HepaRG cells. Drug metabolism and disposition: the biological fate of chemicals 34, 75-83, doi:10.1124/dmd.105.006759 (2006).

74      Ripp, S. L. et al. Use of immortalized human hepatocytes to predict the magnitude of clinical drug-drug interactions caused by CYP3A4 induction. Drug metabolism and disposition: the biological fate of chemicals 34, 1742-1748, doi:10.1124/dmd.106.010132 (2006).

75      Mills, J. B., Rose, K. A., Sadagopan, N., Sahi, J. & de Morais, S. M. Induction of drug metabolism enzymes and MDR1 using a novel human hepatocyte cell line. J Pharmacol Exp Ther 309, 303-309, doi:10.1124/jpet.103.061713 (2004).

76      Hariparsad, N., Carr, B. A., Evers, R. & Chu, X. Comparison of immortalized Fa2N-4 cells and human hepatocytes as in vitro models for cytochrome P450 induction. Drug metabolism and disposition: the biological fate of chemicals 36, 1046-1055, doi:10.1124/dmd.108.020677 (2008).

77      Gripon, P. et al. Infection of a human hepatoma cell line by hepatitis B virus. Proc Natl Acad Sci U S A 99, 15655-15660, doi:10.1073/pnas.232137699 (2002).

78      Cerec, V. et al. Transdifferentiation of hepatocyte-like cells from the human hepatoma HepaRG cell line through bipotent progenitor. Hepatology 45, 957-967, doi:10.1002/hep.21536 (2007).

79      Guillouzo, A. et al. The human hepatoma HepaRG cells: a highly differentiated model for studies of liver metabolism and toxicity of xenobiotics. Chemico-biological interactions 168, 66-73, doi:10.1016/j.cbi.2006.12.003 (2007).

80      Kanebratt, K. P. & Andersson, T. B. Evaluation of HepaRG cells as an in vitro model for human drug metabolism studies. Drug metabolism and disposition: the biological fate of chemicals 36, 1444-1452, doi:10.1124/dmd.107.020016 (2008).

81      Hoekstra, R. et al. The HepaRG cell line is suitable for bioartificial liver application. Int J Biochem Cell Biol 43, 1483-1489, doi:10.1016/j.biocel.2011.06.011 (2011).

82      Nishimura, M., Ueda, N. & Naito, S. Effects of dimethyl sulfoxide on the gene induction of cytochrome P450 isoforms, UGT-dependent glucuronosyl transferase isoforms, and ABCB1 in primary culture of human hepatocytes. Biological & pharmaceutical bulletin 26, 1052-1056 (2003).

83      Hockley, S. L., Arlt, V. M., Brewer, D., Giddings, I. & Phillips, D. H. Time- and concentration-dependent changes in gene expression induced by benzo(a)pyrene in two human cell lines, MCF-7 and HepG2. BMC genomics 7, 260, doi:10.1186/1471-2164-7-260 (2006).

84      van Delft, J. H. et al. Discrimination of genotoxic from non-genotoxic carcinogens by gene expression profiling. Carcinogenesis 25, 1265-1276, doi:10.1093/carcin/bgh108 (2004).

85      Olsavsky, K. M. et al. Gene expression profiling and differentiation assessment in primary human hepatocyte cultures, established hepatoma cell lines, and human liver tissues. Toxicol Appl Pharmacol 222, 42-56, doi:10.1016/j.taap.2007.03.032 (2007).

86      O'Brien, P. J. et al. High concordance of drug-induced human hepatotoxicity with in vitro cytotoxicity measured in a novel cell-based model using high content screening. Archives of toxicology 80, 580-604, doi:10.1007/s00204-006-0091-3 (2006).

87      Fredriksson, L. et al. Diclofenac inhibits tumor necrosis factor-Œ±-induced nuclear factor-ŒƒB activation causing synergistic hepatocyte apoptosis. Hepatology (Baltimore, Md.) 53, 2027-2041, doi:10.1002/hep.24314 (2011).

88      Hewitt, N. J. & Hewitt, P. Phase I and II enzyme characterization of two sources of HepG2 cell

lines. Xenobiotica 34, 243-256, doi:10.1080/00498250310001657568 (2004).

89    Vollmer, C. M. et al. p53 selective and nonselective replication of an E1B-deleted adenovirus in hepatocellular carcinoma. Cancer Res 59, 4369-4374 (1999).

90    Adachi, T. et al. Nrf2-dependent and -independent induction of ABC transporters ABCC1, ABCC2, and ABCG2 in HepG2 cells under oxidative stress. Journal of experimental therapeutics & oncology 6, 335-348 (2007).

91    O'Brien, P. & Haskins, J. R. In vitro cytotoxicity assessment. Methods Mol Biol 356, 415-425 (2007).

92    Schoonen, W. G., Westerink, W. M. & Horbach, G. J. High-throughput screening for analysis of in vitro toxicity. EXS. 99, 401-452 (2009).

93    Abraham, V. C., Towne, D. L., Waring, J. F., Warrior, U. & Burns, D. J. Application of a high-content multiparameter cytotoxicity assay to prioritize compounds based on toxicity potential in humans. J Biomol Screen 13, 527-537 (2008).

94    Westerink, W. M., Stevenson, J. C., Horbach, G. J. & Schoonen, W. G. The development of RAD51C, Cystatin A, p53 and Nrf2 luciferase-reporter assays in metabolically competent HepG2 cells for the assessment of mechanism-based genotoxicity and of oxidative stress in the early research phase of drug development. Mutat Res 696, 21-40, doi:10.1016/j.mrgentox.2009.12.007 (2010).

95    Judson, R. S. et al. In Vitro Screening of Environmental Chemicals for Targeted Testing Prioritization: The ToxCast Project. Environ Health Perspect 118 (2009).

96    Martin, M. T., Judson, R. S., Reif, D. M., Kavlock, R. J. & Dix, D. J. Profiling chemicals based on chronic toxicity results from the U.S. EPA ToxRef Database. Environ Health Perspect 117, 392-399 (2009).

97    Shukla, S. J., Huang, R., Austin, C. P. & Xia, M. The future of toxicity testing: a focus on in vitro methods using a quantitative high-throughput screening platform. Drug Discov Today, doi:S1359-6446(10)00261-8 [pii]10.1016/j.drudis.2010.07.007 (2010).

98    delft, J. v. Toxicogenomics-Based Cellular Models :Alternatives to Animal Testing for Safety Assessment.  (Elsevier, 2014).

99    Gamo, F. J. et al. Thousands of chemical starting points for antimalarial lead identification. Nature 465, 305-310, doi:10.1038/nature09107 (2010).

100   Magkoufopoulou, C. et al. A transcriptomics-based in vitro assay for predicting chemical genotoxicity in vivo. Carcinogenesis 33, 1421-1429, doi:http://dx.doi.org/10.1093/carcin/bgs182 (2012).

101   Jennen, D. G. et al. Comparison of HepG2 and HepaRG by whole-genome gene expression analysis for the purpose of chemical hazard identification. Toxicol Sci 115, 66-79 (2010).

102   Uhl, M. et al. Effect of chrysin, a flavonoid compound, on the mutagenic activity of 2-amino-1-methyl-6-phenylimidazo[4,5- b]pyridine (PhIP) and benzo(a)pyrene (B(a)P) in bacterial and human hepatoma (HepG2) cells. Arch Toxicol 77, 477-484, doi:10.1007/s00204-003-0469-4 (2003).

103   Uhl, M., Helma, C. & Knasmuller, S. Single-cell gel electrophoresis assays with human-derived hepatoma (Hep G2) cells. Mutat Res 441, 215-224 (1999).

104   Gerets, H. H. J. et al. Characterization of primary human hepatocytes, HepG2 cells, and HepaRG cells at the mRNA level and CYP activity in response to inducers and their predictivity for the detection of human hepatotoxins. Cell biology and toxicology, doi:10.1007/s10565-011-9208-4 (2012).

105   Wang, L. & Boyer, J. L. The maintenance and generation of membrane polarity in hepatocytes. Hepatology 39, 892-899, doi:10.1002/hep.20039 (2004).

106   Maurice, M., Rogier, E., Cassio, D. & Feldmann, G. Formation of plasma membrane domains in rat hepatocytes and hepatoma cell lines in culture. J Cell Sci 90 ( Pt 1), 79-92 (1988).

107   Fey, S. J. & Wrzesinski, K. Determination of drug toxicity using 3D spheroids constructed from an immortal human hepatocyte cell line. Toxicol Sci 127, 403-411, doi:10.1093/toxsci/kfs122 (2012).

108   Leite, S. B. et al. 3D HepaRG Model as an attractive tool for toxicity testing. Toxicol Sci, doi:10.1093/toxsci/kfs232 (2012).

109   Tung, Y.-C. et al. High-throughput 3D spheroid culture and drug testing using a 384 hanging drop array. The Analyst 136, 473-478, doi:10.1039/c0an00609b (2011).

110   Dunn, J. C., Tompkins, R. G. & Yarmush, M. L. Hepatocytes in collagen sandwich: evidence for

transcriptional and translational regulation. The Journal of cell biology 116, 1043-1053 (1992).

111     Nakamura, K. et al. Evaluation of drug toxicity with hepatocytes cultured in a micro-space cell culture system. Journal of bioscience and bioengineering 111, 78-84, doi:10.1016/j.jbiosc.2010.08.008 (2011).

112     Khetani, S. R. et al. Use of micropatterned cocultures to detect compounds that cause drug-induced liver injury in humans. Toxicol Sci 132, 107-117, doi:10.1093/toxsci/kfs326 (2013).

113     Lee, J., Kim, S. H., Kim, Y. C., Choi, I. & Sung, J. H. Fabrication and characterization of microfluidic liver-on-a-chip using microsomal enzymes. Enzyme and microbial technology 53, 159-164, doi:10.1016/j.enzmictec.2013.02.015 (2013).

114     Trietsch, S. J., Israels, G. D., Joore, J., Hankemeier, T. & Vulto, P. Microfluidic titer plate for stratified 3D cell culture. Lab on a chip 13, 3548-3554, doi:10.1039/c3lc50210d (2013).

115     Zhang, F., Xu, R. & Zhao, M.-j. QSG-7701 human hepatocytes form polarized acini in three-dimensional culture. Journal of cellular biochemistry 110, 1175-1186, doi:10.1002/jcb.22632 (2010).

116     Matsui, H., Takeuchi, S., Osada, T., Fujii, T. & Sakai, Y. Enhanced bile canaliculi formation enabling direct recovery of biliary metabolites of hepatocytes in 3D collagen gel microcavities. Lab on a chip 12, 1857-1864, doi:10.1039/c2lc40046d (2012).

117     Kim, Y. & Rajagopalan, P. 3D hepatic cultures simultaneously maintain primary hepatocyte and liver sinusoidal endothelial cell phenotypes. PloS one 5, e15456-e15456, doi:10.1371/journal.pone.0015456 (2010).

118     Gunness, P. et al. 3D organotypic cultures of human HepaRG cells: a tool for in vitro toxicity studies. Toxicol Sci 133, 67-78, doi:10.1093/toxsci/kft021 (2013).

119     Ramaiahgari et al. A 3D in vitro model of differentiated HepG2 cell spheroids with improved liver-like properties for repeated dose high-throughput toxicity studies. Archives of toxicology (2014).

120     Lin, J. H. CYP induction-mediated drug interactions: in vitro assessment and clinical implications. Pharm Res 23, 1089-1116, doi:10.1007/s11095-006-0277-7 (2006).

121     Hirano, M., Maeda, K., Shitara, Y. & Sugiyama, Y. Drug-drug interaction between pitavastatin and various drugs via OATP1B1. Drug metabolism and disposition: the biological fate of chemicals 34, 1229-1236, doi:10.1124/dmd.106.009290 (2006).

122     Kanno, Y. & Inouye, Y. A consecutive three alanine residue insertion mutant of human CAR: a novel CAR ligand screening system in HepG2 cells. The Journal of toxicological sciences 35, 515-525 (2010).

123     Naspinski, C. et al. Pregnane X receptor protects HepG2 cells from BaP-induced DNA damage. Toxicological sciences : an official journal of the Society of Toxicology 104, 67-73, doi:10.1093/toxsci/kfn058 (2008).

124     Barrier, M. & Mirkes, P. E. Proteomics in developmental toxicology. Reprod Toxicol 19, 291-304, doi:10.1016/j.reprotox.2004.09.001 (2005).

125     Van Summeren, A., Renes, J., van Delft, J. H., Kleinjans, J. C. & Mariman, E. C. Proteomics in the search for mechanisms and biomarkers of drug-induced hepatotoxicity. Toxicol In Vitro 26, 373-385, doi:10.1016/j.tiv.2012.01.012 (2012).

126     Ruepp, S. et al. Assessment of hepatotoxic liabilities by transcript profiling. Toxicol Appl Pharmacol 207, 161-170 (2005).

127     Natsoulis, G. et al. The liver pharmacological and xenobiotic gene response repertoire. Mol Syst Biol 4, 175 (2008).

128     Hirode, M. et al. Gene expression profiling in rat liver treated with compounds inducing phospholipidosis. Toxicol Appl Pharmacol 229, 290-299 (2008).

129     Waters, M. et al. CEBS--Chemical Effects in Biological Systems: a public data repository integrating study design and toxicity data with microarray and proteomics data. Nucleic Acids Res 36, D892-900, doi:10.1093/nar/gkm755 (2008).

130     McMillian, M. et al. A gene expression signature for oxidant stress/reactive metabolites in rat liver. Biochem Pharmacol 68, 2249-2261 (2004).

131     McMillian, M. et al. Inverse gene expression patterns for macrophage activating hepatotoxicants and peroxisome proliferators in rat liver. Biochem Pharmacol 67, 2141-2165 (2004).

132     Aitman, T. J. et al. Progress and prospects in rat genetics: a community view. Nature genetics 40, 516-522, doi:10.1038/ng.147 (2008).

133     Ellinger-Ziegelbauer, H. et al. The enhanced value of combining conventional and "omics" anal-

yses in early assessment of drug-induced hepatobiliary injury. Toxicol Appl Pharmacol 252, 97-111 (2011).

134 Steiner, G. et al. Discriminating different classes of toxicants by transcript profiling. Environ Health Perspect 112, 1236-1248 (2004).

135 van Ravenzwaay, B. et al. The use of metabolomics for the discovery of new biomarkers of effect. Toxicol Lett 172, 21-28, doi:S0378-4274(07)00159-2 [pii]10.1016/j.toxlet.2007.05.021 (2007).

136 Boitier, E. et al. A comparative integrated transcript analysis and functional characterization of differential mechanisms for induction of liver hypertrophy in the rat. Toxicol Appl Pharmacol 252, 85-96 (2011).

137 Suter, L. et al. EU framework 6 project: predictive toxicology (PredTox)--overview and outcome. Toxicol Appl Pharmacol 252, 73-84 (2011).

138 Edgar, R., Domrachev, M. & Lash, A. E. Gene Expression Omnibus: NCBI gene expression and hybridization array data repository. Nucleic Acids Res 30, 207-210 (2002).

139 Brazma, A. et al. ArrayExpress--a public repository for microarray gene expression data at the EBI. Nucleic Acids Res 31, 68-71 (2003).

140 Mattingly, C. J., Rosenstein, M. C., Colby, G. T., Forrest, J. N., Jr. & Boyer, J. L. The Comparative Toxicogenomics Database (CTD): a resource for comparative toxicological studies. Journal of experimental zoology. Part A, Comparative experimental biology 305, 689-692, doi:10.1002/jez.a.307 (2006).

141 Hayes, K. R. et al. EDGE: a centralized resource for the comparison, analysis, and distribution of toxicogenomic information. Molecular pharmacology 67, 1360-1368, doi:10.1124/mol.104.009175 (2005).

142 Kiyosawa, N., Manabe, S., Yamoto, T. & Sanbuissho, A. Practical application of toxicogenomics for profiling toxicant-induced biological perturbations. International journal of molecular sciences 11, 3397-3412, doi:10.3390/ijms11093397 (2010).

143 Mulrane, L. et al. Creation of a digital slide and tissue microarray resource from a multi-institutional predictive toxicology study in the rat: an initial report from the PredTox group. Experimental and toxicologic pathology : official journal of the Gesellschaft fur Toxikologische Pathologie 60, 235-245, doi:10.1016/j.etp.2007.12.004 (2008).

144 Uehara, T. et al. The Japanese toxicogenomics project: application of toxicogenomics. Molecular nutrition & food research 54, 218-227, doi:10.1002/mnfr.200900169 (2010).

145 Ganter, B., Zidek, N., Hewitt, P. R., Muller, D. & Vladimirova, A. Pathway analysis tools and toxicogenomics reference databases for risk assessment. Pharmacogenomics 9, 35-54, doi:10.2217/14622416.9.1.35 (2008).

146 Kienhuis, A. S. et al. Parallelogram approach using rat-human in vitro and rat in vivo toxicogenomics predicts acetaminophen-induced hepatotoxicity in humans. Toxicol Sci 107, 544-552, doi:10.1093/toxsci/kfn237 (2009).

147 Hart, S. N. et al. A comparison of whole genome gene expression profiles of HepaRG cells and HepG2 cells to primary human hepatocytes and human liver tissues. Drug Metab Dispos 38, 988-994 (2010).

148 Hockley, S. L. et al. Interlaboratory and interplatform comparison of microarray gene expression analysis of HepG2 cells exposed to benzo(a)pyrene. OMICS 13, 115-125 (2009).

149 Lambert, C. B., Spire, C., Claude, N. & Guillouzo, A. Dose- and time-dependent effects of phenobarbital on gene expression profiling in human hepatoma HepaRG cells. Toxicol Appl Pharmacol 234, 345-360 (2009).

150 Dere, E., Lee, A. W., Burgoon, L. D. & Zacharewski, T. R. Differences in TCDD-elicited gene expression profiles in human HepG2, mouse Hepa1c1c7 and rat H4IIE hepatoma cells. BMC Genomics 12, 193, doi:1471-2164-12-193 [pii]10.1186/1471-2164-12-193 (2011).

151 Horiuchi, S. et al. Global gene expression changes including drug metabolism and disposition induced by three-dimensional culture of HepG2 cells-Involvement of microtubules. Biochem Biophys Res Commun 378, 558-562, doi:S0006-291X(08)02282-1 [pii]10.1016/j.bbrc.2008.11.088 (2009).

152 Puigvert, J. C., de Bont, H., van de Water, B. & Danen, E. H. High-throughput live cell imaging of apoptosis. Current protocols in cell biology / editorial board, Juan S. Bonifacino [et al.] Chapter 18, Unit 18 10 11-13, doi:10.1002/0471143030.cb1810s47 (2010).

153 Xu, J. J. et al. Cellular imaging predictions of clinical drug-induced liver injury. Toxicol Sci 105, 97-105, doi:10.1093/toxsci/kfn109 (2008).

# CHAPTER 2

## A 3D *IN VITRO* MODEL OF DIFFERENTIATED HEPG2 CELL SPHEROIDS WITH IMPROVED LIVER-LIKE PROPERTIES FOR REPEATED DOSE HIGH-THROUGHPUT TOXICITY STUDIES

Sreenivasa C. Ramaiahgari[1], Michiel W. den Braver[2], Bram Herpers[1,4], Valeska Terpstra[3], Jan N.M. Commandeur[2], Bob van de Water[1] and Leo S. Price[1,4]

[1]Division of Toxicology, Leiden Academic Centre for Drug Research, Leiden University, Leiden, The Netherlands.

[2]Division of Molecular Toxicology, AIMMS, Vrije University Amsterdam, Amsterdam, The Netherlands.

[3]Department of Pathology, Bronovo hospital, The Hague, The Netherlands.

[4]OcellO B.V. Leiden, The Netherlands.

## ABSTRACT

Immortalized hepatocyte cell lines show only a weak resemblance to primary hepatocytes in terms of gene expression and function, limiting their value in predicting drug induced liver injury. Furthermore, primary hepatocytes cultured on two-dimensional (2D) tissue culture plastic surface rapidly de-differentiate losing their hepatocyte functions and metabolic competence. We have developed a three-dimensional (3D) *in vitro* model using extracellular matrix-based hydrogel for long-term culture of the human hepatoma cell line HepG2. HepG2 cells cultured in this model stop proliferating, self organize and differentiate to form multiple polarized spheroids. These spheroids re-acquire lost hepatocyte functions such as storage of glycogen, transport of bile salts and the formation of structures resembling bile canaliculi. HepG2 spheroids also show increased expression of albumin, urea, xenobiotic transcription factors, phase I and II drug metabolism enzymes and transporters. Consistent with this, cytochrome P450–mediated metabolism is significantly higher in HepG2 spheroids compared to monolayer cultures. This highly differentiated phenotype can be maintained in 384 well microtiter plates for at least 28 days. Toxicity assessment studies with this model showed an increased sensitivity in identifying hepatotoxic compounds with repeated dosing regimens. This simple and robust high throughput-compatible methodology may have potential for use in toxicity screening assays and mechanistic studies and may represent an alternative to animal models for studying drug induced liver injury.

# INTRODUCTION

Drug induced liver injury (DILI) has been a major cause of attrition during drug development [1]. The lack of accurate prediction with animal models and the increasing legislative pressure in implementing 3R's strategy demands an urgent need for robust *in vitro* models in safety assessment. *In vitro* human cell models offer many advantages compared to animal models. However, cells cultured *in vitro* on tissue culture plastic (2D), fail to develop normal tissue architecture, resulting in a poor level of differentiation and loss of tissue-specific functions, limiting their use as alternatives to animal models.

The liver is the principal site for drug metabolism. Liver parenchymal cells or hepatocytes contain the majority of the enzymes required for drug metabolism. Currently human primary hepatocytes are considered as the gold standard for drug metabolism and toxicity studies [2], but the limited availability of human liver samples, short life span, inter-donor differences and cost represent a significant limitation for *in vitro* screening assays [3]. With their unlimited life span, immortalized cell lines - in particular HepG2 cells - are commonly used as an alternative to primary cells [4]. However, in conventional 2D cultures, HepG2 cells express low levels of cytochrome P450 (CYP450) enzymes [5] and the xenobiotic receptors that regulate the expression of drug metabolic enzymes [6, 7]. Since the activity and inducibility of CYP450 enzymes is an important determinant of the pharmacokinetics and toxicity of drugs, poor expression of these and other metabolic enzymes in hepatocyte cell lines is thought to be a key factor in the poor prediction of toxicity in humans.

Hepatocytes are polarized epithelial cells with distinct apical and basolateral domains [8, 9]. The lateral domains of the adjacent hepatocytes form micro-villi-lined bile canaliculi, which collect bile secreted from the hepatocytes [8]. This polarized morphology is lost when cells are restricted to hard plastic surface. Various 3D hepatocyte models have shown a significant improvement in maintaining the morphological and functional characteristics of liver tissue [10-15]. However, these models often require specialized equipment, are costly and/or not compatible with high volume screening. Here we describe a robust high throughput-compatible 3D *in vitro* model using HepG2 cells. HepG2 cells cultured in this model form polarized spheroids with functional bile canaliculi and strongly increased expression of albumin, genes encoding phase I and II drug metabolism enzymes, drug transporters and xenobiotic receptors that mediate induction of CYP450 enzymes. This highly differentiated phenotype can be maintained for more than 28 days in a microtiter plate allowing repeated or sub-chronic drug exposures. A 6-day repeated treatment on 3D HepG2 spheroids showed increased sensitivity in determining cytotoxicity of various hepatotoxic drugs compared to single acute exposures.

Therefore, this 3D HepG2 cell culture model represents a novel, relatively low cost method that is promising for routine high-throughput drug safety assessment containing many features reminiscent of metabolically competent human hepatocytes.

# MATERIALS AND METHODS

### Cell line
Human Hepatoma HepG2 cell line was obtained from American type tissue culture (ATCC, Wesel, Germany), cultured in Dulbecco's modified Eagles medium (DMEM) supplemented with 10% (v/v) fetal bovine serum (Invitrogen, Lot.no. 41F3161K), 25 U/mL penicillin, and 25 µg/mL streptomycin (PSA, Invitrogen).

### 3D cell culture
3D cell culture reagent, Matrigel (Cat.no: 354230; Lot: A6263, 24859, 2306532, 2104930), was obtained from BD Biosciences (Erembodegem, Belgium) and was used to culture liver spheroids. Batches of matrigel vary in the total protein concentration; a stock concentration of 5 mg/ml was prepared and used for culturing spheroids. A CyBi-Selma semi-automatic pipettor was used for liquid handling and dispensing. Cells were incubated at 37°C degrees with 5% $CO_2$ and culture medium was refreshed every 2-3 days. 1000 cells (384 well plate) and 5000 cells (96 well plate) for 3D culture were used for optimal spheroid size. Samples for LC-MS Metabolite analysis, RNA extractions for qPCR, IHC analysis and toxicity assays were performed in 96-well plates. The remaining analyses were performed in 384 well plates.

### Reagents and antibodies
Anti-human albumin (A80-229F, polyclonal), was from Bethyl laboratories Inc (Texas, USA), anti-β1-integrin antibody (MAB1981, monoclonal), was from Millipore (Amsterdam, Netherlands), anti-β-Catenin antibody (610153, monoclonal) and anti-Ezrin antibody (610602, monoclonal) was from BD transduction laboratories (Breda, Netherlands), anti-MRP2 (M2III-6) (AB3373, monoclonal) and anti-Ki-67 (AB15580, polyclonal) antibodies were obtained from Abcam (Cambridge, UK). Goat anti-mouse Alexa-488 (A11001) and anti-rabbit Alexa-488 (A11008) were from Molecular Probes (Breda, Netherlands). Hoechst 33258 from Sigma (Zwijndrecht, Netherlands) (2 µg/ml) was used to visualize the nuclei of fixed cells and Hoechst 33342 (200 ng/mL) from Fisher Scientific (Leiden, The Netherlands) for live cells. Rhodamine phalloidin was obtained from Sigma (Zwijndrecht, Netherlands).

### Albumin and urea measurements
Albumin in cell culture supernatant was measured using human albumin ELISA kit from abcam (ab108788) according to the manufacturer's protocol. Samples were

collected after 72 hours of initial cell seeding from 2D cultures. Changing the culture media every 2-3 days was essential for optimal spheroid growth in 3D cultures and so a 72-hour cumulative albumin secretion was measured at day 3, 7, 14, 21 and 28. Cell number was estimated at each time point using ATPlite reagent (PerkinElmer) and the data normalized to 6x10$^4$ cells. Urea was measured using a colorimetric assay kit from BioVision (California, USA). Cultures were briefly washed with PBS and homogenized with urea assay buffer and analyzed according to manufacturers protocol.

**Histological and immunohistochemical analysis**
HepG2 cell spheroid suspension was collected in PBS and spun at 1000 rpm for 5 minutes. The pellet was fixed in 10% buffered formalin and embedded in paraffin. 3 $\mu$m tissue sections were prepared and stained with haematoxylin and eosin, PAS (Periodic acid-Schiff's reaction) and PAS after treatment with diastase to remove glycogen. Human liver tissue was provided by Bronovo Hospital, The Netherlands, in accordance with the hospital's code of conduct regarding use of patient-derived material. Immunohistochemical detection of cytokeratin 7 and 8 (CAM5.2, 1:20, BD Biosciences, Ref. 345779) and bile canaliculi (polyclonal CEA, 1:200, DAKO, Ref. A0115) was performed using an automated immunostainer (Benchmark ULTRA, Roche Diagnostics).

**RNA extraction and Real time PCR analysis**
Total RNA was extracted using Trizol reagent (Invitrogen) followed by clean up with RNeasy mini kit (Qiagen). 500 ng of RNA was used for cDNA synthesis using Revert aid First strand cDNA synthesis kit (Thermo Scientific) according to the manufacturer's instructions. Real time PCR was performed using SYBR green master mix (Applied Biosystems). mRNA levels of target genes were normalized to housekeeping gene, GAPDH. The list of primer sequences is shown in supplementary table S3.

**Determination of CYP450 enzyme metabolic activity**
2D and 3D cultures were incubated with a mixture of probe substrates, including: diclofenac (CYP2C9, 50 µM), midazolam (CYP3A4, 10 µM), bufuralol (CYP2D6, 20 µM) and chlorzoxazone (CYP2E1, 100 µM).  Cell culture supernatants were collected at 0-, 4-, 24- and 48-h post exposure and stored at -80 degrees. LC-MS analysis of metabolites was performed at Pharmacelsus GmbH (Saarbrucken, Germany). Detailed methodology used is described in supplementary data S4. Diclofenac and chlorzoxazone were obtained from Sigma-Aldrich (Zwijndrecht, Netherlands). Bufuralol HCL was from Corning Gentest (Amsterdam, Netherlands), midazolam was from Actavis (Hafnarfirdi, Iceland).

**Determination of glucuronidation and sulfation activity**

2D and 3D cells were incubated with 500 µM diclofenac and 1 mM acetaminophen to study glucuronidation and sulfation activity. A detailed protocol is in the supplementary data S6.

**Analysis of hepatobiliary transport in HepG2 cells**

Cholyl-lysyl-fluorescein, CLF (BD Biosciences) a synthetic fluorescent bile acid analogue with similar biological activity as cholyl glycine was used to determine the hepatobiliary transport activity. 2D and 3D HepG2 cells were rinsed with 1x Hanks balanced salt solution (Invitrogen, Breda, Netherlands) and incubated with 2 µM CLF in HBSS for 45 minutes similar to the protocol used for primary rat hepatocytes [16]. After the incubation period the cells were washed 3 times with HBSS and imaged live by confocal microscopy (Nikon TiE2000, Nikon). A series of images were collected across the Z-plane of the spheroid and a maximum intensity projection image was generated using the image processing software package, Image J.

**Assessment of drug-induced toxicity**

2D and 3D HepG2 cells were cultured for 24 hours and 21 days respectively prior to compound exposure. Bosentan was obtained from Sequoia Research Products (Pangbourne, UK), all the other compounds were obtained from Sigma-Aldrich (Zwijndrecht, Netherlands). The concentrations of the compounds and solvents used are as shown in the supplementary data S7. A maximum concentration of up to 100X Cmax or above was tested (a reference scaling factor as used in earlier studies with primary hepatocytes [17, 18]). Compounds that are not toxic at 100X Cmax and that are soluble in culture media were tested up to 100 mM (acetaminophen, isoniazid and valproic acid). Cell death was estimated as percentage of viable cells after compound exposure compared to its vehicle control. ATP-lite luminescence assay kit (PerkinElmer) was used to measure cell viability. Measurements were recorded 24-hours after drug exposure. Additionally a repeated drug exposure was performed on 3D cell cultures, by adding the compound every 24 hours for 6 days (at day 22, 23, 24, 25, 26, 27 of spheroid culture) and measuring cell viability on 7th day (day 28 of spheroid culture).

**Statistical analysis**

Data expressed is either representative of 3 independent experiments (mean ± standard deviation (± S.D.) or mean of 3 independent experiments (± S.D.). Graphs were plotted using Graphpad Prism 4 (Graphpad software, San Diego, CA, USA).

# RESULTS

## HepG2 cell proliferation and differentiation in 3D cultures

5000 or 1000 cells in suspension were added on top of a pre-cast gel in 96 or 384-well microplates, respectively. Maintaining this cell number was critical for optimal spheroid size (~100 µm). After seeding, cells settled, adhered to the gel and self-aggregate to form cell clusters (87+/- 16 clusters per well in a 384 microplate) (Supplementary Figure S1). These gradually formed well-defined spheroids over a period of 21 days. The average diameter of the spheroids at day 28 was 118 ± 5 µm (supplem-ementary Figure S1), which is sufficient for oxygen diffusion, as spheroids above 200 µm are known to become hypoxic at the core [19] [20]. To examine the effect of 3D culture on cell proliferation, HepG2 cells were immunostained with antibodies against the proliferation marker Ki-67. The majority of HepG2 cells in 2D
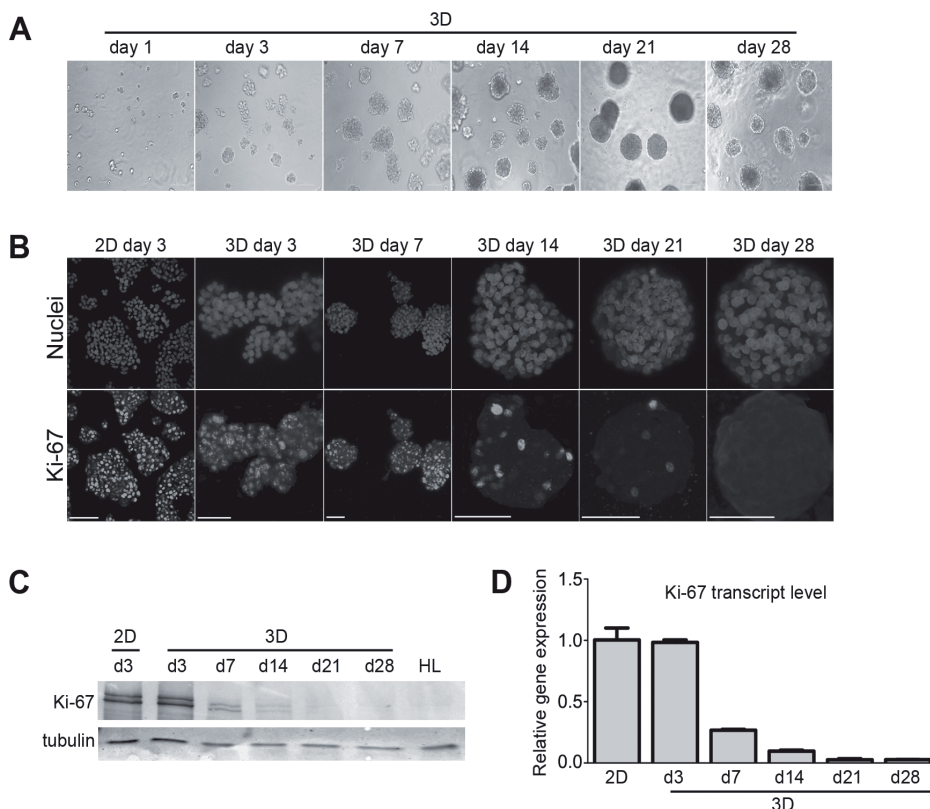


**Figure 1.** *Spheroid development in 3D culture*. Phase contrast images of HepG2 cells cultured in Matrigel (A) scale bar 100 µm. Immunostaining of HepG2 cells for the proliferation marker, Ki-67, counterstained with Hoechst 33358 for nuclei (Blue) (B). Scale bar – 50 µm.  Ki-67 protein level assessed by Western blot analysis; HL= Human Liver (C) and Real time PCR transcript analysis (D), Data is representative of 3 independent experiments.

culture were positive for Ki-67 (Fig. 1B). However, in 3D cultures, there was a sharp decline in Ki-67 positive cells between day 7 and 14, and positive cells were barely present after 21 days. This was confirmed by analyzing the protein and mRNA transcript levels of Ki-67 (Fig. 1C and D). Together, these data demonstrate that HepG2 cells transform from a highly proliferative state in monolayer culture to non-proliferating spheroids after a period in 3D culture.

**HepG2 cells form functionally differentiated spheroids in 3D culture**

Primary hepatocytes cultured as monolayers lose tissue-specific polarity and function and eventually die [21]. Differentiated HepG2 spheroids acquire a uniform size, which remains stable after 21 days. Larger spheroids can show signs of necrosis in the center due to hypoxia [20]. H&E staining of HepG2 spheroids show organized nuclei and cytoplasm and did not show signs of necrosis although the formation of large and multiple cavities was occasionally observed  (Fig. 2B). Since the proliferation of HepG2 cells in 3D culture ceased, we anticipated a probable reprogramming into a more differentiated liver cell phenotype. Positive immunostaining for cytokeratins 7 and 8 at cell-cell junctions in HepG2 spheroids indicate that the cells of the spheroid retain epithelial characteristics (Fig. 2B). To further study the differentiation of the cells in the spheroid we examined the expression of apico-basal surface epithelial markers by immunofluorescent staining. An intense staining of the basal membrane marker, β1 integrin, was seen at the margins of the spheroid where cells contact the extracellular matrix. β-catenin, which is associated with E-cadherin at sites of cell-cell contacts, was localized at lateral junctions. Together, the localization of these two markers indicates that the cells at the periphery of the spheroid establish basal-lateral polarity (Fig. 2A). Finally, we determined the formation of bile canaliculi-like structures by examining the localization of the canalicular marker glycoprotein-1 [22]. HepG2 spheroids showed enhanced punctate staining for this marker between some cells with a similar pattern of immunohistochemical staining to that of human liver (Fig. 2B). We substantiated this with additional immunofluorescent stainings for MRP2 and ezrin (Fig. 2A) that are typically associated in actin rich regions of the bile canaliculi [23, 24]. The localization of these markers was also observed in distinct punctae, which are suggestive of rudimentary canaliculi.

We also investigated the metabolic differentiation by evaluating the glycogen storage capacity, a typical function of liver hepatocytes. 3D spheroids showed the presence of intracellular glycogen as determined by periodic acid-Schiff (PAS) staining. As a control, spheroids were also treated with diastase to digest the glycogen, which resulted in decreased intracellular PAS staining confirming the presence of glycogen in 3D HepG2 spheroids (Fig. 2B).

Cell polarity and ECM signaling have been shown to promote liver-specific
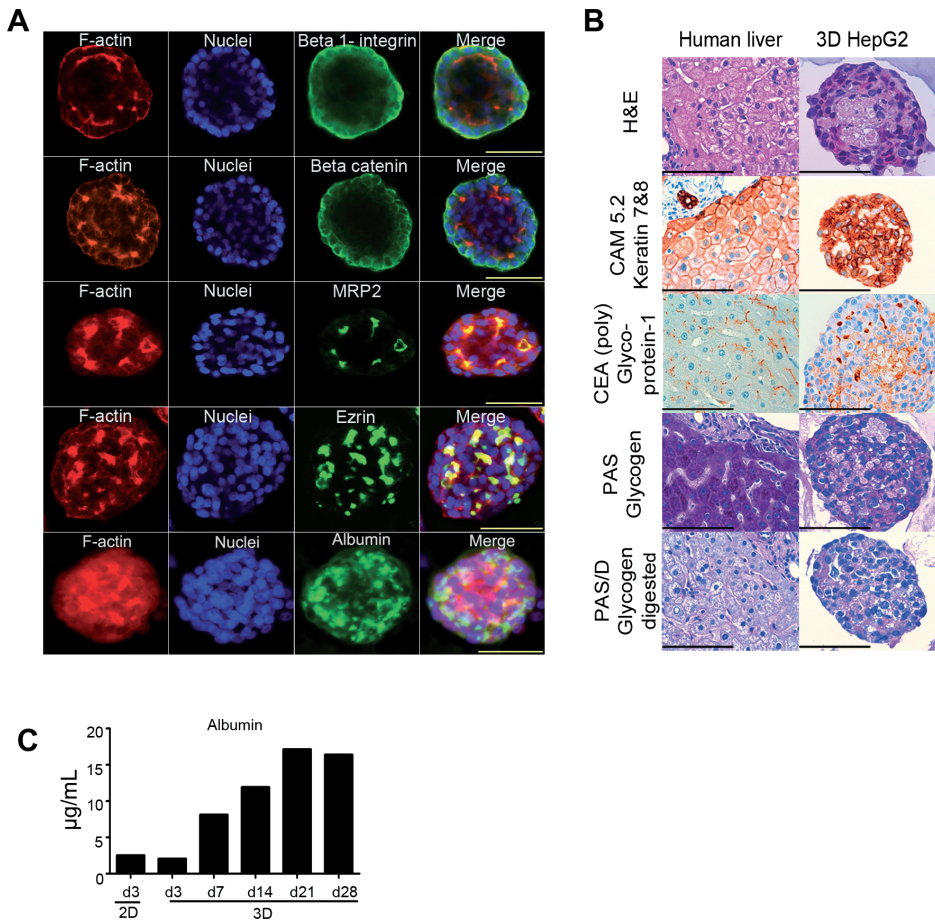
**Figure 2**. *3D HepG2 spheroids show increased expression of markers of differentiated and polarized hepatocytes.* Immunofluorescence staining of 3D HepG2 spheroids with epithelial cell markers β1-integrin, β-catenin, MRP2, ezrin and albumin counterstained with Rhodamine-phalloidin for F-actin and Hoechst 33358 for nuclei (A), scale bars - 50 μm. Histological examination of human liver and HepG2 spheroids (B) scale bars - 100 μm. Albumin production in 2D and 3D HepG2 cells in 72 hours (C) data normalized to 6X104 cells (n=2).

functions such as albumin secretion and metabolic enzyme expression [25]. Immunostaining of HepG2 spheroids showed the presence of albumin (Fig 2A). Consistently, mRNA expression levels of albumin were 10± 4 fold higher in differentiated 3D HepG2 cultures compared to 2D cultures (Fig. 3B). Albumin protein level was approximately 16 μg/mL at day 21 and day 28 (Fig. 2C). Urea production was also found to be higher in spheroids (Supplementary S2). Taken together, these data suggest that HepG2 cells undergo structural and metabolic differentiation in 3D ECM hydrogels.
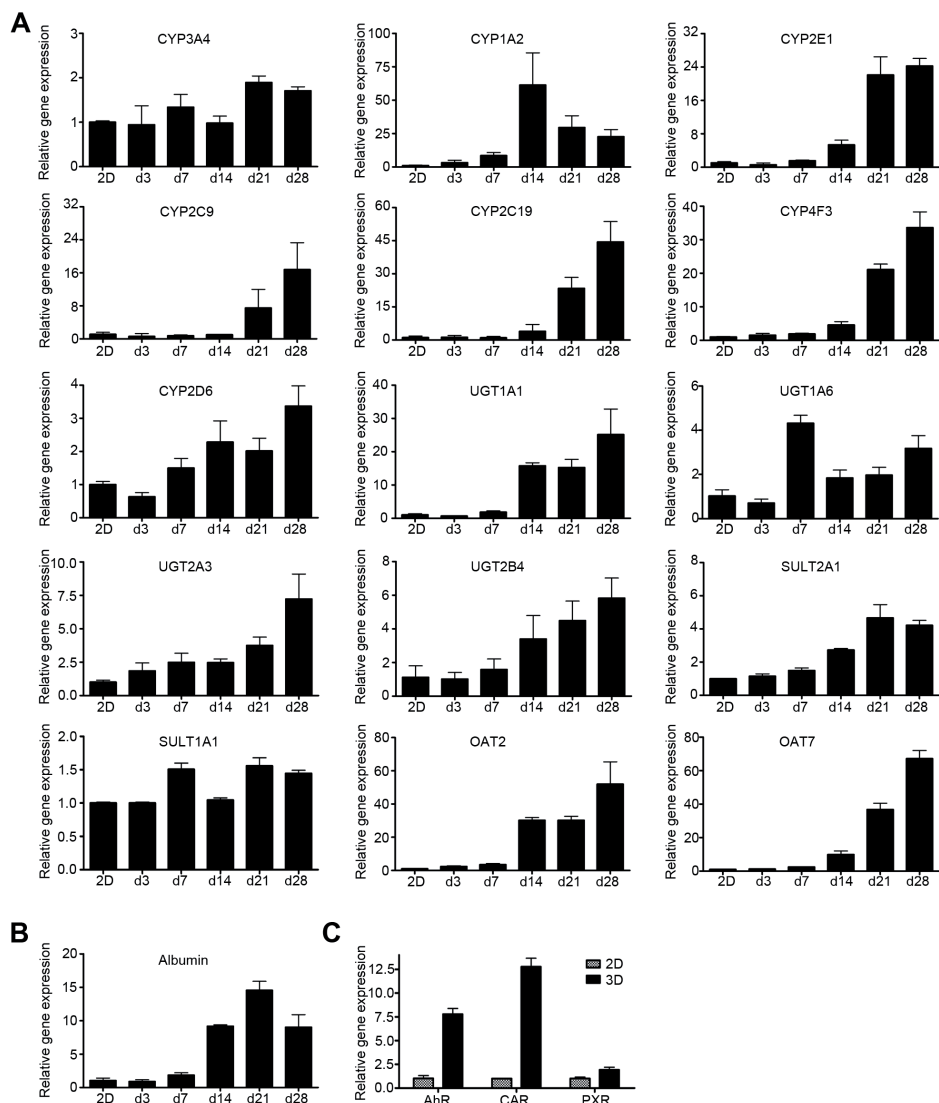
**Figure 3**. *Real-time PCR analysis of liver-specific markers and metabolic enzymes in 2D and 3D culture.* Fold-change gene expression levels of 3D spheroids at day 3 (d3), day 7 (d7), day 14 (d14), day 21 (d21) and day 28 (d28) compared to 3-day cultured 2D HepG2 cells (2D) (A). Data are representative of 4 individual experiments. Real time PCR analysis of Albumin (B); and nuclear receptors AhR, CAR and PXR in 3D cell cultures (C) compared to 2D cultures. Data normalized to GAPDH, representative of 3 independent experiments.

## Metabolic competence is enhanced in 3D-cultured HepG2 spheroids

Low levels of drug metabolism enzymes in HepG2 cells contribute to mis-classification of chemical entities that form toxic metabolites [5]. Real time PCR analysis showed higher expression of various phase I and II metabolizing enzymes and drug

transporters in 3D HepG2 spheroids compared to 2D cultures (Fig. 3A). mRNA transcript levels of phase I xenobiotic metabolic enzymes CYP3A4, CYP1A2, CYP2E1, CYP2C9, CYP2C19, CYP4F3 and CYP2D6 were systematically analyzed over a period of 28 days of spheroid development. Expression levels increased, with a tendency to stabilize after day 14, which coincided with reduced cell proliferation and expression of differentiation markers (Fig. 2). Similarly, the mRNA levels of several phase II xenobiotic metabolizing enzymes UGT1A1, UGT1A6, UGT1A3, UGT2B4, SULT2A1 also increased during 3D culture. Phase III enzyme drug transporters also play a major role in the formation of metabolites and in drug detoxification. The expression levels of OAT2 and OAT7, which represent major transporters of various clinically relevant drug classes [26, 27], were highly increased in spheroids compared to 2D culture.

To evaluate whether increased mRNA levels of metabolic enzymes correlated with an increased functional metabolism, we compared the ability of 2D and 3D cultured HepG2 cells to metabolize CYP450 specific substrates. Rate of formation of 4'-hydroxydiclofenac catalyzed by CYP2C9 was profoundly higher in 3D spheroid cultures and this metabolite was not seen in 2D cultured HepG2 cells (Fig. 4). Day 21 and day 28 spheroid cultures had similar metabolic activity which further substantiates a stable differentiated phenotype after 21-days in 3D culture. Similarly, 1'-hydroxymidazolam, a metabolite of the major CYP450 enzyme, CYP3A4, was approximately 15, 30 and 40 nM at T= 4, 24 and 48, whereas in 2D cells the metabolite reached a maximum of 6 nM at 48 hours. 1'-hydroxybufuralol, a metabolite of bufuralol mediated by CYP2D6, was significantly higher in 3D spheroid cultures (10 nM (4h), 30 nM (24h) and 60 nM (48h) respectively), compared to 2D cultures (3 nM (4h), 10 nM (24h) and 20 nM (48h)). 6'-hydroxychlorzoxazone formation, which is mediated by CYP2E1, was seen in 2D HepG2 cultures but no profound metabolism was observed in 3D spheroids for the concentration used (Fig 4). This was unexpected, since CYP2E1 mRNA was approximately 20-fold higher in 3D compared to 2D cultures. Further investigation is required to determine whether the metabolite is not generated or whether the compound has an affinity to bind to the hydrogel in our 3D model.

Additionally, phase I enzyme activity was assessed by studying the metabolism of testosterone. Testosterone undergoes oxidative metabolism by various CYP450 enzymes, forming several metabolites [28]. The formation of metabolites increased in HepG2 spheroids compared to 2D culture. These include a major metabolite, androstenedione (Supplementary S5) consistent with previous observations [29]. In addition, a small quantity of 6β-hydroxy-testosterone was observed which was significantly increased in spheroids and 1β-hydroxy-testosterone which was detected only in 3D cell cultures but below the detection threshold level in 2D HepG2

**Figure 4.** *Comparison of Phase I enzyme activity in 2D and 3D culture.* CYP450 enzyme activity as measured by rate of formation of OH-diclofenac (CYP2C9), OH-midazolam (CYP3A4), OH-bufuralol (CYP2D6), OH-chlorzoxazone (CYP2E1). Data is represented as mean of three independent experiments ± SD; (n=3), minimum detection level for Diclofenac is 2 nM and Chlorzoxazone is 25 nM.
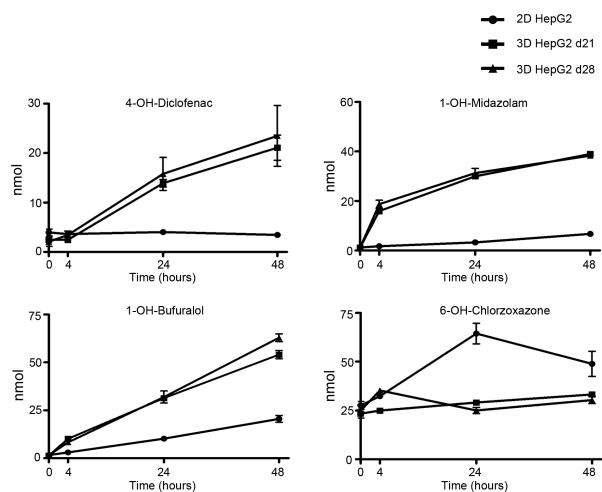


**Figure 5.** *Comparison of Phase II enzyme activity in 2D and 3D culture.* Rate of formation of acyl glucuronides from diclofenac and sulfation activity of acetaminophen in 2D HepG2 cells and 3D day 28 spheroid cultures. Data is representative of two independent experiments.
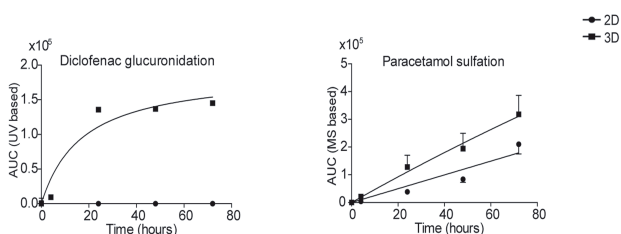


cell cultures (Supplementary S5 D&E). An unidentified hydroxy-metabolite was also observed only in 3D HepG2 cell cultures, although the level was too low for detailed quantification (data not shown).

Phase II metabolism was investigated using diclofenac (glucuronidation) and acetaminophen (sulfation) as probe substrates. The rate of diclofenac glucuronidation was significantly upregulated in 3D HepG2 cultures. The data shown in Fig. 5 was based on the sum of four different acyl glucuronides as described previously [30]. In contrast, there was only a limited difference in acetaminophen sulfation between 2D and 3D cultures (Fig. 5), which was consistent with the expression level of of SULT1A1 mRNA (Fig. 3A), which is involved in sulfation of acetaminophen. The same trends for phase II metabolism (glucuronidation and sulfation) were obtained when 7-hydroxy coumarin was used as substrate (data not shown).

Together, these data indicate that the differentiation of HepG2 cell spheroids is associated with an increased expression of numerous phase I, II and III enzymes

**Figure 6.** *Functional analysis of bile acid transport in 3D HepG2 spheroids.* Cholyl-lysyl-fluorescein (CLF) accumulation in 2D and 3D HepG2 cells (A) scale bars - 100 µm. mRNA transcript level of OATP1B3 in 3D compared to 2D culture (B). mRNA transcript level of OATP1B3 in 3D cell cultures after rifampin treatment (C); data normalized to GAPDH, representative of three independent experiments.
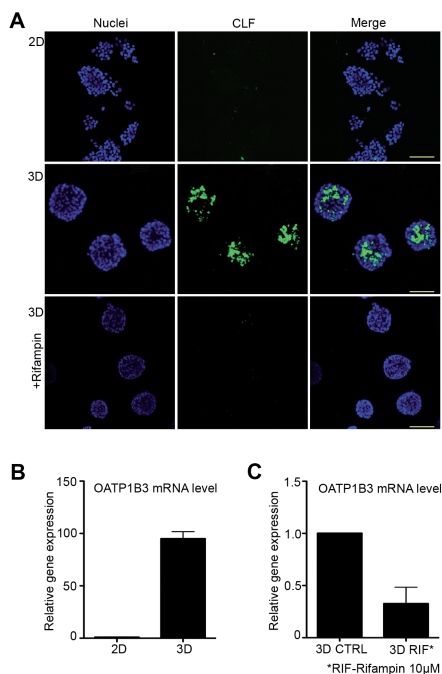
that critically determine ADME of xenobiotics. This functionally correlates with an increased xenobiotic metabolic competence.

## Basal level expression of xenobiotic nuclear receptors in HepG2 cells

Various compounds induce ADME related genes by receptor-mediated mechanisms, resulting in drug-drug interactions that affect the pharmacokinetic and pharmacodynamic properties of a second administered drug [31]. We therefore examined the basal expression level of nuclear receptors AhR, CAR and PXR by real time PCR. These were found to be expressed 7.7-, 12.7-, and 1.9- fold higher respectively in HepG2 spheroids compared to 2D HepG2 cultures (Fig. 3C), suggesting that our spheroid system may be more responsive to the inducers of these receptors.

## Functional bile canaliculi are formed in HepG2 spheroids

Bile salts are transported by hepatocytes into the bile canaliculi. Perturbation of this process is often associated with drug-induced liver injury. To evaluate bile transport, we used a synthetic bile acid analogue, cholyl-lysyl-fluorescein (CLF). CLF accumulated in canaliculi structures of 3D HepG2 spheroids, suggesting that these indeed represent rudimentary canaliculi (Fig. 6A). In contrast, there was no detectable accumulation of CLF in 2D HepG2 cultures. Uptake of CLF into hepatocytes in human liver is mediated by transporter OATP1B3 [32] and excreted into canaliculi via transporters including MRP2 [32]. Immuno-staining of MRP2 on HepG2 spheroids clearly
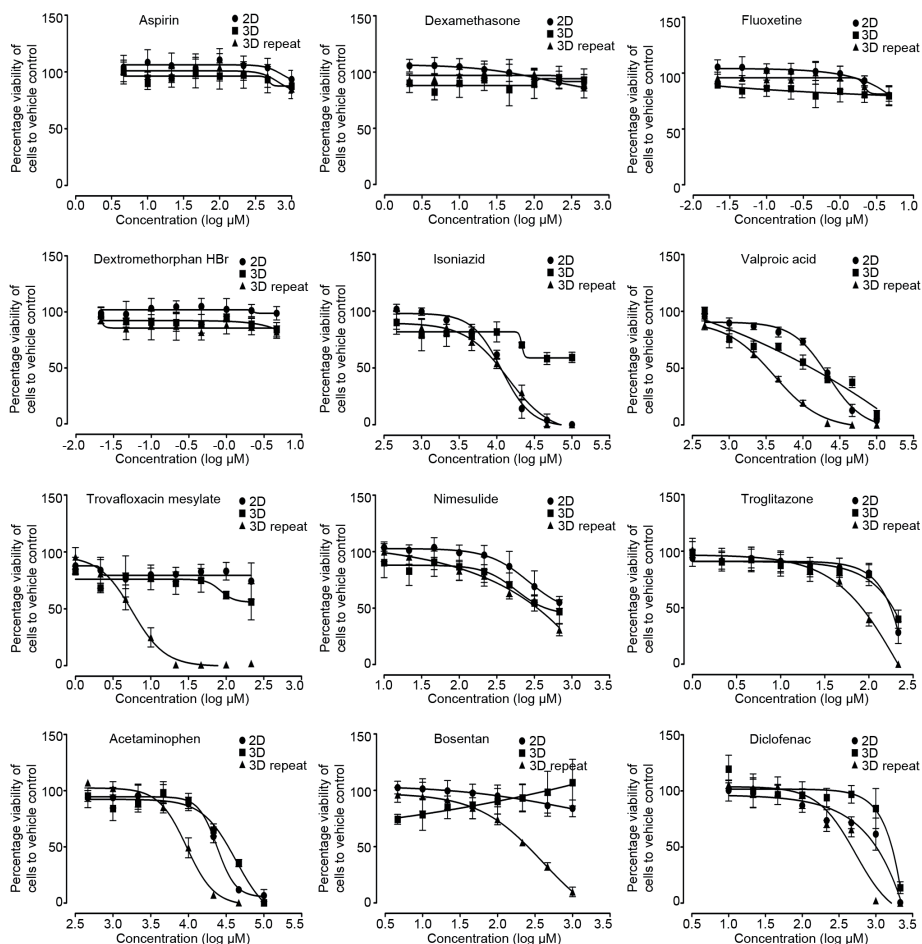
**Figure 7.** *Drug induced cytotoxicity in 2D and 3D HepG2 cells*. ATP content of 2D HepG2 (*filled circle*), 3D HepG2 (*filled square*) after 24 hour drug exposure and 3D HepG2 6-day repeated drug exposure (*filled triangle*) to non-hepatotoxic compounds, ATP-lite assay was performed to measure the cell viability and assess cytotoxicity. Data is mean of 3 independent experiments (±SD).

shows its presence in the apical regions (Fig. 2A). The mRNA level of OATP1B3 was found to be 95–fold higher in HepG2 spheroids compared HepG2 monolayer cultures (Fig. 6B). Inhibition of OATP1B3 with rifampin [25, 33] inhibited the transport of CLF into the bile canicular regions (Fig. 6A). Consistent with this, mRNA level of OATP1B3 was also significantly downregulated after 24-hour treatment with rifampin (Fig. 6C). These results suggest that HepG2 spheroids are able to take up bile salts and actively transport them into canicular structures via known drug transporters.

## Assessment of drug-induced toxicity

In addition to impaired drug metabolism, the scope for chronic drug exposure is restricted in monolayer cultures due to the high rate of proliferation. We evaluated whether our HepG2 spheroid model could overcome these limitations by determining the cytotoxicity of several hepatotoxicants that require bio-activation and typically demonstrate liver injury after repeated dosing. Four compounds that were non-hepatotoxic in previous studies (aspirin, dexamethasone, fluoxetine and dextromethorphan) [17, 18] were similarly not toxic in 2D and 3D HepG2 cell cultures. In contrast, sensitivity to most hepatotoxic compounds was considerably increased with repeated drug exposures in 3D spheroids (Fig. 7). The TC50 of trovafloxacin mesylate, a drug withdrawn from the market, was near to the peak human plasma concentration (Cmax = 4.078 µM; TC50 after repeated dose in 3D is 5.6 µM), whereas in 2D, this compound was not toxic up to 100X Cmax. For most other hepatotoxic compounds, the TC50 was less than or close to 100X Cmax (see supplementary table S7). In conclusion, our 3D spheroid system can report cytotoxicity of known hepatotoxicants, where 2D HepG2 model systems often fail.

# DISCUSSION

One of the major drawbacks with current drug safety evaluation studies is the failure of *in vitro* test models to adequately reflect hepatotoxic responses in humans. Here we present an ECM hydrogel–based 3D cell culture model using HepG2 cells for hepatotoxic studies. This system involves the re-programming of otherwise dedifferentiated HepG2 cells to acquire critical lost functions of *in vivo* hepatocytes including formation of bile canaliculi-like structures, bile acid transport, improved drug metabolism, transporter activity and sensitivity to hepatotoxicants. The compatibility with standard assay plates and automation equipment makes this approach suitable for high-throughput toxicity screening.

HepG2 spheroids in this model differentiate and show many phenotypic characteristics of hepatocytes *in vivo*, such as reduced proliferation, localization of apical and basal-lateral markers and markers for canaliculi. Reduced proliferation may be a result of contact inhibition of growth driven by increased cell-cell interactions. Formation of bile canaliculi was reported earlier in sandwich cultured human and primary rat hepatocytes cultures [21, 34, 35]. Bile-canalicular structures were also observed in hanging drop cultures of HepG2 cells [36, 37]. Recently a 3D peptide nanofiber matrix was also shown to induce a spheroid phenotype and bile canaliculi formation with HepG2 cells, although these spheroids comprised fewer cells and did not result in up-regulation of metabolizing enzymes [38]. In contrast, we found that micro-environmental cues drive both structural organization of canaliculi and the expression and function of drug metabolizing enzymes and transporters.

47

The accumulation of the CLF in HepG2 spheroids resembled accumulation in primary rat hepatocytes cultured on a micro-patterned 3D-collagen gel [16]. Importantly, a pronounced increase in OATP1B3 expression was observed in HepG2 spheroids compared to 2D culture. Inhibition of OATP1B3 by rifampin inhibited CLF accumulation in spheroids, indicating the central role of OATP1B3 in bile acid transport in our system. OATP1B3 plays an important role in hepatic uptake of drugs and various endogenous substrates [39]. Current EMA and FDA guidelines require new chemical entities to be tested for their effects on OATP1B3 (EMA 21 June 2012; FDA Feb 2012) therefore, this HepG2 spheroid model may be suitable for evaluating effects on OATP1B3 activity and bile salt transport.

Induction of CYP450 enzymes is a complex phenomenon mediated by activation of nuclear receptors and gene transcription. It was reported that the low levels of CYP450 enzymes in HepG2 cells is due to the absence of nuclear receptors that regulate their induction [6, 7]. In HepG2 spheroid cultures, the basal levels of nuclear receptors aryl hydrocarbon receptor (AhR), constitutive androstane receptor (CAR) and pregnane X receptor (PXR) were higher compared to monolayer culture. CAR and PXR are regarded as master regulators in drug metabolism [40, 41]. The increased expression of xenobiotic receptors in the spheroid model may make it suitable to study drug-drug interactions mediated by CYP450 enzymes.

Many compounds induce toxicity due to their reactive intermediates [31]. We observed increased functional activity of several important CYP450 enzymes, such as CYP3A4, 2C9 and 2D6 which are involved in metabolism of approximately 80% of marketed drugs [42]. This increased metabolic competence may improve the predictive power of 3D cytotoxic assays. Current in vitro models have limitations for repeated drug exposures studies, which may often be required to accurately reflect drug metabolism in humans. Repeat exposures of HepG2 spheroids resulted in increased sensitivity to DILI compounds compared to a 24 h cytotoxic assessment. Out of 8 hepatotoxic compounds tested, six showed increased sensitivity to repeated drug exposures in 3D cultures. The TC50 of acetaminophen, which is metabolized by CYP2E1 and CYP1A2 was 9.4 mM in 3D repeated exposures, (which is below its 100X Cmax, a scaling factor that represented a reasonable cut-off to differentiate toxic drugs in a study using primary human hepatocytes [17]), whereas for single exposure in 2D cultures, the TC50 was approximately 24 mM. The increased sensitivity with repeated exposures might indicate a mechanistic toxic response over time with DILI compounds. Bosentan, which is metabolized by CYP2C9 and CYP3A4, is known to impair bile acid transport leading to liver toxicity [43]. The TC50 of bosentan in repeat dosing was 400 µM. Although many fold higher than the Cmax (Cmax: 1 µM) no toxicity was observed in 24 h exposures of 2D and 3D cultures. Valproic acid undergoes biotransformation via glucuronidation and CYP2C9, 2A6, 2B6 [44,

45] and liver toxicity is characterized by microvesicular steatosis [46]. The TC50 of valproic acid in 3D repeated exposures was 4 mM, whereas in 2D culture it was ~22 mM. Further development and validation of the 3D spheroid assay may enable its use for prediction of cholestasis and steatosis.

3D spheroids were also sensitive in identifying toxicity induced by the withdrawn drugs, troglitazone and trovafloxacin mesylate. Troglitazone, which is mainly metabolized by CYP3A4, is toxic in our model with a TC50 of 100 µM (15X Cmax). Trovafloxacin mesylate had a TC50 of 5.6 µM, which was close to the human therapeutic Cmax  (~4 µM) whereas single exposures were not toxic below 100 µM, demonstrating the significant effect of repeated exposure on sensitivity. Trovafloxacin is primarily metabolized in liver by phase II metabolism (glucuronidation 13.2%, N-acetylation 10.4% and N-sulphoconjugation 4.1% [47]. The increased sensitivity in 3D compared to 2D may be due to the enhanced phase II activity in HepG2 spheroids. Immune mediators, such as TNFα play an important role in sensitization to trovafloxacin-induced hepatotoxicity [48] under conditions of inflammatory stress. Further studies are needed to establish whether the increased sensitivity of HepG2 spheroids involves autocrine signaling by immune mediators or whether the mechanism of toxicity in vitro differs from the mechanism of toxicity *in vivo*.  Interestingly, troglitazone was not toxic in HepaRG spheroids [13], whereas toxicity was donor dependent for troglitazone and valproic acid in human primary hepatocytes [18], highlighting the differential sensitivities of different *in vitro* models.

In summary, our findings suggest that the culture of HepG2 cells as spheroids on extracellular matrix-rich hydrogels improves their overall suitability for safety assessment studies. Further validation of this model with a large set of compounds is required to assess its potential use in preclinical safety studies. Development of this model by incorporating co-cultures with other hepatic cells (Kupffer cells, stellate cells) may further improve liver characteristics and prediction of drug toxicity in humans.
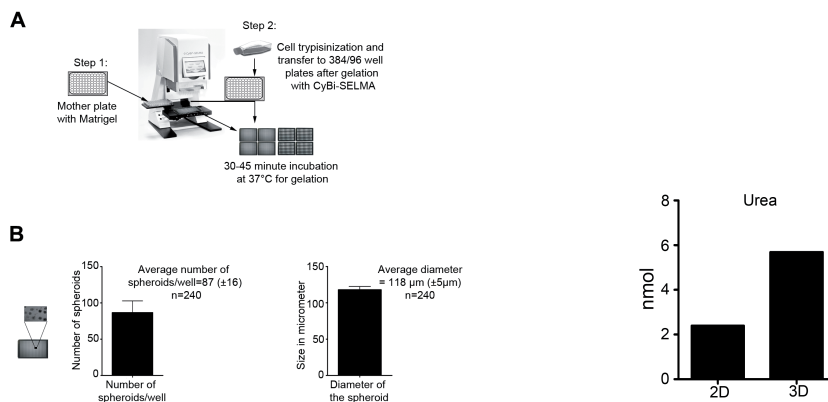
# REFERENCES

1       MacDonald, J. S. & Robertson, R. T. Toxicity testing in the 21st century: a view from the phar-maceutical industry. Toxicol Sci 110, 40-46, doi:10.1093/toxsci/kfp088 (2009).

2       LeCluyse, E. L. Human hepatocyte culture systems for the in vitro evaluation of cytochrome P450 expression and regulation. European journal of pharmaceutical sciences : official journal of the European Federation for Pharmaceutical Sciences 13, 343-368 (2001).

3       Madan, A. et al. Effects of prototypical microsomal enzyme inducers on cytochrome P450 ex-pression in cultured human hepatocytes. Drug metabolism and disposition: the biological fate of chemicals 31, 421-431 (2003).

4       Guo, L. et al. Similarities and differences in the expression of drug-metabolizing enzymes be-tween human hepatic cell lines and primary human hepatocytes. Drug metabolism and dispo-sition: the biological fate of chemicals 39, 528-538, doi:10.1124/dmd.110.035873 (2011).

5       Wilkening, S., Stahl, F. & Bader, A. Comparison of primary human hepatocytes and hepatoma cell line Hepg2 with regard to their biotransformation properties. Drug metabolism and disposi-tion: the biological fate of chemicals 31, 1035-1042, doi:10.1124/dmd.31.8.1035 (2003).

6       Naspinski, C. et al. Pregnane X receptor protects HepG2 cells from BaP-induced DNA damage. Toxicological sciences : an official journal of the Society of Toxicology 104, 67-73, doi:10.1093/toxsci/kfn058 (2008).

7       Kanno, Y. & Inouye, Y. A consecutive three alanine residue insertion mutant of human CAR: a novel CAR ligand screening system in HepG2 cells. The Journal of toxicological sciences 35, 515-525 (2010).

8       Haouzi, D. et al. Three-dimensional polarization sensitizes hepatocytes to Fas/CD95 apoptotic signalling. Journal of cell science 118, 2763-2773, doi:10.1242/jcs.02403 (2005).

9       LeCluyse, E. L., Witek, R. P., Andersen, M. E. & Powers, M. J. Organotypic liver culture models: meeting current challenges in toxicity testing. Critical reviews in toxicology 42, 501-548, doi:10.3109/10408444.2012.682115 (2012).

10      Zhang, F., Xu, R. & Zhao, M.-j. QSG-7701 human hepatocytes form polarized acini in three-di-mensional culture. Journal of cellular biochemistry 110, 1175-1186, doi:10.1002/jcb.22632 (2010).

11      Fey, S. J. & Wrzesinski, K. Determination of drug toxicity using 3D spheroids constructed from an immortal human hepatocyte cell line. Toxicol Sci 127, 403-411, doi:10.1093/toxsci/kfs122 (2012).

12      Nakamura, K. et al. Evaluation of drug toxicity with hepatocytes cultured in a micro-space cell culture system. Journal of bioscience and bioengineering 111, 78-84, doi:10.1016/j.jbiosc.2010.08.008 (2011).

13      Gunness, P. et al. 3D organotypic cultures of human HepaRG cells: a tool for in vitro toxicity studies. Toxicol Sci 133, 67-78, doi:10.1093/toxsci/kft021 (2013).

14      Tostoes, R. M. et al. Human liver cell spheroids in extended perfusion bioreactor culture for repeated-dose drug testing. Hepatology 55, 1227-1236, doi:10.1002/hep.24760 (2012).

15      Godoy, P. et al. Recent advances in 2D and 3D in vitro systems using primary hepatocytes, alternative hepatocyte sources and non-parenchymal liver cells and their use in investigat-ing mechanisms of hepatotoxicity, cell signaling and ADME. Arch Toxicol 87, 1315-1530, doi:10.1007/s00204-013-1078-5 (2013).

16      Matsui, H., Takeuchi, S., Osada, T., Fujii, T. & Sakai, Y. Enhanced bile canaliculi formation en-abling direct recovery of biliary metabolites of hepatocytes in 3D collagen gel microcavities. Lab on a chip 12, 1857-1864, doi:10.1039/c2lc40046d (2012).

17      Xu, J. J. et al. Cellular imaging predictions of clinical drug-induced liver injury. Toxicol Sci 105, 97-105, doi:10.1093/toxsci/kfn109 (2008).

18      Khetani, S. R. et al. Use of micropatterned cocultures to detect compounds that cause drug-in-duced liver injury in humans. Toxicol Sci 132, 107-117, doi:10.1093/toxsci/kfs326 (2013).

19      Asthana, A. & Kisaalita, W. S. Microtissue size and hypoxia in HTS with 3D cultures. Drug Dis-cov Today 17, 810-817, doi:10.1016/j.drudis.2012.03.004 (2012).

20      Hirschhaeuser, F. et al. Multicellular tumor spheroids: an underestimated tool is catching up again. J Biotechnol 148, 3-15, doi:10.1016/j.jbiotec.2010.01.012 (2010).

21      LeCluyse, E. L., Audus, K. L. & Hochman, J. H. Formation of extensive canalicular networks by rat hepatocytes cultured in collagen-sandwich configuration. Am J Physiol 266, C1764-1774

(1994).

22      Bahrami, A., Truong, L. D. & Ro, J. Y. Undifferentiated tumor: true identity by immunohisto-chemistry. Archives of pathology & laboratory medicine 132, 326-348, doi:10.1043/1543-2165(2008)132[326:UTTIBI]2.0.CO;2 (2008).

23      Wang, L. & Boyer, J. L. The maintenance and generation of membrane polarity in hepatocytes. Hepatology 39, 892-899, doi:10.1002/hep.20039 (2004).

24      Jedlitschky, G., Hoffmann, U. & Kroemer, H. K. Structure and function of the MRP2 (ABCC2) protein and its role in drug disposition. Expert opinion on drug metabolism & toxicology 2, 351-366, doi:10.1517/17425255.2.3.351 (2006).

25      Ng, S. et al. Improved hepatocyte excretory function by immediate presentation of polarity cues. Tissue engineering 12, 2181-2191, doi:10.1089/ten.2006.12.2181 (2006).

26      Kobayashi, Y. et al. Transport mechanism and substrate specificity of human organic anion transporter 2 (hOat2 [SLC22A7]). The Journal of pharmacy and pharmacology 57, 573-578, doi:10.1211/0022357055966 (2005).

27      Sweet, D. H. Organic anion transporter (Slc22a) family members as mediators of toxicity. Toxicol Appl Pharmacol 204, 198-215, doi:10.1016/j.taap.2004.10.016 (2005).

28      Choi, M. H., Skipper, P. L., Wishnok, J. S. & Tannenbaum, S. R. Characterization of testosterone 11 beta-hydroxylation catalyzed by human liver microsomal cytochromes P450. Drug metabolism and disposition: the biological fate of chemicals 33, 714-718, doi:10.1124/dmd.104.003327 (2005).

29      Chen, G. et al. Investigation of testosterone, androstenone, and estradiol metabolism in HepG2 cells and primary culture pig hepatocytes and their effects on 17betaHSD7 gene expression. PLoS One 7, e52255, doi:10.1371/journal.pone.0052255 (2012).

30      Fredriksson, L. et al. Diclofenac inhibits tumor necrosis factor-Œ±-induced nuclear factor-ŒſB activation causing synergistic hepatocyte apoptosis. Hepatology (Baltimore, Md.) 53, 2027-2041, doi:10.1002/hep.24314 (2011).

31      Guengerich, F. P. Cytochrome P450s and other enzymes in drug metabolism and toxicity. The AAPS journal 8, E101-111, doi:10.1208/aapsj080112 (2006).

32      de Waart, D. R. et al. Hepatic transport mechanisms of cholyl-L-lysyl-fluorescein. J Pharmacol Exp Ther 334, 78-86, doi:10.1124/jpet.110.166991 (2010).

33      Vavricka, S. R., Van Montfoort, J., Ha, H. R., Meier, P. J. & Fattinger, K. Interactions of rifamycin SV and rifampicin with organic anion uptake systems of human liver. Hepatology 36, 164-172, doi:10.1053/jhep.2002.34133 (2002).

34      Abe, K., Bridges, A. S. & Brouwer, K. L. Use of sandwich-cultured human hepatocytes to predict biliary clearance of angiotensin II receptor blockers and HMG-CoA reductase inhibitors. Drug metabolism and disposition: the biological fate of chemicals 37, 447-452, doi:10.1124/dmd.108.023465 (2009).

35      Hoffmaster, K. A. et al. P-glycoprotein expression, localization, and function in sandwich-cultured primary rat and human hepatocytes: relevance to the hepatobiliary disposition of a model opioid peptide. Pharm Res 21, 1294-1302 (2004).

36      Mueller, D., Kramer, L., Hoffmann, E., Klein, S. & Noor, F. 3D organotypic HepaRG cultures as in vitro model for acute and repeated dose toxicity studies. Toxicol In Vitro 28, 104-112, doi:10.1016/j.tiv.2013.06.024 (2014).

37      Kelm, J. M., Timmins, N. E., Brown, C. J., Fussenegger, M. & Nielsen, L. K. Method for generation of homogeneous multicellular tumor spheroids applicable to a wide variety of cell types. Biotechnol Bioeng 83, 173-180, doi:10.1002/bit.10655 (2003).

38      Malinen, M. M., Palokangas, H., Yliperttula, M. & Urtti, A. Peptide Nanofiber Hydrogel Induces Formation of Bile Canaliculi Structures in Three-Dimensional Hepatic Cell Culture. Tissue Eng Part A, doi:10.1089/ten.TEA.2012.0046 (2012).

39      van de Steeg, E., van Esch, A., Wagenaar, E., Kenworthy, K. E. & Schinkel, A. H. Influence of human OATP1B1, OATP1B3, and OATP1A2 on the pharmacokinetics of methotrexate and paclitaxel in humanized transgenic mice. Clinical cancer research : an official journal of the American Association for Cancer Research, doi:10.1158/1078-0432.CCR-12-2080 (2012).

40      Kublbeck, J. et al. New in vitro tools to study human constitutive androstane receptor (CAR) biology: discovery and comparison of human CAR inverse agonists. Mol Pharm 8, 2424-2433, doi:10.1021/mp2003658 (2011).

41      di Masi, A., De Marinis, E., Ascenzi, P. & Marino, M. Nuclear receptors CAR and PXR: Mo-

lecular, functional, and biomedical aspects. Mol Aspects Med 30, 297-343, doi:10.1016/j. mam.2009.04.002 (2009).

42  Wienkers, L. C. & Heath, T. G. Predicting in vivo drug interactions from in vitro drug discovery data. Nat Rev Drug Discov 4, 825-833, doi:10.1038/nrd1851 (2005).

43  Fattinger, K. et al. The endothelin antagonist bosentan inhibits the canalicular bile salt export pump: a potential mechanism for hepatic adverse reactions. Clinical pharmacology and therapeutics 69, 223-231, doi:10.1067/mcp.2001.114667 (2001).

44  Tang, W. & Abbott, F. S. Bioactivation of a toxic metabolite of valproic acid, (E)-2-propyl-2,4-pentadienoic acid, via glucuronidation. LC/MS/MS characterization of the GSH-glucuronide diconjugates. Chemical research in toxicology 9, 517-526, doi:10.1021/tx950120y (1996).

45  Kiang, T. K. et al. Contribution of CYP2C9, CYP2A6, and CYP2B6 to valproic acid metabolism in hepatic microsomes from individuals with the CYP2C9*1/*1 genotype. Toxicol Sci 94, 261-271, doi:10.1093/toxsci/kfl096 (2006).

46  Silva, M. F. et al. Valproic acid metabolism and its effects on mitochondrial fatty acid oxidation: a review. Journal of inherited metabolic disease 31, 205-216, doi:10.1007/s10545-008-0841-x (2008).

47  Vincent, J., Teng, R., Dalvie, D. K. & Friedman, H. L. Pharmacokinetics and metabolism of single oral doses of trovafloxacin. American journal of surgery 176, 8S-13S (1998).

48  Beggs, K. M., Fullerton, A. M., Miyakawa, K., Ganey, P. E. & Roth, R. A. Molecular Mechanisms of Hepatocellular Apoptosis Induced by Trovafloxacin-Tumor Necrosis Factor-alpha Interaction. Toxicol Sci 137, 91-101, doi:10.1093/toxsci/kft226 (2014).

49  Guideline on the investigation of drug interactions. European Medicines Agency, 2012 June 21, Available at: http://www.ema.europa.eu/docs/en_GB/document_library/Scientific_guideline/2012/07/WC500129606.pdf) Accessed: 31 Jan 2014.

50  FDA guidance for drug interactions- study design, data analysis, implications for dosing and labeling recommendations, CDER, 2012 Feb. Available at: http://www.fda.gov/downloads/Drugs/GuidanceComplianceRegulatoryInformation/Guidances/ucm292362.pdf Accessed: 31 Jan 2014.

# SUPPLEMENTARY DATA

**A**

Step 1:

Mother plate
with Matrigel

Step 2:

Cell trypisinization and
transfer to 384/96 well
plates after gelation
with CyBi-SELMA

30-45 minute incubation
at 37°C for gelation

**B**

Average number of
spheroids/well=87 (±16)
n=240

Average diameter
= 118 µm (±5µm)
n=240

Number of
spheroids/well

Diameter of
the spheroid

Urea

nmol

2D    3D

**Supplementary S1**. *Schematic representation of 3D HepG2 spheroid culture*. (A) Matrigel was added to the plates using the Cybi-Selma semiautomatic pipettor. A 96-well mother plate was prepared by manually pipetting Matrigel into the wells. Plates were then incubated for 30-45 min at 37°C for gelation before adding the required number of cells. (B) Number and area of spheroids after 28-days in 3D cell cultures.

**Supplementary S2**. *Urea production in 2D and 3D HepG2 cells*. Data normalized to $6 \times 10^4$ cells. Data is representative of 2 independent experiments.

**A**

$\times 10^5$

Androstenedione

Counts

Time (minutes)

**C**

$\times 10^4$

6β    1β

Counts

Time (minutes)

**B**

$\times 10^5$

Androstenedione

AUC (UV based)

Time (hours)

● 2D
■ 3D

**D**

$\times 10^3$

6β-OH testosterone

AUC (UV based)

Time (hours)

**E**

$\times 10^3$

1β-OH testosterone

AUC (UV based)

Time (hours)
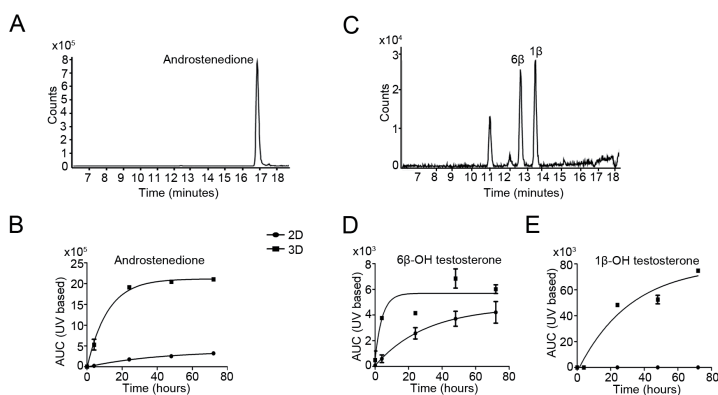
**Supplementary S5**. *Biotransformation of testosterone in 2D and 3D HepG2 cultures*. Extracted ion chromatogram of androstenedione (m/z 287,20) in a 72hr 3D sample (A). Time curves of androstenedione formation after exposure of 2D/3D cell cultures (B). Data is representative of two independent experiments. Extracted ion chromatogram of hydroxylated testosterone (m/z 305, 19) in a 72hr 3D sample (C), Time curves of 1-β and 6β-hydroxy testosterone formation (D and E) after exposure. Quantification is based on UV, and corrected for background. Data is representative of two independent experiments.

| Gene | Forward primer | Reverse primer |
|------|----------------|----------------|
| GAPDH | AGCCACATCGCTCAGACACC | ACCCGTTGACTCCGACCTT |
| CYP3A4[1] | CAGGAGGAAATTGATGCAGTTTT | GTCAAGATACTCCATCTGTAGCACAGT |
| CYP1A2 | GCCTTCATCCTGGAGACCTT | AGCGTTGTGTCCCTTGTTG |
| CYP2E1 | TTCAGCGGTTCATCACCCT | GAGGTATCCTCTGAAAATGGTGTC |
| CYP2C9[2] | ACATCAGCAAATCCTTAACCAATCT | GGGTTTCAGGCCAAAATACAGA |
| CYP2C19 | GTCCAGAGATACATCGACCTCA | AGTGAGGGAAGTTAATATGGTTGTG |
| CYP4F3 | CATCAAGCCTGTGCTCTTTG | CTTTTCACCAGCACTCAGCA |
| CYP2D6[2] | CGCATCCCTAAGGGAACGA | TTCCAGACGGCCTCATCCT |
| UGT1A1[3] | AACTTTCTGTGCGACGTGGTT | GTCACCTCTCTCTGAAGGAATTCTG |
| UGT1A6[3] | AGCCCAGACCCTGTGTCCTA | CCACTCGTTGGGAAAAAGTCA |
| UGT2A3 | GGTCACTGTTTCAAAATGTTACAGAA | TTCCTTTGTACCTCCATAACACC |
| UGT2B4 | CCAAATGTTGAGTTCGTTGG | GCTCTGGACAAACTCTTCCATT |
| SULT2A1 | TGAGAGAGGAGAAAAACTT | TCTTTCCCAGGAATTGAC |
| OAT2 | TAGCTGTCACCCTGCCTTGT | CATGGCCTTGGGTCAGAA |
| OAT7 | GCATCCTAGGCGGTCATTTA | TGGCAACCTGGAGGTAACAC |
| AHR | CAACATCACCTACGCCAGTC | GCTTGGAAGGATTTGACTTGA |
| CAR | CAGGTGACATGCTGCCTAAG | TCAGCTCATCTTCCCTACTGG |
| PXR | GGACGCTCAGATGAAAACCT | AACTCGCAGCCACTGCTAAG |
| Ki67 | CCAAAAGAAAGTCTCTGGT | CCTGATGGTTGAGGCTGTTC |

**Supplementary S3.** Primer sequences used for real-time PCR analysis.

[1] Kikuchi R, McCown M, Olson P, Tateno C, Morikawa Y, Katoh Y, et al. Effect of hepatitis C virus infection on the mRNA expression of drug transporters and cytochrome p450 enzymes in chimeric mice with humanized liver. Drug metabolism and disposition: the biological fate of chemicals 2010;38:1954-1961.
[2] Westerink WMa, Schoonen WGEJ. Cytochrome P450 enzyme levels in HepG2 cells and cryopreserved primary human hepatocytes and their induction in HepG2 cells. Toxicology *in vitro* : an international journal published in association with BIBRA 2007;21:1581-1591.
[3] Westerink WM, Schoonen WG. Phase II enzyme levels in HepG2 cells and cryopreserved primary human hepatocytes and their induction in HepG2 cells. Toxicol *In Vitro* 2007;21:1592-1602.

**Supplementary S4**. Protocol used to analyse phase I metabolites at Pharmacelsus GmBH.

**Compound exposure:**

Substrate mix was exposed to 2D and 3D cells in 96-well plates. Spheroids stop proliferating after day 14 and they have equal cell number between 21-day and 28-days as determined using ATPlite assay. Same amount of cells ($20 \times 10^3$ cells/well) were seeded to 2D plates and after 24 hours substrate mix was added to the cells and samples were collected at 0, 4, 24 and 48 h from a pool of 8 wells of 96-well plate at each time point and the data indicates nmol of metabolite formed/ $1.6 \times 10^5$ cells initial cell density. Samples were stored at -80 degrees and shipped on dry ice to Pharmacelsus GmBH for further analysis as explained below.

**Sample preparation:**

Cell culture supernatants were precipitated with the twofold volume of acetonitrile supplemented with the internal standard (1 $\mu$M griseofulvin), vigorously shaken (10

min) and centrifuged (5,000xg).

**LC-MS conditions:**

The HPLC system consisted of U-HPLC pump and an auto sampler (both by Thermo Fisher Scientific, Dreieich, Germany). Mass spectrometry was performed on a Q-Exactive mass spectrometer (Orbitrap technology, Thermo Fisher Scientific) equipped with a heated electrospray interface (Thermo Fisher Scientific) and connected to a PC running the standard software Xcalibur 2.2. The HPLC pump flow rate was set to 600 $\mu$l/min and the compounds were separated on a Gemini C6-phenyl 3 $\mu$m, 50x2.0 mm analytical column (Phenomenex, Aschaffenburg, Germany) with corresponding precolumn. Analytes were separated by gradient elution with acetonitrile as organic phase (A) and 10 mM ammonium acetate as aqueous phase (B) (% A (t (min), 0(0-0.1)-97(0.4-1.7)-0(1.8–3.0). The mass resolution of the Orbitrap was set to 17,500. Further analyser settings were as follows: max. trap injection time 120 ms, sheath gas 40, aux gas 10, sweep gas 2, capillary voltage 4 kV, capillary temperature 350°C, H-ESI heater temperature 350°C. Full MS selected ion monitoring (SIM) analysis was applied using fast scan-to-scan polarity switching to analyse all metabolites in a single sample run. Target ions for SIM analysis ([M+H]+ or [M-H]-, respectively) were m/z 278.1751 (1-hydroxybufuralol), m/z 342.0804 (1'-hydroxymidazolam) and m/z 353.0786 (griseofulvin, internal standard) in the positive mode and m/z 183.9796 (6-hydroxychlorzoxazone) and m/z 310.0033 (4'-hydroxydiclofenac) in the negative mode. Retention times were 1.07 min (1-hydroxybufuralol), 1.20 min (1'-hydroxymidazolam), 1.10 min (6-hydroxychlorzoxazone), 1.13 min (4'-hydroxydiclofenac) and 1.23 min (griseofulvin).

**Calibration standards and quantification:**

The stock solutions of each metabolite were prepared in acetonitrile/water (1:1, v/v), except for 6-hydroxychlorzoxazone was prepared in acetonitrile and methanol, respectively. A cocktail working solution was prepared containing all metabolites at a concentration of 250 $\mu$M. Calibration samples were generated in cell culture medium to achieve the final concentrations of 5000, 2400, 1200, 400, 100, 25, 6.25, 2.08, 1.04, and 0.52 nM for each metabolite. Calibration curves for each metabolite were represented by the plots of the peak-area ratio (metabolite/internal standard) versus the nominal concentration of the metabolite in cell culture medium. The line of best fit was generated using quadratic regression and weighing as appropriate. Metabolite concentrations in experimental samples were calculated from the resulting area ratio and the regression equation of the calibration curve.

**Supplementary S6.** Protocol used to analyze testosterone metabolism and phase II metabolism (Glucuronidation and sulphation).

**Qualitative and quantitative analysis of phase I (Testosterone) and Phase II (Diclofenac glucuronidation and Paracetamol Sulfation).**

The total number of cells/well in 3D cell culture was measured by ATP-lite assay and an equal number of cells were seeded in 2D culture. 2D and 3D HepG2 cells were incubated with testosterone (500 µM), paracetamol (1mM) and diclofenac (500 µM). Incubations were terminated at 0, 4, 24, 48 and 72 hours by adding perchloric acid (1% v/v) final concentration in case of testosterone, perchloric acid (1%V/V) in 50% v/v acetonitrile for paracetamol and ice cold methanol (50% v/v) for diclofenac.

The samples were centrifuged at 14,000 rpm for 15 minutes. Supernatants were stored at -80°C until analysis. The analytical method used for diclofenac was described previously (1). For paracetamol the same method was used, with the only difference using of a Luna C18 reversed-phase column (150 mm x 4.6mm, 5 µm i.d.) (Phenomenex, Torrance, CA). For testosterone the analysis of metabolites was done using a Shimadzu Prominence HPLC system equipped with a Luna C18 reversed-phase column (150 mm x 4.6mm, 5 µm i.d.) (Phenomenex, Torrance, CA) and a SPD-2A UV/VIS detector (Shimadzu, Kyoto, Japan). The mobile phase for both HPLC and LC-MS/MS analysis (flow rate 0.5 mL/min) consisted of a gradient constructed of 0.1% formic acid in water (solution A) and 0.1% formic acid in methanol (solution B). Testosterone and its metabolites were eluted using an isocratic elution at 50% B for 1 min after sample loading, followed by a linear gradient from 50 to 99% B from 1 to 19 minutes. The final gradient composition was maintained for 1 minute, after which the column was re-equilibrated with the initial gradient composition. Metabolites were quantified by integration of analytes detected at 254 nm. Retention times of analytes were: 6β-hydroxy testosterone at 12.8 min, 1β-hydroxy testosterone at 13.5 min, androstenedione at 16.8 min, testosterone at 18 min.

To identify metabolites by LC-MS, the final time points were pooled and extracted with 3 volumes of dichloromethane. The combined fractions were evaporated to dryness under a stream of nitrogen and reconstituted in 200µL 50% methanol. An Agilent 1200 Series Rapid resolution LC system was connected to a hybrid quadrupole-time-of-flight (Q-TOF) Agilent 6520 mass spectrometer (Agilent Technologies, Waldbronn, Germany), equipped with an electrospray ionization (ESI) source operating in the positive mode. The MS ion source parameters were set with a capillary voltage of 3500 V; nitrogen was used as the desolvation (12L/min) and nebulizing gas (pressure 60 psig) at a constant gas temperature of 350°C. Nitrogen was used as a collision gas with collision energy of 25 V. MS spectra were acquired using automated full scan MS/MS analysis over m/z range of 50–1000 using a scan rate of 1.003 spectra/s. Metabolite identification was established by comparison with refer-

ence compounds. Androstenedione was obtained from Sigma Aldrich (Zwijndrecht, the Netherlands). Hydroxy metabolites of testosterone were identified by comparison with metabolites formed by recombinant CYP3A4 (2).

1. Dragovic S. Boerma JS, Vermeulen NP, Commandeur JN Effect of human glutathione S-transferases on glutathione-dependent inactivation of cytochrome P450-dependent reactive intermediates of diclofenac .Chem Res Toxicol 2013;26:1632-41
2. Krauser JA, Voehler M, Tseng LH, Schefer AB, Godejohann M, Guengerich FP. Testosterone 1 beta-hydroxylation by human cytochrome P450 3A4. Eur J Biochem 2004;271:3962-3969.

**Supplementary S7.** List of compounds used for toxicity assessment.

| | Compound | Solvent | cMax (µM) | 100XCmax (µM) | Concentration range tested (µM) | TC50 (µM) |
|---|---|---|---|---|---|---|
| 1 | Aspirin | DMSO | 5.526 | 552.6 | 4.64 to 1000 | N/A |
| 2 | Dexamethasone | DMSO | 0.224 | 22.4 | 2.15 to 464 | N/A |
| 3 | Fluoxetine | DMSO | 0.049 | 4.9 | 0.0215 to 4.64 | N/A |
| 4 | Dextromethorphan HBr | DMSO | 0.028 | 2.8 | 0.010 to 2.15 | N/A |
| 5 | Isoniazid | Culture media | 76.6 | 7660 | 464 to 100000 | ~14000 |
| 6 | Troglitazone | DMSO | 6.387 | 638.7 | 1 to 215 | ~100 |
| 7 | Acetaminophen | Culture media | 139 | 13900 | 464 to 100000 | ~9400 |
| 8 | Nimesulide | DMSO | 6.5 | 650 | 10 to 2150 | ~1000 |
| 9 | Bosentan | DMSO | 1 | 100 | 4.64 to 1000 | ~400 |
| 10 | Trovafloxacin mesylate | DMSO | 4.078 | 407.8 | 1 to 215 | ~5.6 |
| 11 | Diclofenac | DMSO | 8.023 | 802.3 | 10 to 2150 | ~530 |
| 12 | Valproic acid | Culture media | 30.086 | 3008.6 | 464 to 100000 | ~4000 |

# CHAPTER 3

## 3D CELL CULTURE IMPROVES LIVER-SPECIFIC CHARACTERISTICS OF HEPG2 CELLS: A GENE EXPRESSION ANALYSIS-BASED COMPARISON OF DIFFERENT *IN VITRO* HEPATOCYTE MODELS

Sreenivasa C. Ramaiahgari[1], Maarten Coonen[2,3], John Meerman[1], Danyel Jennen[2,3], Bob van de Water[1], Joost van Delft[2,3] and Leo S. Price[1,4]

[1]Division of Toxicology, Leiden Academic Centre for Drug Research, Leiden University, Leiden, The Netherlands.

[2]Department of Toxicogenomics, Maastricht University, Maastricht, The Netherlands.

[3]Netherlands Toxicogenomics Centre, Maastricht University, Maastricht, The Netherlands.

[4]OcellO B.V Leiden, The Netherlands.

# ABSTRACT

Hepatocytes rapidly de-differentiate when isolated from their natural tissue environment. Three dimensional cell cultures provide physical and chemical cues that improve and preserve the differentiated status of hepatocytes for extended periods. Our recent findings have shown that HepG2 cells differentiate in 3D matrix hydrogels, more closely recapitulating the polarized morphology and functions of *in vivo* hepatocytes compared to conventional monolayer cultures. Here we report the findings from whole genome expression analysis of 2D and 3D HepG2 cell models and also a comparative analysis of these models together with other hepatocyte models including HepaRG and primary human hepatocytes. With increasing duration in 3D culture up to 28 days, HepG2 cells showed coordinated regulation of various signaling pathways associated with cellular differentiation, development, and metabolism reminiscent of *in vivo* hepatocytes. Pathway analysis was used to identify canonical pathways that are differentially changed in HepG2 spheroids in 3D culture during differentiation. Comparative pathway analysis of various *in vitro* models with human liver highlighted the similarities and differences that are inherently associated with specific cell lines. PCA analysis of genes associated with some important biological pathways such as cell cycle regulation and xenobiotic metabolism showed a different expression profile of HepG2 cells in 3D culture than 2D and a similarity with human liver and primary human hepatocytes and/or HepaRG cells. In conclusion, the gene expression of 3D HepG2 spheroids was significantly different from 2D cultures; some important physiological pathways that are absent in monolayer cultures were induced in 3D HepG2 cultures and showed similarity to primary hepatocytes and human liver. Though the expression profile is not similar to current 'gold standard' primary human hepatocytes, the presence of active xenobiotic metabolism pathways, anti-oxidant response pathways and pathways involved in maintaining normal physiology of liver and possibility for a long term culture makes our 3D HepG2 model a powerful tool to detect and understand the mechanisms of drug-induced toxicity.

# INTRODUCTION

Various test models are used for assessing toxicity of new chemical entities, mostly, relying on animal models for short and long-term effects of compounds. With the potential risks in species-specific variation in toxic response with animal studies, human cell models are a preferred choice. But it is a major challenge to maintain the differentiated status of human cells in an *in vitro* culture condition. In the absence of a physiological niche, cells rapidly lose their tissue specific properties leading to poor biological responses and a failure to predict the toxicity of the compounds in humans. Different hepatocyte cell lines have been evaluated for their competence in drug screening assays, but an approved cell model that is efficient in accurately predicting the toxic effects of chemicals is still lacking. Currently, human primary hepatocyte cell lines are considered as gold standards for safety assessment studies but these cells rapidly lose their differentiated status in two-dimensional (2D) monolayer cultures [1].

Cells can be cultured as three-dimensional (3D) tissues using extra cellular matrix hydrogels including collagen, matrigel, peptide nanofiber gels and using hanging drop methods, all of which have shown an improvement in hepatocyte function. Although primary hepatocytes cultured as two-dimensional (2D) monolayer cultures or on a single layer of collagen rapidly lose liver tissue properties, sandwich culturing was shown to improve the maintenance of specialized functions [1]. The limited availability of human primary cells, donor-specific variability and cost, drives a demand for the models that use cell lines that are functionally stable and metabolically competent. HepaRG, a cell line derived from a hepatocarcinoma patient [2] are 'bi-potent' progenitor cells which, when cultured in the presence of DMSO differentiate into biliary and hepatocyte like cells and have drug-metabolizing enzymes similar to primary human hepatocytes [2-4]. However, culture of HepaRG cells in DMSO lead to a 3-4 fold increase in LDH and AST release, reduction in proliferation and decreased hepatic functions [5], which may adversely affect assessment of chemical-induced cytotoxicity. Nonetheless, the drug metabolism enzymes and metabolic capacity were found to be similar to or higher than PHH in HepaRG cells [6, 7].

The other widely used cell line for hepatotoxic studies is HepG2. These cells are also of carcinoma origin but have low levels of cytochrome P450 enzymes compared to primary human hepatocytes [8, 9]. Despite their carcinoma origin, these cells have functionally active p53 and an active Nrf2 system, which is an advantage for cytotoxic studies [10, 11]. A high content screening assay using HepG2 cells, measuring calcium levels, mitochondrial membrane potential, DNA content and plasma membrane potential was shown to be 93% sensitive in identifying DILI com-

pounds [12]. A comparative toxicogenomics profiling of HepaRG and HepG2 for their ability to discriminate genotoxic and non-genotoxic compounds showed that HepG2 could better predict chemical carcinogens [13]. However, the low-levels of CYP450 enzymes and nuclear xenobiotic receptors [14, 15] have been a major drawback for their use in drug safety testing. Our previous studies showed that HepG2 cells cultured in 3D form differentiated polarized spheroids that re-acquire many of the properties of hepatocytes *in vivo* [16]. These specialized functions could be maintained for at least 28 days in 3D culture allowing long-term assessment of toxic effects. Functions such as bile acid transport, glycogen storage were present in 3D HepG2 spheroids and levels of phase I, II and III enzymes were also higher increasing its metabolic competency and the capacity to identify hepatotoxic compounds.

In the present study we analyzed the gene expression profiles of HepG2 cells at different stages of spheroid development and differentiation in 3D culture, comparing these with two-dimensional monolayer HepG2 culture, HepaRG, primary human hepatocytes (PHH) and human liver. We observed that HepG2 spheroids showed upregulation of genes associated with hepatocyte development, differentiation and metabolism, which stabilized after 21 days in 3D culture. Ingenuity Pathway Analysis (IPA) was used to examine changes in the core signaling pathways upon culture in 3D and to compare these with other hepatocyte models. Many functional pathways associated with *in vivo* hepatocytes were significantly enriched in HepG2 spheroids. Cell cycle regulation, xenobiotic metabolism pathways such as PXR/RXR, complement system, bile-acid biosynthesis and coagulation system were significantly upregulated and showed a close similarity to the human liver expression compared to other hepatocyte cells. Overall, the gene expression analysis of 3D spheroids showed robust improvement in the physiological and metabolic profile of HepG2 cells, indicating that this model may represent a powerful *in vitro* tool for studying liver biology.

# MATERIALS AND METHODS

### Cell line and 3D cell culturing
Human hepatoma HepG2 cell line was obtained from American type tissue culture (ATCC, Wesel, Germany), cultured in Dulbecco's modified Eagles medium (DMEM) supplemented with 10% (v/v) fetal bovine serum (Invitrogen, The Netherlands), 25 U/mL penicillin, and 25 $\mu$g/mL streptomycin (PSA, Invitrogen). The cells were cultured at 37°C with 5% CO2. Matrigel (Erembodegem,BD Biosciences) was used to culture 3D spheroids as previously described [16].

### RNA isolation and microarray analysis of 2D and 3D HepG2 cells
RNA was extracted from 3 day cultured 2D HepG2 cells and 3D HepG2 cells cul-

tured at day 3, 7 14, 21 and 28. Total RNA was extracted from 2D/3D cultured cells using Trizol reagent (Invitrogen) followed by clean up using RNeasy mini kit (Qiagen, Hilden, Germany). RNA integrity quality and integrity was determined using the Agilent bioanalyser (Agilent Technologies Inc, Santa Clara, USA). Biotinylated cRNA was prepared using the Affymetrix 3' IVT-Express Labeling Kit (Affymetrix, Santa Clara, USA) and hybridization steps were performed by Service XS B.V (Leiden, The Netherlands) on Affymetrix HT Human Genome U133 plus PM plate. Array plates were scanned using the Affymetrix GeneTitan scanner. BRB Array Tools software (developed by Dr. Richard Simon and BRB-ArrayTools Development Team) was used to normalize the .cel data using the Robust Multichip Average (RMA) method. Differentially expressed genes (p-value < 0.001) between the various experimental conditions were identified with an ANOVA test followed by calculation of the false discovery rate according to Benjamini and Hochber [17]. Classification of the selected genes according to their biological and toxicological functions was performed using the Ingenuity Pathway Analysis IPA® software (Ingenuity Systems, Redwood, USA). Heatmap representations and hierarchical clustering (using Pearson correlation) were performed using the Multi Experiment Viewer software [18].

**Re-annotation, normalization, and data filtering for comparative gene expression profiling**

To compare basal gene expression data from 2D and 3D HepG2 cells with other cell models, different data sources were combined. Raw data files from untreated HepaRG and HepG2 cells were obtained from the department of Toxicogenomics, Maastricht University [13, 19]. Primary cryopreserved human hepatocyte data was downloaded from TG-GATEs [20]; 16 microarrays of untreated conditions were randomly selected from this database. Post-mortem liver data was obtained through GEO, accession numbers GSE13471 and GSE3526 respectively. Raw data files were loaded into R version 2.15.2 for Windows (64-bit) [21], re-annotated to Entrez Gene using Brainarray's custom CDF version 15.1.0 [22]. The R-packages used was obtained from BioConductor version 2.11 [23] Since the combined data set was originating from the Affymetrix Human Genome U133 Plus 2.0 and Affymetrix HT Human Genome U133 plus PM (GeneTitan) platforms, normalization was performed in a multi-step procedure. Data from different chip types were merged based on 18909 overlapping Entrez Gene ID's, followed by scaling of the GeneTitan data and quantile normalization on the merged set.

**Principal component analysis**

Principal Component Analysis (PCA) was applied to identify data patterns and to

highlight data similarity and differences between the treated and untreated cell lines at different time points. Therefore, the normalized intensities of the combined data sets were uploaded into the PCA module of ArrayTrack [24]. PCA analysis was performed on whole genome expression and filtered gene sets of hepatocyte-specific canonical pathways. PCA data were visualized using Tibco Silver Spotfire (Paulo Alto, CA, USA).

**Ingenuity Pathway analysis**

To better understand the biological processes and canonical pathways that changed significantly and to make a comparative overview of gene expression profiles in the different cell models, differentially expressed genes (DEG's) with a p value <0.001 were uploaded onto ingenuity pathway analysis (Ingenuity® systems, www.ingenuity.com).

# RESULTS

**Gene expression profile of HepG2 cells in 3D culture correlates with differentiation of hepatocytes**

When HepG2 cells are cultured in an extracellular matrix (ECM) protein-rich hydrogel that simulates a tissue microenvironment, cells form spheroids and exhibit many features of hepatocytes *in vivo* [16]. A significant change in the gene expression was observed during the 3D culture period with a gradual increase in DEG's (P<0.001, Fold change>1.5) until day 14. Thereafter, the change in gene expression follows a downward trend with a steady gene expression between day 21 and 28 (Fig. 1A). Spheroid development in the 3D culture seems to recapitulate ontogeny of a developing liver. Genes that are associated with the fetal liver CYP3A7, CYP1A1 [25, 26] are highly expressed in the initial culture period until 7 days and their expression was reduced later during the culture (Fig. 2C). Similarly genes that are expressed by adult liver such as Flavin containing monooxygenase 5 (FMO5), haptoglobin (HP) [27, 28] were induced after 7-days in 3D culture and highly expressed from 14–days (Fig. 2C). The terminal hepatocyte differentiation marker glucose-6-phosphate (G6PC) was 150-fold higher after 14 days and 230-fold at both 21 and 28 day cultures, indicating that the differentiation process stabilizes between day 14 and 21 days. Differentiated liver marker genes albumin, transferrin, fibronectin, aldolase-b, apolipoprotein, IGF2, fibrinogen beta-chain and fibrinogen gamma chain, which previous studies showed were either absent in HepG2 cells or weakly expressed (Yu *et al.* 2001) were increased in HepG2 spheroid cultures (Fig.1B). Recently, human iPSC-LB were shown to form vascularized and functional human liver [29] with up-regulation of a set of 83-genes that are involved in liver development. Almost all of

these genes were also serially upregulated in the HepG2 spheroid cultures (Fig. 2B). Hepatocyte specific gene expression is controlled by liver-enriched transcriptional factors belonging to HNF, C/EBP family members, which act synergistically to maintain tissue functions [30]. The transcript levels of HNF4α, C/EBPβ were also increased with time in HepG2 spheroids (Supplementary data S1). Taken together, these results indicate that HepG2 cells display a trend toward liver-like differentiation when cultured as 3D spheroids.
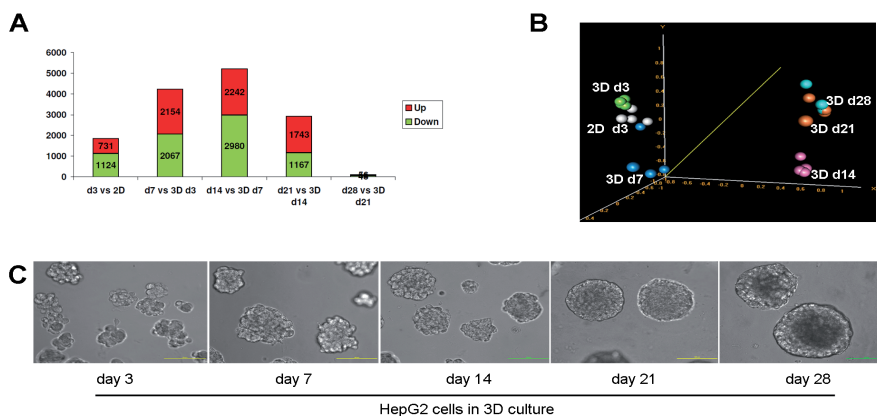


**Figure 1.** *Gene expression changes in differentiated HepG2 spheroids.* Differentially expressed genes which are significantly changed (p<0.001 and FC >1.5 fold) in time during 3D culture (A) Green represents number of genes downregulated / Red represents the upregulated genes. PCA plot showing the distribution of genes in 2D HepG2 cells and at different times in 3D culture where HepG2 cells differentiate into a spheroid (B). Phase contrast images of HepG2 cells in 3D culture with time (C) scale bars 100 $\mu$m.

**Drug detoxifying enzyme gene expression coordinately increases with (spheroid) differentiation**

One of the major limitations of HepG2 cells in drug screening assays is their low level of cytochrome P450 enzymes, phase II conjugating enzymes and drug transporters. Furthermore, the key transcription factors that regulate the drug metabolizing enzymes are also poorly expressed in HepG2 cultures [31]. Xenobiotic metabolism involves various phase I and phase II drug metabolism as well as phase III mediated excretion processes. Expression of these drug-metabolizing enzymes and transporters is higher in differentiated HepG2 spheroids compared to 2D monolayer cultured HepG2 cells. Xenobiotic CYP450 enzymes CYP 2C18, 3A5, 7A1, 4F2 and others (Fig. 2A) were upregulated upon 3D culturing. Also other CYP450 enzymes mainly involved in sterol and fatty acid metabolism, including CYP 7A1, 8B1, 17A1, 19A1, 51A1, 2J2, 4B1, 4F12, had a significantly higher expression in 3D HepG2 spheroids. Phase II enzymes, which are involved in glutathione, glucuronidation and sulfation conjugation reactions were also upregulated in HepG2 spheroids. Glutathione- S- transferases GSTA1, K1, M3, M4 and sulfotransferases SULT2A1, 1C2,

1E1; UDP-glucoronosyltransferases UGT1A1, 1A6, 1A7, 1A8, 1A9,1A10, 2A3, 2B4, 2B28 were significantly upregulated in 3D HepG2 spheroids (Fig. 2A). Besides these, alcohol dehydrogenases and aldehyde dehydrogenases showed an increased expression with time in 3D culture.
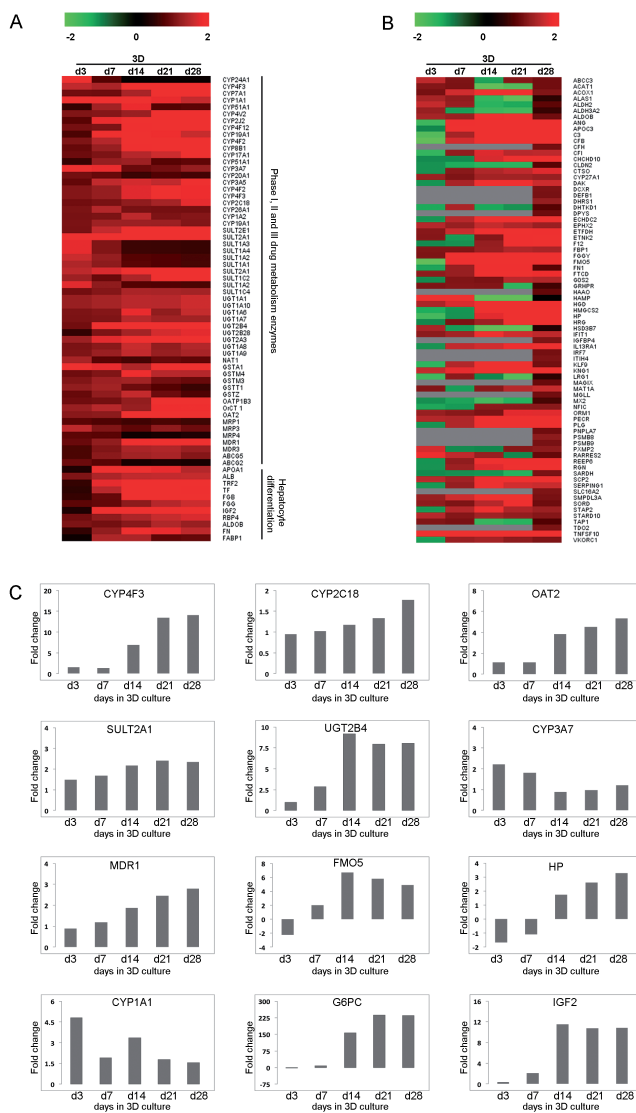


**Figure 2.** *Expression of genes associated with differentiated hepatocytes in 3D culture.* Heat map showing fold change gene expression changes in Phase I, II and III drug metabolism enzymes (A). Fold change expression of genes involved in differentiation and development of the liver (B) in HepG2 spheroids compared to 2D monolayer cultures, data is average (4 experiments) fold change compared to 2D HepG2 gene expression. Fold change gene expression of individual genes corresponding to xenobiotic metabolism, differentiation markers, fetal and adult liver markers over time in 3D culture (C).
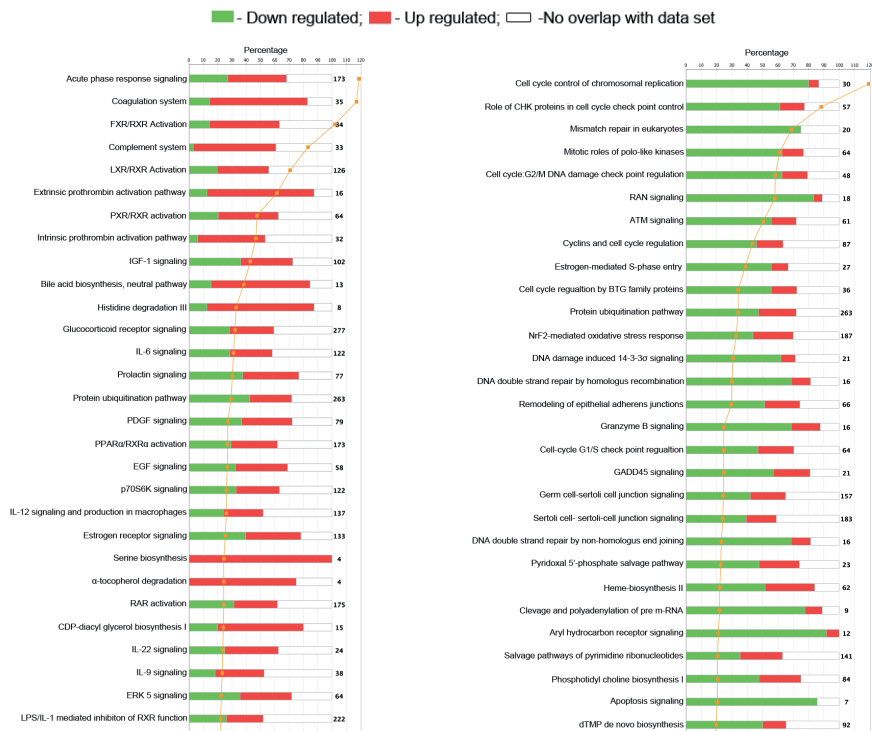
**Figure 3.** *Canonical pathways that are significantly induced in HepG2 cells cultured as spheroids.* Significantly enriched pathways in day 28 differentiated HepG2 spheroids compared to 2D cultured HepG2 cells from Ingenuity Pathway Analysis (IPA), upregulated pathways (A), downregulated pathways (B).

## Liver-specific functions are enriched in 3D HepG2 spheroids

Besides the metabolic competence it is important for an in vitro system to emulate liver specific functions in order to accurately predict a human stress response. Ingenuity Pathway Analysis was used to identify the canonical pathways that are significantly enriched in differentiated HepG2 spheroids compared to HepG2 cells grown as monolayer cultures. The principal upregulated pathways included many xenobiotic metabolism pathways (FXR/RXR, LXR/RXR, PXR/RXR activation) and hepatocyte specific pathways related to liver physiology (coagulation system, complement system, extrinisic prothrombin activation, bile acid biosynthesis) and many pathways related to functional hepatocytes are significantly upregulated (Fig. 3A). The principal downregulated pathways mostly belonged to cell cycle regulation with canonical pathway 'cell cycle control of chromosomal replication' being most strongly downregulated pathway with 80% of downregulated genes (Fig 3B). This indicates that HepG2 spheroids are functionally and metabolically differentiated at the pathway level.

67
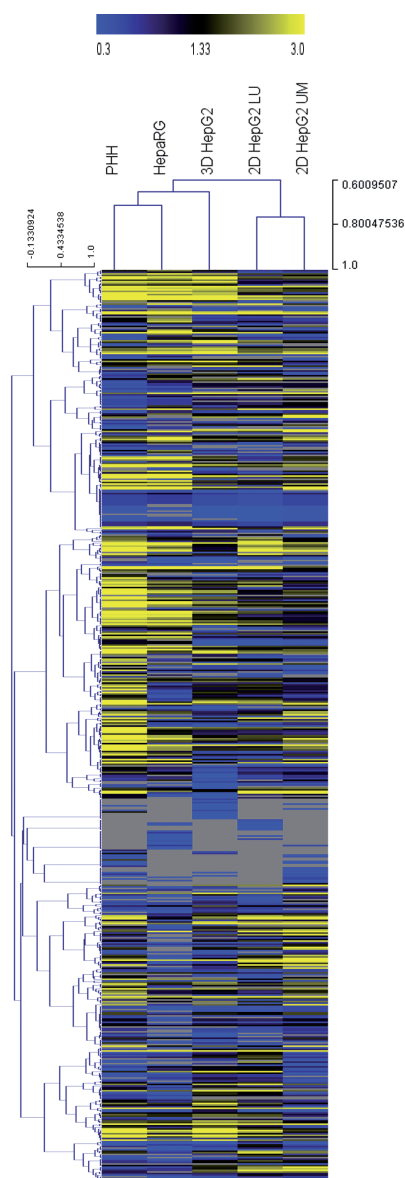
**Figure 4.** *Heat map showing regulation of canonical pathways across hepatocyte models in comparison to human liver.* Scale is – log (p-value); -log (pvalue) 1.3 (p=0.05) represent pathways that are significantly different from human liver. 2D HepG2 LU/2D HepG2 UM: Two sources of HepG2 cells from Leiden University (LU); Maastricht University (UM).

**Pathway analysis of *in vitro* cellular models compared to human liver**

It is anticipated that *in vitro* cultured hepatocytes derived from liver tissue exhibit a different expression profile to intact liver. Ingenuity Pathway Analysis was used to examine the similarities and overall changes in the expression profiles of *in vitro* cellular models compared to human liver. HepG2 cells in 2D culture from 2 different sources showed a close association, but there was also a difference in several molecular pathways, highlighting the effects of source and culture conditions of the HepG2 cells as observed in earlier studies [32]. A close similarity in regulation of molecular pathway was observed between HepaRG and cryopreserved PHH. 3D HepG2 gene expression was different from monolayer cultured HepG2 cells and an association with PHH and HepaRG was observed in hierarchical clustering (Fig. 4). A detailed heat map showing the changes in individual molecular canonical pathways compared to human liver is in supplementary figure S3.

Pathways that are differentially regulated or that are similar to human liver, specific to a cell type are listed in Supplementary data S4. Canonical pathways related to cytokine signaling, MAPK signaling, xenobiotic receptor signaling were similar in PHH and human liver. In HepaRG cells apoptosis signaling, hepatocyte functional pathways such as coagulation system, gluconeogenesis, cell cycle regulation etc. are some of the hepatocyte specific canonical pathways that are not differentially regulated compared to hu-

man liver expression. Pathways related to protein biosynthesis, cytokine signaling, aryl hydrocarbon signaling in xenobiotic metabolism were some of the pathways that were unaltered in HepG2 monolayer cultures compared to human liver. Cell cycle regulation, coagulation system, complement system, PXR/RXR, FXR/RXR xenobiotic signaling, epithelial adherens junction signaling etc. were similar in 3D HepG2 cells and human liver.

To further understand the relationship between different liver models, important functional pathways of hepatocytes were selected and their distribution was
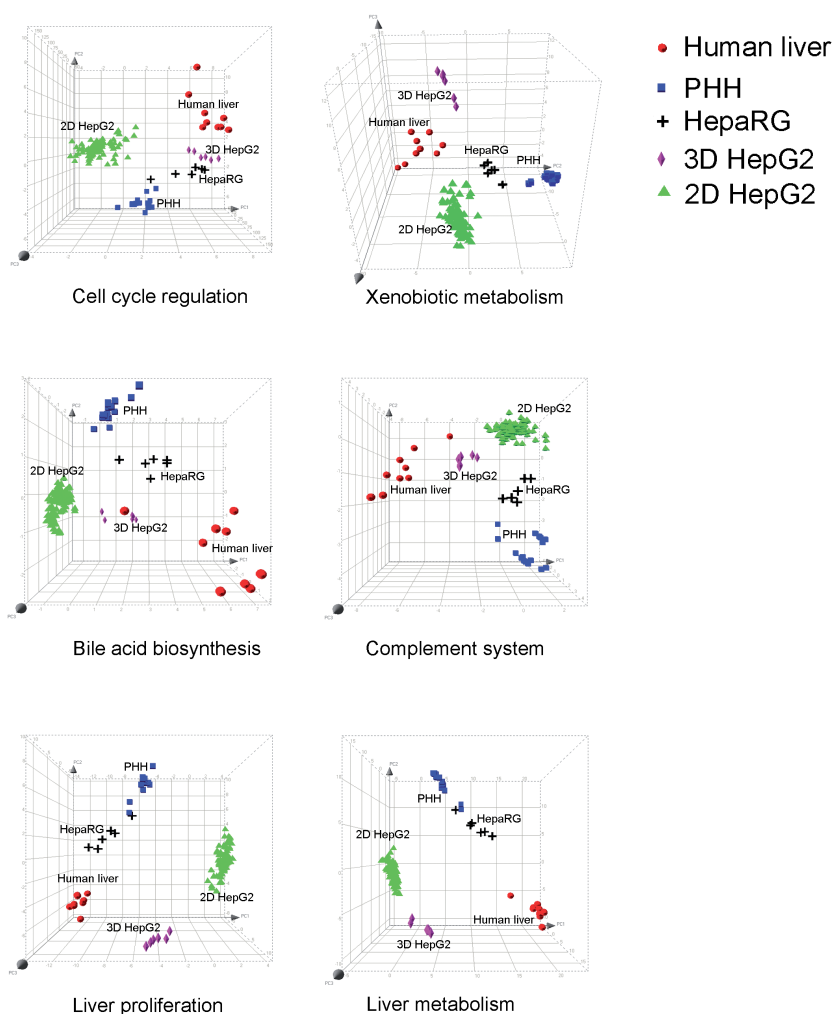


**Figure 5.** *PCA of physiologically relevant molecular pathways.* PCA of selected pathways related to hepatocyte function and differentiation, cell cycle regulation, xenobiotic metabolism, bile acid biosynthesis, complement system, liver proliferation and liver metabolism, in 2D/ 3D HepG2 cells, primary human hepatocytes, HepaRG and human liver.

analyzed using PCA. Pathways related to liver proliferation, liver metabolism, bile acid biosynthesis, complement system, xenobiotic metabolism and cell cycle regulation were analyzed by plotting the normalized log2 intensities of the genes from the groups on PCA (Fig. 5). As observed in IPA analysis, 3D HepG2 cells showed close similarity with human liver expression for cell cycle pathway, supporting the previous observations that the proliferation is ceased in HepG2 spheroids [16]. The expression of cell cycle regulation genes were closely associated in HepaRG and 3D HepG2 spheroids. For other pathways 3D HepG2 spheroid expression was different from 2D HepG2 cells with a trend moving towards human liver. Primary human hepatocytes and HepaRG had a close association both at whole genome level and for selected pathways in this study. Bile acid biosynthesis and complement system pathways in 3D HepG2 spheroids showed a close similarity to human liver than other models, as observed in ingenuity pathway analysis. Together, this data suggests that HepG2 cells in 3D culture transformed into differentiated hepatocytes acquiring various specialized functions of a liver tissue.

## DISCUSSION

Hepatocytes extracted from fresh liver tissue are considered as 'gold standards' for assessing liver toxicity, but their rapid deterioration in culture and high variability is a major limitation for their reliability in drug screening assays. In the wake of high-drug attrition rates due to liver injury, there is a significant interest in developing a robust model that can predict hepatotoxicity in humans. We previously showed that 3D HepG2 spheroids show many of the morphological and functional properties of human liver [16]. In this study we made a detailed investigation of the transcriptomic profile of HepG2 spheroids comparing these with those of HepG2 monolayer cultures, primary human hepatocytes, HepaRG cell line and human liver tissue

Our findings suggest that the differentiation of HepG2 cells in 3D culture recapitulate many of the early ontogenetic events of a developing liver. After 21 days in 3D culture, HepG2 spheroids showed a steady state gene expression profile, after which there was no significant change in the gene expression up to day 28. Genes expressed by human fetal liver (CYP3A7, CYP1A1) were highly expressed during the first 7 days in 3D culture whereas genes associated with differentiated adult liver (Flavin containing mono-oxygenase 5 and haptoglobin) were expressed after day 7 [27, 33].

Under optimal conditions hepatocyte cell lines also have the capacity to generate well-differentiated functional hepatocytes and also may have the capacity to form a liver tissue. Similarly iPSC co-cultures in 3D ECM matrigel allowed the formation of liver buds, and upon transplantation into immuno-deficient mice developed vasculature resembling adult liver, [29] opening new avenues to develop organs for

liver transplantation. In these experiments a set of 83 genes that were serially up-regulated in liver development were analyzed in iPSC's. Interestingly, almost all of these genes were also up regulated in 3D HepG2 spheroids over time, suggestive of a similar differentiation process in our hydrogel cultures.

Differentiation of HepG2 in 3D spheroids also led to induction of various drug-metabolizing enzymes that are typically poorly expressed in 2D HepG2 cell cultures. Phase I enzymes belonging to CYP3A CYP2C, CYP1A, CYP2D families are major enzymes involved in metabolism of 90% of prescribed drugs [34-36]. Most of the members belonging to these families are upregulated in differentiated HepG2 spheroids. Also various enzymes belonging to phase II drug metabolism and trans-porters were also highly expressed in HepG2 spheroids compared to its native ori-gin. The increased expression was observed after 14 days in 3D culture and a sta-ble expression remained up to 28 days, thus providing a window for studying more chronic/repeated dose effects of novel drugs or other chemical entities.

The higher expression of drug metabolic enzymes does not imply that a cellular model is sufficiently robust to detect a toxic stress response. Though, the presence of Phase I, II and drug metabolizing enzymes is promising for making an accurate estimation of toxicity, stress signaling pathways need various other co-reg-ulatory genes in order to show an actual biological response. Ingenuity pathway analysis (IPA) on differentiated 3D HepG2 spheroids showed significantly enriched xenobiotic metabolism pathways. The top upregulated pathway in the list was 'acute response singling pathway' which is required for a proper inflammatory response. Other xenobiotic signaling pathways PXR/RXR, PPARα/RXR, FXR/RXR, LXR/RXR, were also significantly enriched during 3D spheroid culture, suggesting that 3D HepG2 spheroids might be more sensitive for a xenobiotic response. PXR together with RXR plays an important role in drug metabolism, most importantly they activate the CY3A4 gene, which is involved in the metabolism of 50% of current drugs. Upon activation PXR/RXR induces the expression of various phase II and drug metabo-lizing enzymes [37, 38]. It also plays a major role in regulating bile acid synthesis, gluconeogenesis and lipid metabolism [39, 40]. PPARα is also an important target for various pharmacological agents and play a major role in xenobiotic metabolism [41]. FXR/RXR and LXR/RXR pathways are also involved in regulating both en-dogenous and xenobiotic responses [39, 42], suggesting 3D HepG2 spheroids might be more responsive to xenobiotics and would serve as a useful model to help investigate the mechanisms of toxicity.

Principal component analysis on whole genome gene expression profiles of different hepatocyte models was in agreement with previous studies for PHH and HepaRG [4, 6]. A close similarity of HepaRG gene expression profile with cryopre-served PHH suggest that HepaRG may offer a suitable alternative to PHH in toxicity

assays. This still needs to be investigated, but until now there were no large scale toxicity screens comparing these two models. However, in a comparative toxicogenomics analysis both HepG2 and HepaRG cells performed similar compared to PHH [43] and in another transcriptomic study, HepG2 cells performed better in identifying genotoxic compounds than HepaRG cells [13]. The gene expression profile of 3D HepG2 spheroids was different from 2D HepG2 cells and was not closely associated with any other models at the global gene expression level, but showed a close similarity with human liver for important xenobiotic metabolism pathways such as PXR/RXR. Furthermore, the reduced expression of cell cycle genes and the absence of cell cycle, which might represent a physiologically relevant tissue level toxicity assessment and therefore may be advantageous in studying mechanistic toxic responses. Further toxicogenomics studies on HepG2 spheroids would validate their xenobiotic response and similarity to higher models, which may be more similar to an *in vivo* response.

In this study we did not make a direct comparison of drug metabolizing enzymes in various models due to the source of transcriptomic data from primary human hepatocytes and HepaRG. These data sets were from 0.5% DMSO treated controls from another study. Though DMSO will not have an effect on overall gene expression, it is known that DMSO induces expression of various phase I, II xenobiotic metabolizing enzymes and transporters, which therefore might overestimate the comparison with untreated 2D and 3D HepG2 cells. Instead a comparative pathway analysis was performed across different models to understand the similarity and association of different data sets.

In conclusion, HepG2 spheroids in 3D culture showed transcriptional features recapitulating liver development and differentiation. Phase I, II drug metabolic enzymes and drug transporters are highly upregulated in spheroid cultures. Canonical pathways of functional hepatocytes are highly enriched and had a close similarity to human liver. With a higher complexity and amenability to high-throughput assays, 3D HepG2 spheroid model could prove to be promising tool for future drug discovery and development research.

# REFERENCES

1    LeCluyse, E. et al. Expression and regulation of cytochrome P450 enzymes in primary cultures of human hepatocytes. Journal of biochemical and molecular toxicology 14, 177-188 (2000).
2    Gripon, P. et al. Infection of a human hepatoma cell line by hepatitis B virus. Proc Natl Acad Sci U S A 99, 15655-15660, doi:10.1073/pnas.232137699 (2002).
3    Cerec, V. et al. Transdifferentiation of hepatocyte-like cells from the human hepatoma HepaRG cell line through bipotent progenitor. Hepatology 45, 957-967, doi:10.1002/hep.21536 (2007).
4    Aninat, C. et al. Expression of cytochromes P450, conjugating enzymes and nuclear receptors in human hepatoma HepaRG cells. Drug metabolism and disposition: the biological fate of chemicals 34, 75-83, doi:10.1124/dmd.105.006759 (2006).
5    Hoekstra, R. et al. The HepaRG cell line is suitable for bioartificial liver application. Int J Biochem Cell Biol 43, 1483-1489, doi:10.1016/j.biocel.2011.06.011 (2011).
6    Hart, S. N. et al. A comparison of whole genome gene expression profiles of HepaRG cells and HepG2 cells to primary human hepatocytes and human liver tissues. Drug metabolism and disposition: the biological fate of chemicals 38, 988-994, doi:10.1124/dmd.109.031831 (2010).
7    Lubberstedt, M. et al. HepaRG human hepatic cell line utility as a surrogate for primary human hepatocytes in drug metabolism assessment in vitro. Journal of pharmacological and toxicological methods 63, 59-68, doi:10.1016/j.vascn.2010.04.013 (2011).
8    Westerink, W. M. a. & Schoonen, W. G. E. J. Cytochrome P450 enzyme levels in HepG2 cells and cryopreserved primary human hepatocytes and their induction in HepG2 cells. Toxicology in vitro : an international journal published in association with BIBRA 21, 1581-1591, doi:10.1016/j.tiv.2007.05.014 (2007).
9    Wilkening, S., Stahl, F. & Bader, A. Comparison of primary human hepatocytes and hepatoma cell line Hepg2 with regard to their biotransformation properties. Drug metabolism and disposition: the biological fate of chemicals 31, 1035-1042, doi:10.1124/dmd.31.8.1035 (2003).
10   Vollmer, C. M. et al. p53 selective and nonselective replication of an E1B-deleted adenovirus in hepatocellular carcinoma. Cancer Res 59, 4369-4374 (1999).
11   Westerink, W. M., Stevenson, J. C., Horbach, G. J. & Schoonen, W. G. The development of RAD51C, Cystatin A, p53 and Nrf2 luciferase-reporter assays in metabolically competent HepG2 cells for the assessment of mechanism-based genotoxicity and of oxidative stress in the early research phase of drug development. Mutat Res 696, 21-40, doi:10.1016/j.mrgentox.2009.12.007 (2010).
12   O'Brien, P. J. et al. High concordance of drug-induced human hepatotoxicity with in vitro cytotoxicity measured in a novel cell-based model using high content screening. Archives of toxicology 80, 580-604, doi:10.1007/s00204-006-0091-3 (2006).
13   Jennen, D. G. et al. Comparison of HepG2 and HepaRG by whole-genome gene expression analysis for the purpose of chemical hazard identification. Toxicol Sci 115, 66-79, doi:10.1093/toxsci/kfq026 (2010).
14   Kanno, Y. & Inouye, Y. A consecutive three alanine residue insertion mutant of human CAR: a novel CAR ligand screening system in HepG2 cells. The Journal of toxicological sciences 35, 515-525 (2010).
15   Naspinski, C. et al. Pregnane X receptor protects HepG2 cells from BaP-induced DNA damage. Toxicological sciences : an official journal of the Society of Toxicology 104, 67-73, doi:10.1093/toxsci/kfn058 (2008).
16   Ramaiahgari, S. A 3D in vitro model of differentiated HepG2 cell spheroids with improved liver-like properties for repeated dose high-throughput toxicity studies. Archives of toxicology (2014).
17   Benjamini, Y. & Hochberg, Y. Controlling the False Discovery Rate: A Practical and Powerful Approach to Multiple Testing. Journal of the Royal Statistical Society. Series B (Methodological) 57, 289-300, doi:10.2307/2346101 (1995).
18   Saeed, A. I. et al. TM4: a free, open-source system for microarray data management and analysis. BioTechniques 34, 374-378 (2003).
19   Deferme, L. et al. Time series analysis of oxidative stress response patterns in HepG2: a toxicogenomics approach. Toxicology 306, 24-34, doi:10.1016/j.tox.2013.02.001 (2013).
20   Uehara, T. et al. The Japanese toxicogenomics project: application of toxicogenomics. Molecular nutrition & food research 54, 218-227, doi:10.1002/mnfr.200900169 (2010).

21      R: A language and environment for statistical computing (R foundation for statistical computing, Vienna, Austria, 2012).

22      Dai, M. et al. Evolving gene/transcript definitions significantly alter the interpretation of GeneChip data. Nucleic Acids Res 33, e175, doi:10.1093/nar/gni179 (2005).

23      Gentleman, R. C. et al. Bioconductor: open software development for computational biology and bioinformatics. Genome biology 5, R80, doi:10.1186/gb-2004-5-10-r80 (2004).

24      Tong, W. et al. ArrayTrack--supporting toxicogenomic research at the U.S. Food and Drug Administration National Center for Toxicological Research. Environmental health perspectives 111, 1819-1826 (2003).

25      Sharma, S. et al. Metabolism of 17alpha-hydroxyprogesterone caproate, an agent for preventing preterm birth, by fetal hepatocytes. Drug metabolism and disposition: the biological fate of chemicals 38, 723-727, doi:10.1124/dmd.109.029918 (2010).

26      Marongiu, F. et al. Hepatic differentiation of amniotic epithelial cells. Hepatology 53, 1719-1729, doi:10.1002/hep.24255 (2011).

27      Zhang, J. & Cashman, J. R. Quantitative analysis of FMO gene mRNA levels in human tissues. Drug metabolism and disposition: the biological fate of chemicals 34, 19-26, doi:10.1124/dmd.105.006171 (2006).

28      Bensi, G., Raugei, G., Klefenz, H. & Cortese, R. Structure and expression of the human haptoglobin locus. EMBO J 4, 119-126 (1985).

29      Takebe, T. et al. Vascularized and functional human liver from an iPSC-derived organ bud transplant. Nature 499, 481-484, doi:10.1038/nature12271 (2013).

30      Cereghini, S. Liver-enriched transcription factors and hepatocyte differentiation. FASEB journal : official publication of the Federation of American Societies for Experimental Biology 10, 267-282 (1996).

31      Castell, J. V., Jover, R., Martinez-Jimenez, C. P. & Gomez-Lechon, M. J. Hepatocyte cell lines: their use, scope and limitations in drug metabolism studies. Expert opinion on drug metabolism & toxicology 2, 183-212, doi:10.1517/17425255.2.2.183 (2006).

32      Hewitt, N. J. & Hewitt, P. Phase I and II enzyme characterization of two sources of HepG2 cell lines. Xenobiotica 34, 243-256, doi:10.1080/00498250310001657568 (2004).

33      Ring, J. A., Ghabrial, H., Ching, M. S., Smallwood, R. A. & Morgan, D. J. Fetal hepatic drug elimination. Pharmacology & therapeutics 84, 429-445 (1999).

34      Wilkinson, G. R. Drug metabolism and variability among patients in drug response. The New England journal of medicine 352, 2211-2221, doi:10.1056/NEJMra032424 (2005).

35      Slaughter, R. L. & Edwards, D. J. Recent advances: the cytochrome P450 enzymes. The Annals of pharmacotherapy 29, 619-624 (1995).

36      Lynch, T. & Price, A. The effect of cytochrome P450 metabolism on drug response, interactions, and adverse effects. American family physician 76, 391-396 (2007).

37      Istrate, M. A., Nussler, A. K., Eichelbaum, M. & Burk, O. Regulation of CYP3A4 by pregnane X receptor: The role of nuclear receptors competing for response element binding. Biochemical and biophysical research communications 393, 688-693, doi:10.1016/j.bbrc.2010.02.058 (2010).

38      Kliewer, S. A., Goodwin, B. & Willson, T. M. The nuclear pregnane X receptor: a key regulator of xenobiotic metabolism. Endocrine reviews 23, 687-702, doi:10.1210/er.2001-0038 (2002).

39      Xu, C., Li, C. Y. & Kong, A. N. Induction of phase I, II and III drug metabolism/transport by xenobiotics. Archives of pharmacal research 28, 249-268 (2005).

40      Ihunnah, C. A., Jiang, M. & Xie, W. Nuclear receptor PXR, transcriptional circuits and metabolic relevance. Biochim Biophys Acta 1812, 956-963, doi:10.1016/j.bbadis.2011.01.014 (2011).

41      Rakhshandehroo, M., Knoch, B., Muller, M. & Kersten, S. Peroxisome proliferator-activated receptor alpha target genes. PPAR research 2010, doi:10.1155/2010/612089 (2010).

42      Menke, J. G. et al. A novel liver X receptor agonist establishes species differences in the regulation of cholesterol 7alpha-hydroxylase (CYP7a). Endocrinology 143, 2548-2558, doi:10.1210/endo.143.7.8907 (2002).

43      Jetten, M. J., Kleinjans, J. C., Claessen, S. M., Chesne, C. & van Delft, J. H. Baseline and genotoxic compound induced gene expression profiles in HepG2 and HepaRG compared to primary human hepatocytes. Toxicol In Vitro 27, 2031-2040, doi:10.1016/j.tiv.2013.07.010 (2013).

# SUPPLEMENTARY DATA
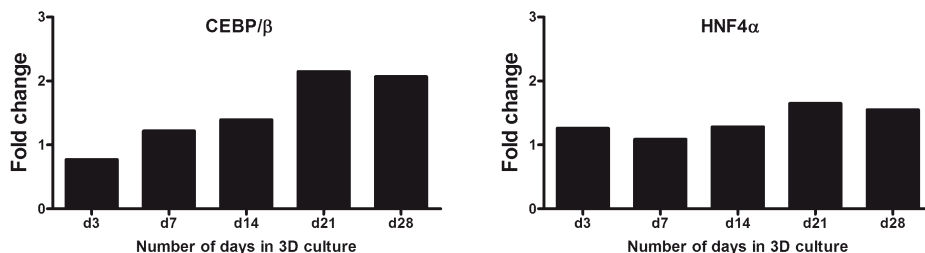


**Supplementary S1.** Transcript level of HNF4α and C/EBPβ in HepG2 spheroids with time in 3D culture.

**Supplementary S2.** Entrez ID of genes used in PCA for figure 5.

**Xenobiotic metabolism pathway**

| | | | | | | | | | |
|---|---|---|---|---|---|---|---|---|---|
| 5243 | 124 | 126 | 127 | 130 | 196 | 8644 | 1109 | 126133 | 5832 |
| 216 | 160428 | 8659 | 501 | 405 | 472 | 1066 | 9469 | 56548 | 113189 |
| 51363 | 1387 | 1562 | 1573 | 66002 | 9451 | 2098 | 2330 | 2938 | 3265 |
| 9653 | 3845 | 3990 | 4128 | 5608 | 6885 | 5594 | 5599 | 5601 | 5603 |
| 5469 | 4257 | 22808 | 8648 | 4780 | 4790 | 1728 | 4835 | 8856 | 4893 |
| 5289 | 5287 | 8503 | 10891 | 5515 | 5520 | 5522 | 5578 | 5581 | 9978 |
| 6256 | 6819 | 6783 | 6822 | 7363 | | | | | |

**Cyclins and cell cycle regulation**

| | | | | | | | | | |
|---|---|---|---|---|---|---|---|---|---|
| 472 | 545 | 8945 | 890 | 891 | 9133 | 595 | 898 | 9134 | 993 |
| 983 | 1017 | 1019 | 1026 | 1031 | 1869 | 1870 | 1871 | 1876 | 2932 |
| 8841 | 9759 | 10014 | 55869 | 5515 | 5520 | 5522 | 5925 | 25942 | |
| 6500l728622 | | 6502 | 6839 | 7027 | 7040 | | | | |

**Bile acid biosynthesis**

| | | | | | | |
|---|---|---|---|---|---|---|
| 8644 | 1109 | 570 | 1581 | 1582 | 80270 | 6342 |

**Complement system**

| | | | | | | | | | |
|---|---|---|---|---|---|---|---|---|---|
| 717 | 718 | 727 | 728 | 731 | 732 | 733 | 1604 | 629 | 5648 |
| 4153 | | | | | | | | | |

**Liver proliferation**

| | | | | | | | | | |
|---|---|---|---|---|---|---|---|---|---|
| 100 | 185 | 196 | 405 | 718 | 727 | 595 | 898 | 1017 | 1026 |
| 1050 | 1051 | 11113 | 1490 | 23405 | 10395 | 1869 | 1906 | 1956 | 957 |
| 2056 | 2147 | 355 | 2305 | 10468 | 2932 | 3172 | 3265 | 3480 | 3484 |
| 3557 | 3570 | 3643 | 3725 | 4254 | 3953 | 3956 | 3958 | 5594 | 5599 |
| 5601 | 4192 | 5469 | 4493 | 4609 | 4780 | 4790 | 9971 | 8856 | 113791 |
| 5340 | 5465 | 5467 | 5468 | 5562 | 5925 | 6256 | 6342 | 6502 | 4088 |
| 4092 | 9021 | 6696 | 6772 | 7039 | 7040 | 7048 | 7057 | 7076 | 7132 |
| 8743 | 8805 | 7422 | | | | | | | |

**Liver metabolism**

| | | | | | | | | | |
|---|---|---|---|---|---|---|---|---|---|
| 100 | 185 | 196 | 405 | 718 | 727 | 595 | 898 | 1017 | 1026 |
| 1050 | 1051 | 11113 | 1490 | 23405 | 10395 | 1869 | 1906 | 1956 | 957 |
| 2056 | 2147 | 355 | 2305 | 10468 | 2932 | 3172 | 3265 | 3480 | 3484 |
| 3557 | 3570 | 3643 | 3725 | 4254 | 3953 | 3956 | 3958 | 5594 | 5599 |
| 5601 | 4192 | 5469 | 4493 | 4609 | 4780 | 4790 | 9971 | 8856 | 113791 |
| 5340 | 5465 | 5467 | 5468 | 5562 | 5925 | 6256 | 6342 | 6502 | 4088 |
| 4092 | 9021 | 6696 | 6772 | 7039 | 7040 | 7048 | 7057 | 7076 | 7132 |
| 8743 | 8805 | 7422 | 2 | 2152 | 2153 | 2155 | 2159 | 2160 | 2161 |
| 2165 | 2243 | 2244 | 3818 | 3827 | 5624 | 3053 | 5054 | 5345 | 7035 |
| 28976 | 39 | 51 | 51703 | 124 | 126 | 127 | 130 | 216 | 8659 |
| 501 | 1374 | 1562 | 1573 | 66002 | 3033 | 3028 | 3712 | 717 | 728 |
| 731 | 732 | 733 | 1604 | 629 | 5648 | 4153 | 80781 | 1280 | 8644 |
| 1109 | 570 | 1581 | 1582 | 80270 | 10797 | 441024 | 4548 | 6470 | 226 |
| 229 | 2027 | 2597 | 5223 | 5230 | 5313 | 5315 | 10841 | 3034 | |

**Supplementary S3.** Heat map of molecular canonical pathways in various *in vitro* models compared to human liver gene expression. Scale is – log  (p-value); -log  (pvalue)  1.3 (p=0.05) represent pathways that are significantly different from human liver.

| PHH | HepaRG | 3D HepG2 | 2D HepG2 |
|---|---|---|---|
| The Visual Cycle | Lactose Degradation III | L-carnitine Biosynthesis | Tetrapyrrole Biosynthesis II |
| TNFR1 Signaling | NAD Biosynthesis III | Tetrahydrobiopterin Biosynthesis I | Sphingosine and Sphingosine-1-phosphate Metabolism |
| GABA Receptor Signaling | Rapoport-Luebering Glycolytic Shunt | Tetrahydrobiopterin Biosynthesis II | Vitamin-C Transport |
| DNA Double-Strand Break Repair by Homologous Recombination | Retinoate Biosynthesis II | Role of IL-17A in Psoriasis | Oleate Biosynthesis II (Animals) |
| nNOS Signaling in Skeletal Muscle Cells | Histidine Degradation VI | GDP-mannose Biosynthesis | Tumoricidal Function of Hepatic Natural Killer Cells |
| Pregnenolone Biosynthesis | NADH Repair | TWEAK Signaling | Creatine-phosphate Biosynthesis |
| Lipid Antigen Presentation by CD1 | D-myo-inositol (1,4,5)-Trisphosphate Biosynthesis | Histamine Degradation | Acetyl-CoA Biosynthesis III (from Citrate) |
| Acetate Conversion to Acetyl-CoA | IL-17A Signaling in Fibroblasts | B Cell Development | Methylthiopropionate Biosynthesis |
| Glutamate Degradation III (via 4-aminobutyrate) | Ethanol Degradation II | Role of RIG1-like Receptors in Antiviral Innate Immunity | Inhibition of Matrix Metalloproteases |
| Heparan Sulfate Biosynthesis | Glutaryl-CoA Degradation | Circadian Rhythm Signaling | Androgen Signaling |
| Phenylalanine Degradation IV (Mammalian, via Side Chain) | Altered T Cell and B Cell Signaling in Rheumatoid Arthritis | Activation of IRF by Cytosolic Pattern Recognition Receptors | Dopamine-DARPP32 Feedback in cAMP Signaling |
| GADD45 Signaling | NAD Biosynthesis from 2-amino-3-carboxymuconate Semialdehyde | DNA damage-induced 14-3-37 Signaling | CREB Signaling in Neurons |
| Ubiquinol-10 Biosynthesis (Eukaryotic) | RhoA Signaling | 1D-myo-inositol Hexakisphosphate Biosynthesis II (Mammalian) | Macropinocytosis Signaling |
| Airway Pathology in Chronic Obstructive Pulmonary Disease | Phototransduction Pathway | Choline Biosynthesis III | P2Y Purigenic Receptor Signaling Pathway |
| Tetrahydrofolate Salvage from 5,10-methenyltetrahydrofolate | CMP-N-acetylneuraminate Biosynthesis I (Eukaryotes) | Superpathway of D-myo-inositol (1,4,5)-trisphosphate Metabolism | Axonal Guidance Signaling |
| Fatty Acid ?-oxidation I | IL-17A Signaling in Airway Cells | PXR/RXR Activation | Cell Cycle: G2/M DNA Damage Checkpoint Regulation |
| Nicotine Degradation III | Role of IL-17A in Arthritis | Intrinsic Prothrombin Activation Pathway | Neurotrophin/TRK Signaling |
| Folate Transformations I | Pyridoxal 5'-phosphate Salvage Pathway | Glycolysis I | Synaptic Long Term Potentiation |
| IL-12 Signaling and Production in Macrophages | Tryptophan Degradation III (Eukaryotic) | Cell Cycle: G1/S Checkpoint Regulation | G Beta Gamma Signaling |
| | Catecholamine Biosynthesis | FXR/RXR Activation | ?-Adrenergic Signaling |
| | Pentose Phosphate Pathway (Oxidative Branch) | Complement System | Neuropathic Pain Signaling In Dorsal Horn Neurons |
| | Toll-like Receptor Signaling | PI3K/AKT Signaling | Endothelin-1 Signaling |
| | Salvage Pathways of Pyrimidine Ribonucleotides | Prolactin Signaling | Hepatic Fibrosis / Hepatic Stellate Cell Activation |
| | tRNA Charging | Ovarian Cancer Signaling | Neuregulin Signaling |
| | Pyrimidine Deoxyribonucleotides De Novo Biosynthesis I | Inhibition of Angiogenesis by TSP1 | ?-Adrenergic Signaling |
| | Actin Cytoskeleton Signaling | | Role of NFAT in Regulation of the Immune Response |
| | 5-aminoimidazole Ribonucleotide Biosynthesis I | | Role of NANOG in Mammalian Embryonic Stem Cell Pluripotency |
| | G Protein Signaling Mediated by Tubby | | HER-2 Signaling in Breast Cancer |
| | Cleavage and Polyadenylation of Pre-mRNA | | Phospholipase C Signaling |
| | IL-17 Signaling | | NF-?B Activation by Viruses |
| | Small Cell Lung Cancer Signaling | | IL-4 Signaling |
| | Purine Nucleotides De Novo Biosynthesis II | | Non-Small Cell Lung Cancer Signaling |
| | Assembly of RNA Polymerase II Complex | | Antiproliferative Role of Somatostatin Receptor 2 |
| | G?12/13 Signaling | | IMLP Signaling in Neutrophils |
| | HIF-1a Signaling | | Corticotropin Releasing Hormone Signaling |
| | Ceramide Signaling | | |
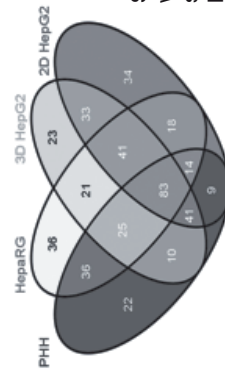


**Supplementary S4 (A).** List of pathways (generated from IPA) that have not significantly changed when compared to human liver expression and that are unique to specific model. Venn diagram showing the overlap of all the pathways in various models that are not significantly changed with human liver.

| PHH | HepaRG | 3D HepG2 | 2D HepG2 |
|---|---|---|---|
| Gluconeogenesis I | Heparan Sulfate Biosynthesis | G-Protein Coupled Receptor Signaling | D-myo-inositol (1,4,5)-trisphosphate Degradation |
| Estrogen Receptor Signaling | Fcγ Receptor-mediated Phagocytosis in Macrophages and Monocytes | Type I Diabetes Mellitus Signaling | D-myo-inositol-5-phosphate Metabolism |
| Apoptosis Signaling | Methionine Degradation I (to Homocysteine) | IGXR0 Signaling Pathway | Crosstalk between Dendritic Cells and Natural Killer Cells |
| Role of PI3K/AKT Signaling in the Pathogenesis of Influenza | Synaptic Long Term Depression | Notch Signaling | D-glucuronate Degradation I |
| Nucleotide Excision Repair Pathway | Granulocyte Adhesion and Diapedesis | Methionine Salvage II (Mammalian) | Inosine-5'-phosphate Biosynthesis II |
| Adenine and Adenosine Salvage III | Ceramide Biosynthesis | mTOR Signaling | Fatty Acid Activation |
| Selenocysteine Biosynthesis II (Archaea and Eukaryotes) | Glycogen Biosynthesis II (from UDP-D-Glucose) | | Choline Biosynthesis III |
| Superpathway of Serine and Glycine Biosynthesis I | Gγi Signaling | | Telomere Extension by Telomerase |
| Agrin Interactions at Neuromuscular Junction | Mechanisms of Viral Exit from Host Cells | | Adenosine Nucleotides Degradation II |
| ERK5 Signaling | Atherosclerosis Signaling | | Superpathway of D-myo-inositol (1,4,5)-trisphosphate Metabolism |
| DNA damage-induced 14-3-3? Signaling | Tight Junction Signaling | | ?-linolenate Biosynthesis II (Animals) |
| Cell Cycle: G2/M DNA Damage Checkpoint Regulation | p38 MAPK Signaling | | 1D-myo-inositol Hexakisphosphate Biosynthesis II (Mammalian) |
| Phosphatidylethanolamine Biosynthesis II | Human Embryonic Stem Cell Pluripotency | | Histidine Degradation III |
| Role of IL-17A in Psoriasis | Sperm Motility | | Extrinsic Prothrombin Activation Pathway |
| Regulation of Cellular Mechanics by Calpain Protease | PPAR Signaling | | Valine Degradation I |
| Cyclins and Cell Cycle Regulation | | | DNA Double-Strand Break Repair by Homologous Recombination |
| CTLA4 Signaling in Cytotoxic T Lymphocytes | | | |
| Lysine Degradation II | | | |
| Lysine Degradation V | | | |
| Renal Cell Carcinoma Signaling | | | |
| Maturity Onset Diabetes of Young (MODY) Signaling | | | |
| FGF Signaling | | | |
| G Protein Signaling Mediated by Tubby | | | |
| IL-17A Signaling in Gastric Cells | | | |
| DNA Double-Strand Break Repair by Non-Homologous End Joining | | | |
| VEGF Signaling | | | |
| RAN Signaling | | | |
| AMPK Signaling | | | |
| CD28 Signaling in T Helper Cells | | | |
| T Cell Receptor Signaling | | | |
| RhoGDI Signaling | | | |
| Thyroid Cancer Signaling | | | |
| Purine Ribonucleosides Degradation to Ribose-1-phosphate | | | |
| Remodeling of Epithelial Adherens Junctions | | | |
| Bladder Cancer Signaling | | | |
| Aryl Hydrocarbon Receptor Signaling | | | |
| Rac Signaling | | | |



**Supplementary S4 (B).** List of pathways (generated from IPA) that have significantly changed when compared to human liver expression and that are unique to specific model. Venn diagram showing the overlap of all the pathways in various models that are not significantly changed with human liver.

| Common pathways in "PHH" and "3D HepG2" (9) | Common pathways in "PHH" and "HepaRG" (17) | Common pathways in "PHH" and "2D HepG2" (11) |
|---|---|---|
| Glycine Cleavage Complex | Huntington's Disease Signaling | Methylglyoxal Degradation III |
| Lymphotoxin Receptor Signaling | Sphingosine-1-phosphate Signaling | Serotonin Degradation |
| Regulation of Actin-based Motility by Rho | Superpathway of Methionine Degradation | Coagulation System |
| CNTF Signaling | VEGF Family Ligand-Receptor Interactions | Noradrenaline and Adrenaline Degradation |
| IL-17A Signaling in Gastric Cells | Sucrose Degradation V (Mammalian) | MSP-RON Signaling Pathway |
| Angiopoietin Signaling | Leptin Signaling in Obesity | Clathrin-mediated Endocytosis Signaling |
| iCOS-iCOSL Signaling in T Helper Cells | Epithelial Adherens Junction Signaling | Protein Ubiquitination Pathway |
| iNOS Signaling | Melanocyte Development and Pigmentation Signaling | Bile Acid Biosynthesis, Neutral Pathway |
| Ephrin A Signaling | CDK5 Signaling | Role of CHK Proteins in Cell Cycle Checkpoint Control |
| | CCR5 Signaling in Macrophages | PXR/RXR Activation |
| | PPAR/RXR Activation | Cell Cycle Control of Chromosomal Replication |
| | PTEN Signaling | |
| | Role of p14/p19ARF in Tumor Suppression | |
| | Leukocyte Extravasation Signaling | |
| | Docosahexaenoic Acid (DHA) Signaling | |
| | Role of JAK1 and JAK3 in Cytokine Signaling | |
| | FcRIIB Signaling in B Lymphocytes | |
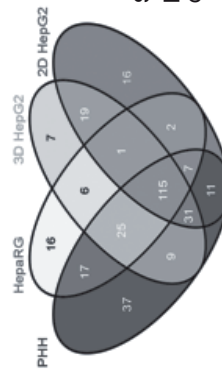


**Supplementary S5.** List of pathways (generated from IPA) that have significantly changed compared to human liver expression and that are common in primary human hepatocytes. Venn diagram showing the overlap of the pathways .

# CHAPTER 4

## SYSTEMIC COMPARISON OF DICLOFENAC INDUCED GENE EXPRESSION CHANGES IN DIVERSE *IN VITRO* AND *IN VIVO* MODELS AND SPECIES

Sreenivasa C. Ramaiahgari[1], Steven Wink[1], Mackenzie Hadi[3],
John Meerman[1], Mirjam Luijten[2], Geny Groothuis[3],
Bob van de Water[1] and Leo S. Price[1]

[1]Division of Toxicology, Leiden Academic Centre for Drug Research,
Leiden University, Leiden, The Netherlands.

[2]Laboratory for Health Protection Research,
National Institute for Public Health and the Environment,
Bilthoven, The Netherlands.

[3]Division of Pharmacokinetics, Toxicology and Targeting,
Department of Pharmacy, University of Groningen,
Groningen, The Netherlands.

# ABSTRACT

Drug-induced liver injury (DILI) is a major clinical concern. Various models are proposed to investigate DILI, but a gold-standard model that could predict human DILI is still lacking. A systematic comparison of *in vitro*/*in vivo* models would help to characterize the responses associated with the drug-induced hepatotoxicity and identify better model(s) that could closely predict human DILI. Here we performed a comparative transcriptomic analysis using ex-vivo human precision cut liver slices (PCLS), *in vitro* primary human hepatocytes, mouse hepatocytes, rat hepatocytes, the human hepatoma cell line HepG2, cultured in 2D monolayer or 3D spheroids, and *in vivo* rat and mouse livers. All models were exposed to the drug diclofenac, which causes idiosyncratic DILI. To dissect the canonical cellular stress responses upon diclofenac treatment in the different models we used Ingenuity pathway analysis, where human PCLS with its heterogeneous cell population representing intact liver tissue was used as a reference for all other models. Protein ubiquitination, Nrf2-associated oxidative stress and xenobiotic metabolism pathways were found to be significantly altered upon diclofenac treatment. Genes involved in liver diseases including cholestasis and steatosis were significantly upregulated providing an early evidence for long-term effects of diclofenac treatment. HepG2 cells in 3D culture were more responsive and showed a significant upregulation of stress signaling pathways and genes related to diclofenac induced liver diseases with a similarity to human PCLS. Compared to mouse, rat gene expression profiles were more similar to human gene expression. In conclusion, transcriptomic analysis will allow us to identify various drug-induced cellular stress responses. Functionally and phenotypically stable HepG2 spheroids could serve as a better alternative model to identify human relevant biomarkers of DILI.

# INTRODUCTION

Adverse drug reactions are a major concern for the safe use of drugs. These reactions are undetected during early clinical trials in small groups of patients and are often idiosyncratic in nature [1]. With the first pass effect and its central role in drug metabolism, the liver is prone to adverse drug reactions leading to drug induced liver injury (DILI) or causing liver diseases after chronic treatment. DILI has been the major reason for pre- and post-marketed attrition of drugs [2]. There is an urgent need for improved methods and models that could reflect drug metabolism in a human system and ultimately predict DILI risk during early preclinical drug development.

Animal models are the primary source for toxicity studies, as they are the only available laboratory models with the complexity approaching that of humans. But several studies have shown that the toxicity assessment using animal models and its translation to human toxicological responses is quite poor [3]. In order to predict human DILI, human cell-based models possessing tissue specific characteristics are preferred. Current *in vitro* models are not feasible for long-term culture giving us no choice but to rely on animal models for studying repeated drug exposure effects. Ex-vivo models such as precision cut liver slices (PCLS) can represent an intact functional liver with heterogeneous cell population [4], which could respond similar to *in vivo* liver tissue [5]. But, major disadvantages of liver slices are a rapid decline of its functional properties ex vivo [6] and the low throughput limiting its value in repeated dose-effect studies. Primary human hepatocytes are considered as gold standards for compound screening assays [7]. But they also show a rapid decline of liver function and due to its high variability between donors; even replicate samples of a single transcriptomic study can differ [8]. In this respect, immortalized cell lines might provide an advantage in maintaining a stable gene expression and models using HepG2 and HepaRG have been studied for their efficiency in toxicogenomics [9, 10]. Recent developments in *in vitro* cell culture methodologies have helped to maintain the differentiated phenotype of cells for extended periods [11-14]. Systems such as bioreactors, micropatterning and ECM gels for 3D growth have been proposed that provide a physiological niche to various primary and immortal cell lines. Due to the ease of use and availability of HepG2 cells and the ability to maintain a highly differentiated spheroid phenotype with improved metabolic competence in 3D cultures [14], HepG2 spheroids could be an optimal choice for the evaluation of DILI. Drug-induced cytotoxicity is typically identified by simple cell death measurements in *in vitro* models. For accurate human translation it is important to determine whether the molecular initiation events and the subsequent cell state changes that trigger cytotoxicity are translatable from simple *in vitro* models to humans.

Genome-wide microarray analysis allows the detailed evaluation of altered gene expression upon toxic insults, thereby representing the altered cell status after drug-induced cellular perturbations. Likewise, such a transcriptomics analysis is highly suited to identify the cellular stress responses that underlie DILI-related cytotoxicity as well as the comparison of such stress responses between models. A wealth of toxicogenomics data from human, mouse, rat, canine *in vitro* and *in vivo* liver models has helped to identify promising biomarkers for liver injury [15]. These toxicogenomics data are available in the public domain Gene Expression Omnibus (GEO) [16], Array Express [17], Comparative Toxicogenomics Database (CTD) [18], EDGE [19, 20], Chemical Effects in Biological Systems (CEBS) [21], TG-GATES (Genomics Assisted Toxicity Evaluation System). TG-GATES has a database of *in vivo* and *in vitro* gene expression profiles of liver and kidney upon exposure to 150 chemicals, mainly drugs that are currently used for patients [22]. These databases can be used as a reference for comparing the gene expression profiles in different models upon exposure to toxicants relevant for DILI.

In the present study we compared the gene expression profiles of human PCLS, primary human hepatocytes, HepG2 cells, mouse primary hepatocytes, mouse liver, rat primary hepatocytes and rat liver treated with a widely used non-steroidal anti-inflammatory drug diclofenac. Diclofenac is one of the most frequent causes of adverse drug injury to the liver, with 180 confirmed cases reported by FDA during the initial marketing period [23]. Several possible mechanisms of diclofenac induced liver injury have been proposed which involve formation of reactive metabolites, mitochondrial injury, ROS formation as well as interference with the immune system signaling, but the molecular mechanism leading to the liver damage is largely unknown [24-26].

Using Ingenuity pathway analysis, molecular pathways that were altered upon diclofenac exposure in human PCLS, rat and mouse *in vivo*, human, rat and mouse cultured primary hepatocytes, and human hepatoma cell line HepG2 cultured in 2D monolayer or 3D spheroids were compared and a similarity of gene expression profiles at the pathway level was analyzed across species. Since fresh PCLS most closely represented *in vivo* human liver tissue, it was used as a standard reference for the other models. Genes associated with diclofenac-induced chronic liver injury were found to be significantly activated in human PCLS. Several xenobiotic metabolism and stress-induced pathways were significantly enriched highlighting their potential role in diclofenac induced liver injury. HepG2 spheroid cultures were more responsive than 2D HepG2 cultures and showed a high similarity to PCLS. Ingenuity classified toxicity-related pathways of HepG2 spheroids were very similar to PCLS.

# MATERIALS AND METHODS

### Cell culture and diclofenac exposure

HepG2 cells: HepG2 cell line was obtained from American type tissue culture (ATCC, Wesel, Germany), cultured in Dulbecco's modified Eagles medium (DMEM) supplemented with 10% (v/v) fetal bovine serum, (Invitrogen, The Netherlands), 25 U/mL penicillin and 25 μg/mL streptomycin (PSA, Invitrogen) and used for culture. 3D cultures were prepared as described earlier [14]. 500 μM Diclofenac (Sigma Aldrich, Zwijndrecht, The Netherlands) was incubated for 24 hours before RNA extraction. HepG2 cells in 2D culture were incubated with 500 μM diclofenac for 14 hours before RNA extraction. Human PCLS: Human PCLS were prepared and incubated with diclofenac as described earlier [27] Mouse liver and hepatocytes: Mouse hepatocytes were obtained as described earlier [28] and exposed with 500 μM diclofenac. Rat liver and hepatocytes: Rat liver and hepatocyte data was obtained from public transcriptomics data base, Toxicogenomics Project-Genomics Assisted Toxicity Evaluation system' (TG-GATEs). Rat *in vitro* hepatocytes were treated with 400 μM diclofenac for 24 h. Rat *in vivo* data single exposure with 100 mg/kg for 24 hours and for repeat exposures 100mg/kg daily dose via gavage until day 29 were used for analysis. Primary human hepatocytes: data set from primary human hepatocytes exposed with 400 μM diclofenac for 24 h obtained from public transcriptomics data base, Toxicogenomics Project-Genomics Assisted Toxicity Evaluation system' (TG-GATEs) was used for analysis.

### RNA extraction for microarrays

Total RNA was extracted from 3D cultured HepG2 cells using Tri reagent (Sigma) followed by clean up using RNeasy® mini kit (Qiagen, Venlo, The Netherlands). Purity and concentration of the RNA were analyzed using NanoDrop ND-1000 spectrophotometer (Nanodrop technologies, Wilmington, DE, USA). RNA quality and integrity was further determined using the Agilent bioanalyser (Agilent Technologies Inc, Santa Clara, CA, USA). Biotinylated cRNA was prepared using the Affymetrix 3' IVT-Express Labeling Kit (Affymetrix, Santa clara, CA, USA) and hybridization steps were performed by Service XS B.V (Leiden, The Netherlands) on Affymetrix HT Human Genome U133 plus PM plate. Array plates were scanned using the Affymetrix GeneTitan scanner.

### Microarray analysis

Probe annotation was performed using the hthgu133pluspmhsentrezg.db package version 17.1.0 and Probe mapping was performed with hthgu133pluspmhsentrezg-cdf file downloaded from NuGO (http://nmg-r.bioinformatics.nl/NuGO_R.html).

Probe-wise background correction, between-array (within same datasets) normalization and probe set summaries calculation was performed using the RMA function of the Affy package (Affy package, version 1.38.1) [29, 30]. The normalized data were statistically analyzed for differential gene expression using a linear model [31, 32] with coefficients for each experimental group using the Limma package (Limma package, version 1.22.0; [30]). A contrast analysis was applied to compare each exposure with the corresponding vehicle control. For hypothesis testing the moderated t-statistics by empirical Bayes moderation was used followed by an implementation of the multiple testing correction of Benjamini and Hochberg.

Array and normalization quality control was performed with the arrayQualityMetrics, a bioconductor package for quality assessment of microarray data [33]. All analysis was performed in the R statistical language environment (R development core team 2012).

## Pathway analysis

Differentially expressed genes with P<0.05 (and FDR <0.05) were uploaded onto Ingenuity Pathway Analysis IPA® (Ingenuity® systems, Redwood, CA, USA). Genes that were </> 1.5 fold changed compared to vehicle control were selected for pathway enrichment analysis. Activation of canonical pathways is predicted by calculating p-value using right-tailed Fisher Exact Test from the DEG's and p-values less than 0.05 (-log=1.3) are said to be significantly activated. Heatmap and hierarchical clustering using Pearson correlation was performed using TM4: MultiExperiment Viewer program [34].

| Sl.no | Test model | DEG's | (up"^") or (down"ᵛ") r e g u l a t e d | Diclofenac Conc. | Exposure time |
|---|---|---|---|---|---|
| 1 | Human liver slices | 3737 | (1690^/2047ᵛ) | 500 µM | 24 h |
| 2 | Primary human hepatocytes | 4165 | (2125ᵛ/2040ᵛ) | 400 µM | 24 h |
| 3 | HepG2 cells 3D | 3183 | (1523ᵛ/1660ᵛ) | 500 µM | 24 h |
| 4 | HepG2 cells 2D | 4241 | (2246ᵛ/1995ᵛ) | 500 µM | 14 h |
| 5 | Primary mouse hepatocytes | 4012 | (2073ᵛ/1939ᵛ) | 500 µM | 24 h |
| 6 | In vivo mouse liver | 500 | (192^/308ᵛ) | 100 mg/kg | 24 h |
| 7 | Primary rat hepatocytes | 3421 | (1973ᵛ/1448ᵛ) | 400 µM | 24 h |
| 8 | *In vivo* rat liver | 2461 | (1073ᵛ/1388ᵛ) | 100 mg/kg | 24 h |
| 9 | *In vivo* rat liver repeat exposure | 1141 | (573^ /568ᵛ) | 100 mg/kg | 29 days |

**Table 1:** Differentially expressed genes after diclofenac treatment in various *in vitro* and *in vivo* models. Selection was based on genes that are significant P<0.05, FDR<0.05.

# RESULTS

**Diclofenac induced differential gene expression in human and rodent models**

Differentially expressed genes (FDR & $P<0.05$) upon diclofenac treatment in various models are as shown in table 1. This included in almost all cases a 24-hour time point post exposure, except 2D HepG2 cultures (14-hour) and a chronic exposure in rat *in vivo* model (29-day); *In vivo* mouse and rat (repeated exposure) had the lowest number of DEGs of all models models (Fig 1A). Next, transcriptomic changes induced by diclofenac were compared across all models. 471 DEG's were found to have an overlap in the human models (Fig 1B). IPA analysis demonstrated that these genes are functionally associated with signaling pathways including remodeling of epithelial adherens junction, NRF2 mediated oxidative stress response and p53-signaling pathway. A complete list of pathways associated with these 471 genes is shown in
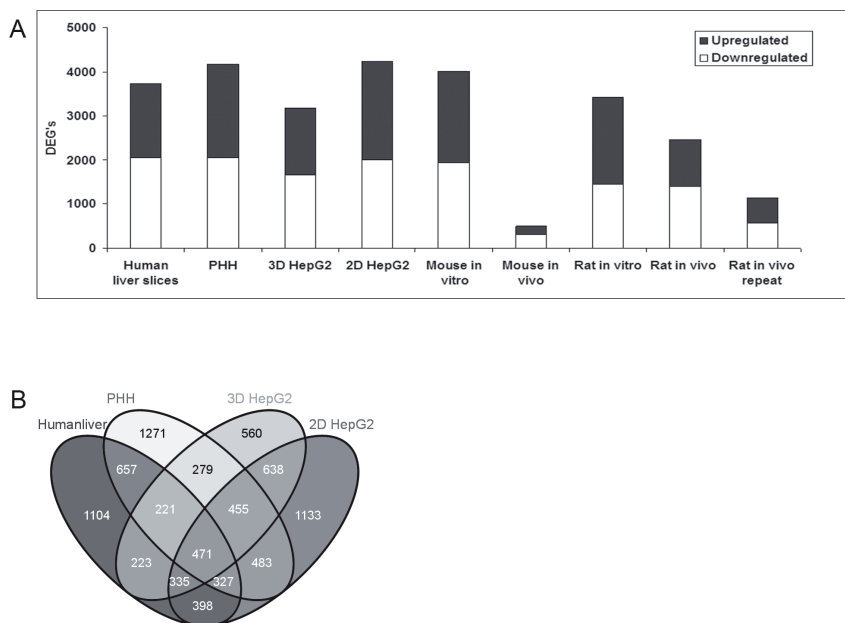


**Figure 1:** *Similarity of differentially expressed genes in various models.* Differentially expressed genes in various *in vitro/in vivo* models (A). Venn diagrams of DEG's from human derived cell lines (B); DEG's with $P<0.05$ (and FDR $P<0.05$) were selected.

supplementary figure S2. The overlap of DEGs in 2D/3D HepG2, hPCLS to primary hepatocyte models of human, mouse and rat was also analyzed: 214 genes were in common for 3D HepG2 spheroids; 242 for 2D HepG2 and 267 for human PCLS (Supplementary S2). Molecular pathways associated with these overlapping genes
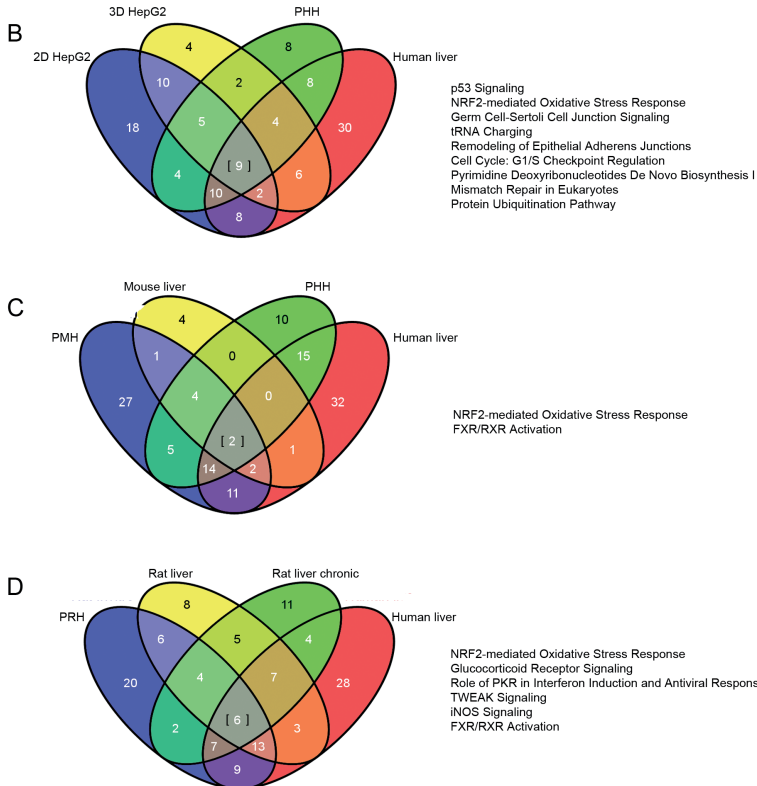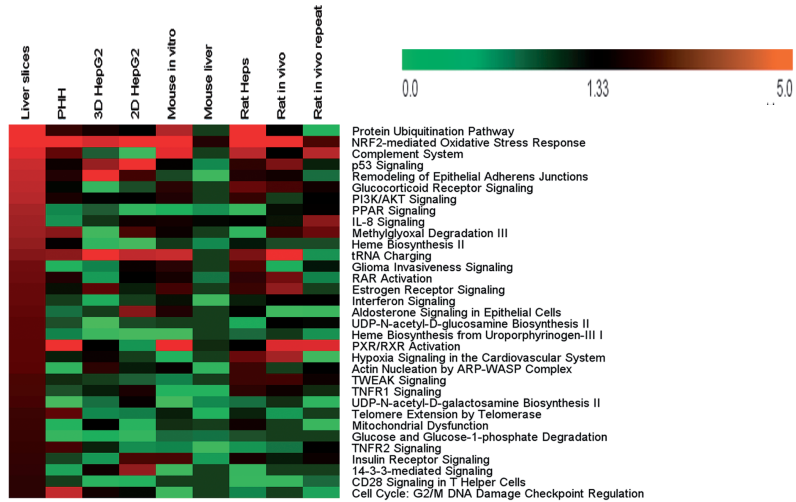
**Figure 2:** *Altered canonical pathways upon diclofenac exposure.* Heatmap showing significantly altered canonical pathways in human PCLS and their expression on other models from ingenuity pathway analysis (A). Venn diagram comparing significantly altered pathways in human cell models (B), Mouse models compared to human PCLS and PHH (C), Rat models compared to human PCLS (D). Significance calculated based on the ratio of the genes that are associated with specific canonical pathway, -log (p-value) 1.3 = P (0.05).

are as shown in supplementary S4. A closer similarity in overlapping pathways was seen between 3D HepG2 spheroids and human PCLS than 2D HepG2 and hPCLS (Supplementary S4). *In vivo* mouse liver exposed to diclofenac for 24 hours showed only 500 genes that were significantly changed, yet almost half of them overlapped with the mouse primary hepatocytes (Supplementary S1). Similarly, almost 50% of the DEGs of the single dose treatment of rat *in vivo* overlapped with the DEGs of the primary rat hepatocytes; also repeated diclofenac exposures in rats gave more than 60% concordance with either rat liver *in vivo* or rat hepatocytes *in vitro*. Venn diagrams showing association of DEG's between other models are in supplementary S1. Overall these data indicate that although there is quite a good concordance between all models, the highest concordance is reached within one species, either human, rat or mouse.

**Differentially regulated canonical pathways upon diclofenac treatment**
Although the overlap between the DEGs between species was relatively low, overall, DEGs could be part of similar cellular stress response pathways. Therefore, for all the models the molecular pathways that are associated with DEG's from diclofenac exposure were analyzed using Ingenuity Pathway Analysis (IPA®). We ranked the pathways of the different models according to the significance levels in the human PCLS model (Fig 2A). This demonstrates quite a differential modulation of pathways in the different models. Significant activation of the Nrf2 oxidative stress pathway was seen in all the models, highlighting its prime role in diclofenac induced liver injury. A higher number of significantly activated canonical pathways are seen in mouse primary hepatocytes than mouse liver, which is due to less number of significant genes in mouse liver samples (Table 1).

Next we evaluated the overlap of the differentially modulated pathways in the different models. Nine pathways had an overlap in human models (Fig. 2B), which included some important stress pathways such as Nrf2 oxidative stress response and p53 signaling. Only two pathways overlapped between mouse models, PHH and human PCLS: Nrf2 pathway and PXR/RXR activation (Fig. 2A and C). Six pathways showed an overlap with rat models and human PCLS, which also included Nrf2 signaling (Fig. 2A and D).

The pathways that are activated are not necessarily determined by the same gene sets. Therefore, for the most common pathways we first extracted the genes that are significantly affected for the individual pathways for the human PCLS model, and then extracted the fold change values for all these individual genes from the other models. We focused on some of the top affected pathways that also contained sufficient DEGs (Fig. 3).

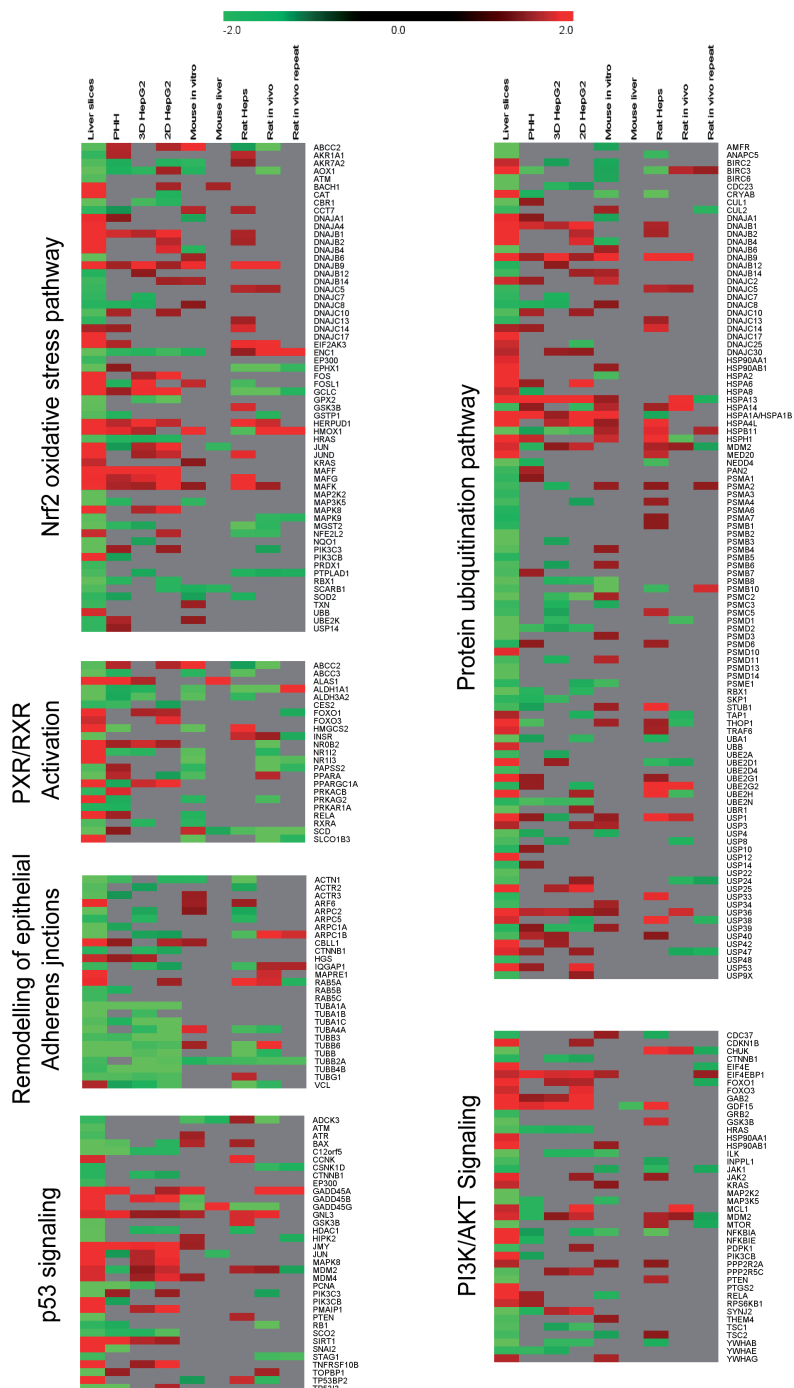**Figure 3:** Individual genes associated with altered canonical pathways upon diclofenac treatment in human PCLS and their expression in other models. Fold change gene expression compared to vehicle controls.

Nrf2 oxidative stress response was a major common pathway that was induced upon diclofenac exposure. Diclofenac metabolites may cause mitochondrial impairment, ROS generation and subsequent oxidative stress, which is proposed as a possible mechanism of diclofenac-induced liver injury [35-38]. Oxidative stress activates the Nrf2 pathway to adapt to a more pro-oxidant environment. Genes regulated by Nrf2, such as HO-1 (heame oxygenase 1), are important markers for oxidative stress [39] and upregulation of HO-1 has been observed after diclofenac treatment [35, 36]. Here, HO-1 gene expression was seen in *in vivo* rodent models, human PCLS, primary hepatocytes and 3D HepG2 spheroids (Fig 3), but not in HepG2 cells in 2D culture in agreement with earlier reports [35]. This could be due to poor metabolism of diclofenac in 2D HepG2 cultures, since HO-1 expression was seen in HepG2 cells with S9 mixture [36]. In contrast, HepG2 cells cultured in hydrogels as spheroids expressed HO-1 supporting an increased metabolic competence in these HepG2 spheroids. Another Nrf2 target, DNAJB9, a HSP40 family protein, [40, 41] was induced >2-fold in human PCLS, rat primary cells and liver and 3D HepG2 cells. The expression of DNAJB9 was lower or not seen (mouse liver and rat repeated exposures) in other models (Fig 3). Interestingly, MafK expression was upregulated upon diclofenac exposure in all the models except mouse liver and rat chronic exposures where it was unchanged with diclofenac treatment (Fig 3). Nrf2/MafK heterodimer binds and activate anti-oxidant responsive elements (ARE), inducing the expression of phase II enzymes [42, 43]. It was also reported that over expression of MafK resulted in negative regulation of ARE-dependent transcription [44, 45]. The positive and negative regulation of antioxidant responsive elements by Nrf2/MafK may play an important role in balancing the oxidative stress response upon toxicant exposure.

Next we evaluated the p53 signaling pathway in more detail. Cellular injury-induced mitochondrial dysfunction and subsequent generation of ROS was shown to be involved in upstream activation of p53 mediated apoptotic signaling [46]. p53 plays a major role in DNA damage response, cell cycle regulation and apoptosis [47]. p53 signaling pathway is significantly altered upon diclofenac exposure in the all models studied, except mouse liver (Fig 2A). Downstream targets of p53 involved in cell cycle regulation and apoptosis showed a varied response in different models. GADD45a, is induced upon DNA damage and is involved in G2-M cell cycle arrest [48]. GADD45a is upregulated after diclofenac exposure in all the models except primary rat hepatocytes, 3D HepG2 and mouse liver (Fig 3A). Earlier studies have reported that diclofenac induces oxidative stress leading to DNA fragmentation and apoptotic cell death [49]. Activation of GADD45a may indicate induction of a DNA damage response upon diclofenac exposure in this study. Up regulation of p53 mediated apoptosis inducer, Bax, was seen only in mouse and rat primary hepatocytes (Fig 3A). MDM2, a negative regulator of p53 [50] was down-regulated in primary

human hepatocytes and rat repeated diclofenac exposures, but not differentially expressed in mouse models and is upregulated in other models.

PXR/RXR activation, PI3K/AKT signaling, protein ubiquitination pathway and remodeling of epithelial adherens junctions were all significantly altered upon diclofenac treatment. For these models the highest concordance for individual gene expression was observed amongst the human models. Overall these data indicate that, while in the different models diclofenac may activate similar pathways, overall the genes that are affected in these pathways is quite different. Most concordance is observed for species-specific changes. Regardless, some genes do overlap amongst all models, with the exception for mouse liver *in vivo* and rat repeated dose.
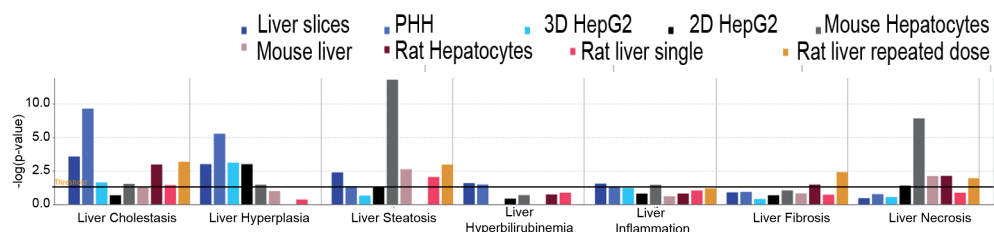


**Figure 4.** *Diclofenac induced gene expression changes associated with liver diseases*. Significance calculated based on the ratio of the genes that are associated with the onset or mechanism of liver disease manifestation, -log (p-value)1.3 = P 0.05 from Ingenuity Pathway Analysis.

## Gene expression analysis identifies liver diseases associated with diclofenac treatment

Several cases have shown that long-term use of diclofenac lead to overt liver diseases. We used our transcriptomics data from different models to relate gene expression to disease models. FDA reports show that cholestasis was an adverse effect in 8% of patients taking diclofenac in 180 reported cases [23]. Analysis of genes involved in manifestation of liver diseases showed a significant induction of genes associated with cholestatic liver injury in all the models except 2D HepG2 cultures (Fig 4). Genes involved in liver hyperplasia were also significantly present in human cell models and mouse hepatocytes. Liver steatosis was significantly activated in human PCLS, primary human hepatocytes, 2D HepG2 cells, mouse and *in vivo* rat models. In particular, mouse primary hepatocytes showed a significant activation of genes involved in steatotic injury, ~4 fold higher than the human PCLS. Steatosis is not reported with diclofenac treatment in clinical use. Genes associated with liver hyperbilirubinemia and inflammation were significantly induced in human PCLS and primary human hepatocytes. Clinical cases associated with inflammation leading to hepatitis and hyperbilirubinemia were reported earlier with diclofenac use [51, 52]. Our data suggest that transcriptomic analysis could provide early evidence to potential drug-induced liver diseases.
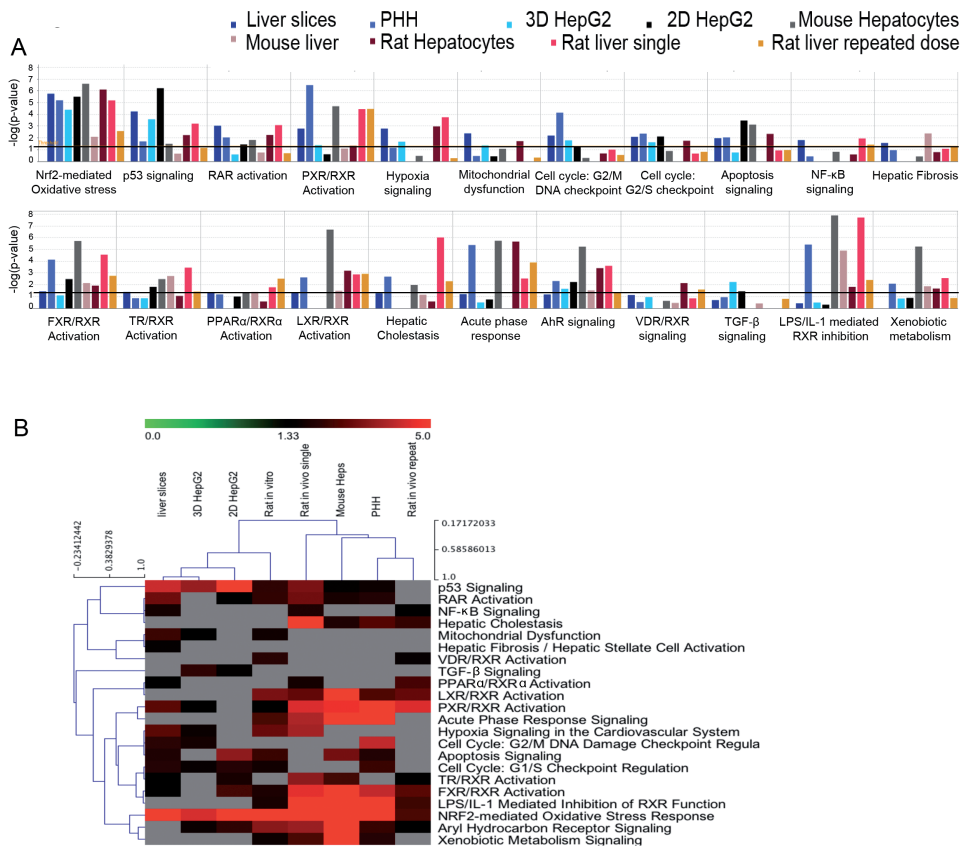
**Figure 5.** *Toxicity pathways from 'IPA Tox pathways' and their induction upon diclofenac treatment*. Canonical toxicity pathways in various models (A); Hierarchical clustering of toxicity pathways (B).

## Toxicity pathways activated upon diclofenac exposure

Our initial IPA analysis involved all signaling pathways and networks, without a focus on pathways involved in toxicity. Therefore, as a final step we focused solely on pathways that are related to toxicity. 22 pathways that are listed in the IPA program that have a significant role in xenobiotic toxicity response were further analyzed (Fig. 5A and B). Overall, mouse hepatocytes and rat *in vivo* single dose showed the strongest toxicity pathway activation. Genes involved in mitochondrial dysfunction were significantly activated in human PCLS, 3D HepG2 spheroids and rat primary hepatocytes. Cell cycle pathways; G2/M and G2/S checkpoint were significantly activated in all human cell models and rat hepatocytes (Fig. 5A). NF-κB signaling was significantly active in human PCLS and *in vivo* rat models. Other xenobiotic metabolism pathways FXR/RXR, TR/RXR, LXR/RXR were primarily activated in rodent models. Pathways involved in inflammatory signaling and acute phase response signaling were significantly activated in primary human hepatocytes, mouse hepatocytes and

rat models (Fig 5A).

Next we performed unsupervised hierarchical clustering of toxicity pathways to determine which model was closest to human PCLS (Fig 5B). The 3D HepG2 spheroid model was in closest proximity to PCLS with high similarity in the activation of mitochondrial dysfunction, PXR/RXR pathway, p53 signaling, hypoxia signaling, cell cycle: G2/M DNA damage checkpoint regulation and Nrf2 signaling. All primary hepatocyte models were also in close similarity in particular with respect to PXR/RXR activation, AhR signaling, LXR/RXR activation, hepatic cholestasis.

# DISCUSSION

With several *in vitro* and *in vivo* models in practical use as surrogates to study human specific DILI, comparative gene expression profiling of these models will provide an improved insight into the molecular changes that occur upon xenobiotic exposure. This type of comparative analysis will also help in characterizing the value of different *in vitro*/ *in vivo* models in predicting human specific responses associated with xenobiotic insult. In this study we used transcriptomics data to compare the effect of diclofenac treatment in human and rodent *in vitro*/*in vivo* models. Human PCLS showed a clear upregulation of molecular pathways that are associated with the pathogenicity of diclofenac induced liver injury. We anticipated a similar xenobiotic response in primary human hepatocytes (PHH). Although we observed a similar level of gene expression changes in PCLS and PHH, there were quite significant differences in the expression profile and even less similarities in the significantly affected cellular stress signaling pathways. Intriguingly, HepG2 cells cultured as spheroids showed diclofenac-induced activation of various stress signaling pathways comparable to human PCLS models; this was not observed in HepG2 cells cultured as 2D monolayer cells. This is likely due to increased metabolic competence observed in differentiated HepG2 spheroid cultures [14]. Phase 1 metabolism enzymes CYP2C9, CYP3A4 and phase II UGT's are involved in metabolism of diclofenac [37]; acyl glucuronides from glucuronosyl-transferse UGT2B7 and 4-hydroxy diclofenac from CYP2C9 are the major metabolites in diclofenac metabolism [53, 54]. These metabolites were previously shown to form in HepG2 spheroids exposed to diclofenac [14], suggesting a mechanistic response in HepG2 spheroids which is not seen in HepG2 2D cultures where drug metabolism enzymes are poorly expressed [55].

Diclofenac induces apoptosis by disrupting mitochondrial function and generating reactive oxygen species [24]. Genes that lead to mitochondrial dysfunction were seen only in human PCLS, 3D HepG2 spheroids and rat hepatocytes. Due to large inter-individual variability, primary human hepatocytes from 10 different cryopreserved donors were used for this transcriptomic study. However, the genes as-

sociated with mitochondrial dysfunction were not significantly activated in PHH, or in other primary hepatocytes or HepG2 cells in 2D culture. The differentiated HepG2 spheroids responded similarly to PCLS and rats treated with diclofenac, suggesting an increased functional complexity that has developed during differentiation of cells in 3D culture. Mitochondrial dysfunction has been proposed to be one of the under-lying causes of idiosyncrasy [56, 57]; failure to identify mitochondrial toxicity in some models is a caveat for predictive toxicogenomics assays.

Nrf2-mediated oxidative stress response is a major signaling pathway that was reported in diclofenac hepatotoxicity and significantly activated in all the mod-els in the current study. Earlier studies have shown that Heameoxyenase-1 (HO-1) in Nrf2 pathway is significantly induced upon diclofenac treatment [35]. Induction of HO-1 is seen in 3D HepG2 spheroids and other models compared in this study but not in 2D cultured HepG2 cells. FXR/RXR activation pathway was significantly activated upon diclofenac treatment in human (except 3D HepG2), rat and mouse models. FXR/RXR plays a role in bile acid regulation, lipid and glucose metabolism, [58] activation of drug metabolism enzymes [59] and protection against xenobiotic injury [60]. Activation of FXR/RXR pathway was also seen in diclofenac exposed rat livers in earlier studies [61] suggesting a role in diclofenac metabolism.

Genes and molecular events associated with diclofenac injury were highly enriched in DEG's from PCLS. PCLS may be a better alternative in understanding the short-term responses induced by the drugs, but its dependency on availability of human liver samples, variability due to different genetic backgrounds of individual samples and rapid decline of its native liver physiology have to be addressed for its relevance in exploring long-term effects of the xenobiotics. Similarly PHH have several limitations as described earlier for its dependence in toxicological assays. Although important stress signaling pathways such as Nrf2 oxidative stress pathway, genes associated with liver diseases such as cholestasis and steatosis were activat-ed in both PCLS and PHH there was a considerable difference in activated pathways between PCLS and PHH.

DEG's in rat and mouse primary hepatocytes shared higher similarity to their *in vivo* counterparts than to human models. Mouse hepatocytes had similar enriched pathways as mouse *in vivo*, and in some aspects genes associated with liver dis-eases were significantly higher in mouse hepatocytes, although this may be due to the low number of DEG's in mouse *in vivo* treatments. DEG's in rat had higher sim-ilarity to humans than mouse, highlighting the increased capacity of rat compared to mouse in predicting human specific responses. Nonetheless, animal models are poor in predicting human responses and their current dependency is mainly due to lack of complex models that closely reflect complex human systems. Human derived immortalized hepatocytes with improved metabolic competence and polarized he-

patocyte morphology such as 3D HepG2 spheroids used in this study gave similar responses as PCLS. 3D HepG2 spheroids showed upregulation of genes and pathways that are associated with the mechanism of diclofenac injury, which were not seen in same cells cultured in a 2D monolayer. The ability to sustain a stable phenotype for a longer period whilst maintaining their polarized morphology and increased metabolic competence is also ideal for studying repeated dose effects of drugs.

In the current investigation we have used transcriptomics data from in-house and publicly available sources. Moreover, the isolation procedures and culturing protocols have been different for all individual models. In addition, concentrations of diclofenac, mRNA isolation and Affymetrix hybridization procedures may have been slightly different. Despite these discrepancies we find quite strong overlap in various pathways that are activated in the different models. Moreover, several individual genes that are modulated across different models and that represent individual pathway activation are likely ideal markers for cross species comparison and human translation. Future next generation sequencing approaches of similar comparative treatment samples across species and models will further limit the variability and likely identify additional candidate translational biomarkers for DILI.

In conclusion, this study provides an overview of transcriptional responses in various models upon diclofenac exposure and their commonality. The ability to predict long-term effects of diclofenac and its toxicity pathways at gene level further supports toxicogenomic approaches in predicting toxicity of new chemical entities. New improved *in vitro* models such as the HepG2 spheroid model used in this analysis would be valuable to consider in future toxicogenomic approaches.

# REFERENCES

1       Naranjo, C. A., Busto, U. & Sellers, E. M. Difficulties in assessing adverse drug reactions in clinical trials. Progress in neuro-psychopharmacology & biological psychiatry 6, 651-657 (1982).

2       Kaplowitz, N. Idiosyncratic drug hepatotoxicity. Nat Rev Drug Discov 4, 489-499, doi:10.1038/nrd1750 (2005).

3       Knight, A. Systematic reviews of animal experiments demonstrate poor human clinical and toxicological utility. Altern Lab Anim 35, 641-659 (2007).

4       Graaf, I. A., Groothuis, G. M. & Olinga, P. Precision-cut tissue slices as a tool to predict metabolism of novel drugs. Expert opinion on drug metabolism & toxicology 3, 879-898, doi:10.1517/17425255.3.6.879 (2007).

5       Elferink, M. G. et al. Microarray analysis in rat liver slices correctly predicts in vivo hepatotoxicity. Toxicol Appl Pharmacol 229, 300-309, doi:10.1016/j.taap.2008.01.037 (2008).

6       de Graaf, I. A. et al. Preparation and incubation of precision-cut liver and intestinal slices for application in drug metabolism and toxicity studies. Nat Protoc 5, 1540-1551, doi:10.1038/nprot.2010.111 (2010).

7       LeCluyse, E. et al. Expression and regulation of cytochrome P450 enzymes in primary cultures of human hepatocytes. Journal of biochemical and molecular toxicology 14, 177-188 (2000).

8       Hart, S. N. et al. A comparison of whole genome gene expression profiles of HepaRG cells and HepG2 cells to primary human hepatocytes and human liver tissues. Drug metabolism and disposition: the biological fate of chemicals 38, 988-994, doi:10.1124/dmd.109.031831 (2010).

9       Jennen, D. G. et al. Comparison of HepG2 and HepaRG by whole-genome gene expression analysis for the purpose of chemical hazard identification. Toxicol Sci 115, 66-79, doi:10.1093/toxsci/kfq026 (2010).

10      Jetten, M. J., Kleinjans, J. C., Claessen, S. M., Chesne, C. & van Delft, J. H. Baseline and genotoxic compound induced gene expression profiles in HepG2 and HepaRG compared to primary human hepatocytes. Toxicol In Vitro 27, 2031-2040, doi:10.1016/j.tiv.2013.07.010 (2013).

11      Khetani, S. R. et al. Use of micropatterned cocultures to detect compounds that cause drug-induced liver injury in humans. Toxicol Sci 132, 107-117, doi:10.1093/toxsci/kfs326 (2013).

12      Guillouzo, A. et al. The human hepatoma HepaRG cells: a highly differentiated model for studies of liver metabolism and toxicity of xenobiotics. Chemico-biological interactions 168, 66-73, doi:10.1016/j.cbi.2006.12.003 (2007).

13      Gunness, P. et al. 3D organotypic cultures of human HepaRG cells: a tool for in vitro toxicity studies. Toxicol Sci 133, 67-78, doi:10.1093/toxsci/kft021 (2013).

14      Ramaiahgari et al. A 3D in vitro model of differentiated HepG2 cell spheroids with improved liver-like properties for repeated dose high-throughput toxicity studies. Archives of toxicology (2014).

15      Kiyosawa, N., Ando, Y., Manabe, S. & Yamoto, T. Toxicogenomic biomarkers for liver toxicity. Journal of toxicologic pathology 22, 35-52, doi:10.1293/tox.22.35 (2009).

16      Edgar, R., Domrachev, M. & Lash, A. E. Gene Expression Omnibus: NCBI gene expression and hybridization array data repository. Nucleic Acids Res 30, 207-210 (2002).

17      Brazma, A. et al. ArrayExpress--a public repository for microarray gene expression data at the EBI. Nucleic Acids Res 31, 68-71 (2003).

18      Mattingly, C. J., Rosenstein, M. C., Colby, G. T., Forrest, J. N., Jr. & Boyer, J. L. The Comparative Toxicogenomics Database (CTD): a resource for comparative toxicological studies. Journal of experimental zoology. Part A, Comparative experimental biology 305, 689-692, doi:10.1002/jez.a.307 (2006).

19      Hayes, K. R. et al. EDGE: a centralized resource for the comparison, analysis, and distribution of toxicogenomic information. Molecular pharmacology 67, 1360-1368, doi:10.1124/mol.104.009175 (2005).

20      Kiyosawa, N., Manabe, S., Yamoto, T. & Sanbuissho, A. Practical application of toxicogenomics for profiling toxicant-induced biological perturbations. International journal of molecular sciences 11, 3397-3412, doi:10.3390/ijms11093397 (2010).

21      Waters, M. et al. CEBS--Chemical Effects in Biological Systems: a public data repository integrating study design and toxicity data with microarray and proteomics data. Nucleic Acids Res 36, D892-900, doi:10.1093/nar/gkm755 (2008).

22      Uehara, T. et al. The Japanese toxicogenomics project: application of toxicogenomics. Molecu-

lar nutrition & food research 54, 218-227, doi:10.1002/mnfr.200900169 (2010).

23  Banks, A. T., Zimmerman, H. J., Ishak, K. G. & Harter, J. G. Diclofenac-associated hepatotoxicity: analysis of 180 cases reported to the Food and Drug Administration as adverse reactions. Hepatology 22, 820-827 (1995).

24  Gomez-Lechon, M. J. et al. Diclofenac induces apoptosis in hepatocytes by alteration of mitochondrial function and generation of ROS. Biochemical pharmacology 66, 2155-2167 (2003).

25  Bort, R., Ponsoda, X., Jover, R., Gomez-Lechon, M. J. & Castell, J. V. Diclofenac toxicity to hepatocytes: a role for drug metabolism in cell toxicity. J Pharmacol Exp Ther 288, 65-72 (1999).

26  Chung, H. et al. Comprehensive analysis of differential gene expression profiles on diclofenac-induced acute mouse liver injury and recovery. Toxicol Lett 166, 77-87, doi:10.1016/j.toxlet.2006.05.016 (2006).

27  Hadi, M. et al. Human precision-cut liver slices as an ex vivo model to study idiosyncratic drug-induced liver injury. Chemical research in toxicology 26, 710-720, doi:10.1021/tx300519p (2013).

28  Schaap, M. M. et al. Dissecting modes of action of non-genotoxic carcinogens in primary mouse hepatocytes. Arch Toxicol 86, 1717-1727, doi:10.1007/s00204-012-0883-6 (2012).

29  Irizarry, R. A. et al. Summaries of Affymetrix GeneChip probe level data. Nucleic Acids Res 31, e15 (2003).

30  Irizarry, R. A. et al. Exploration, normalization, and summaries of high density oligonucleotide array probe level data. Biostatistics 4, 249-264, doi:10.1093/biostatistics/4.2.249 (2003).

31  Smyth, G. K., Yang, Y. H. & Speed, T. Statistical issues in cDNA microarray data analysis. Methods Mol Biol 224, 111-136, doi:10.1385/1-59259-364-X:111 (2003).

32  Wolfinger, R. D. et al. Assessing gene significance from cDNA microarray expression data via mixed models. Journal of computational biology : a journal of computational molecular cell biology 8, 625-637, doi:10.1089/106652701753307520 (2001).

33  Kauffmann, A., Gentleman, R. & Huber, W. arrayQualityMetrics--a bioconductor package for quality assessment of microarray data. Bioinformatics 25, 415-416, doi:10.1093/bioinformatics/btn647 (2009).

34  Saeed, A. I. et al. TM4: a free, open-source system for microarray data management and analysis. BioTechniques 34, 374-378 (2003).

35  Cantoni, L. et al. Induction of hepatic heme oxygenase-1 by diclofenac in rodents: role of oxidative stress and cytochrome P-450 activity. Journal of hepatology 38, 776-783 (2003).

36  Miyamoto, Y., Ohshida, K. & Sasago, K. Protein assay for heme oxygenase-1 (HO-1) induced by chemicals in HepG2 cells. J Toxicol Sci 34, 709-714 (2009).

37  Tang, W. The metabolism of diclofenac--enzymology and toxicology perspectives. Current drug metabolism 4, 319-329 (2003).

38  Cosgrove, B. D. et al. Synergistic drug-cytokine induction of hepatocellular death as an in vitro approach for the study of inflammation-associated idiosyncratic drug hepatotoxicity. Toxicol Appl Pharmacol 237, 317-330, doi:10.1016/j.taap.2009.04.002 (2009).

39  Gu, Q. et al. Heme oxygenase-1 alleviates mouse hepatic failure through suppression of adaptive immune responses. J Pharmacol Exp Ther 340, 2-10, doi:10.1124/jpet.111.186551 (2012).

40  Fink, A. L. Chaperone-mediated protein folding. Physiol Rev 79, 425-449 (1999).

41  Thimmulappa, R. K. et al. Identification of Nrf2-regulated genes induced by the chemopreventive agent sulforaphane by oligonucleotide microarray. Cancer Res 62, 5196-5203 (2002).

42  van Bladeren, P. J. Glutathione conjugation as a bioactivation reaction. Chemico-biological interactions 129, 61-76 (2000).

43  Itoh, K. et al. An Nrf2/small Maf heterodimer mediates the induction of phase II detoxifying enzyme genes through antioxidant response elements. Biochemical and biophysical research communications 236, 313-322 (1997).

44  Nguyen, T., Huang, H. C. & Pickett, C. B. Transcriptional regulation of the antioxidant response element. Activation by Nrf2 and repression by MafK. J Biol Chem 275, 15466-15473, doi:10.1074/jbc.M000361200 (2000).

45  Dhakshinamoorthy, S. & Jaiswal, A. K. Small maf (MafG and MafK) proteins negatively regulate antioxidant response element-mediated expression and antioxidant induction of the NAD(P)H:Quinone oxidoreductase1 gene. J Biol Chem 275, 40134-40141, doi:10.1074/jbc.M003531200 (2000).

46  Karawajew, L., Rhein, P., Czerwony, G. & Ludwig, W. D. Stress-induced activation of the p53

tumor suppressor in leukemia cells and normal lymphocytes requires mitochondrial activity and reactive oxygen species. Blood 105, 4767-4775, doi:10.1182/blood-2004-09-3428 (2005).

47    Levine, A. J. p53, the cellular gatekeeper for growth and division. Cell 88, 323-331 (1997).

48    Jin, S. et al. GADD45-induced cell cycle G2-M arrest associates with altered subcellular distribution of cyclin B1 and is independent of p38 kinase activity. Oncogene 21, 8696-8704, doi:10.1038/sj.onc.1206034 (2002).

49    Hickey, E. J., Raje, R. R., Reid, V. E., Gross, S. M. & Ray, S. D. Diclofenac induced in vivo nephrotoxicity may involve oxidative stress-mediated massive genomic DNA fragmentation and apoptotic cell death. Free radical biology & medicine 31, 139-152 (2001).

50    Wang, X. p53 regulation: teamwork between RING domains of Mdm2 and MdmX. Cell Cycle 10, 4225-4229, doi:10.4161/cc.10.24.18662 (2011).

51    Sallie, R. W., McKenzie, T., Reed, W. D., Quinlan, M. F. & Shilkin, K. B. Diclofenac hepatitis. Australian and New Zealand journal of medicine 21, 251-255 (1991).

52    Ramakrishna, B. & Viswanath, N. Diclofenac-induced hepatitis: case report and literature review. Liver 14, 83-84 (1994).

53    King, C., Tang, W., Ngui, J., Tephly, T. & Braun, M. Characterization of rat and human UDP-glucuronosyltransferases responsible for the in vitro glucuronidation of diclofenac. Toxicol Sci 61, 49-53 (2001).

54    Leemann, T., Transon, C. & Dayer, P. Cytochrome P450TB (CYP2C): a major monooxygenase catalyzing diclofenac 4'-hydroxylation in human liver. Life sciences 52, 29-34 (1993).

55    Westerink, W. M. a. & Schoonen, W. G. E. J. Cytochrome P450 enzyme levels in HepG2 cells and cryopreserved primary human hepatocytes and their induction in HepG2 cells. Toxicology in vitro : an international journal published in association with BIBRA 21, 1581-1591, doi:10.1016/j.tiv.2007.05.014 (2007).

56    Liguori, M. J. et al. Microarray analysis in human hepatocytes suggests a mechanism for hepatotoxicity induced by trovafloxacin. Hepatology 41, 177-186, doi:10.1002/hep.20514 (2005).

57    Li, A. P. A review of the common properties of drugs with idiosyncratic hepatotoxicity and the "multiple determinant hypothesis" for the manifestation of idiosyncratic drug toxicity. Chemico-biological interactions 142, 7-23 (2002).

58    Matsukuma, K. E. et al. Coordinated control of bile acids and lipogenesis through FXR-dependent regulation of fatty acid synthase. Journal of lipid research 47, 2754-2761, doi:10.1194/jlr.M600342-JLR200 (2006).

59    Gnerre, C., Blattler, S., Kaufmann, M. R., Looser, R. & Meyer, U. A. Regulation of CYP3A4 by the bile acid receptor FXR: evidence for functional binding sites in the CYP3A4 gene. Pharmacogenetics 14, 635-645 (2004).

60    Lee, F. Y. et al. Activation of the farnesoid X receptor provides protection against acetaminophen-induced hepatic toxicity. Mol Endocrinol 24, 1626-1636, doi:10.1210/me.2010-0117 (2010).

61    Deng, X. et al. Gene expression profiles in livers from diclofenac-treated rats reveal intestinal bacteria-dependent and -independent pathways associated with liver injury. J Pharmacol Exp Ther 327, 634-644, doi:10.1124/jpet.108.140335 (2008).

# SUPPLEMENTARY DATA

| Ingenuity Canonical Pathways | -log(p-value) |
|---|---|
| Remodeling of Epithelial Adherens Junctions | 3.66E+00 |
| tRNA Charging | 2.63E+00 |
| 14-3-3-mediated Signaling | 2.61E+00 |
| Epithelial Adherens Junction Signaling | 2.49E+00 |
| NRF2-mediated Oxidative Stress Response | 2.32E+00 |
| Bladder Cancer Signaling | 2.26E+00 |
| p53 Signaling | 1.95E+00 |
| Sertoli Cell-Sertoli Cell Junction Signaling | 1.94E+00 |
| Gap Junction Signaling | 1.88E+00 |
| Germ Cell-Sertoli Cell Junction Signaling | 1.83E+00 |
| Activation of IRF by Cytosolic Pattern Recognition Receptors | 1.78E+00 |
| TCA Cycle II (Eukaryotic) | 1.78E+00 |
| Cell Cycle: G1/S Checkpoint Regulation | 1.70E+00 |
| Neuregulin Signaling | 1.70E+00 |
| Breast Cancer Regulation by Stathmin1 | 1.69E+00 |
| IL-17A Signaling in Gastric Cells | 1.63E+00 |
| Thio-molybdenum Cofactor Biosynthesis | 1.60E+00 |
| Glutamate Removal from Folates | 1.60E+00 |
| Lipoate Salvage and Modification | 1.60E+00 |
| L-cysteine Degradation II | 1.60E+00 |
| Asparagine Biosynthesis I | 1.60E+00 |
| Chronic Myeloid Leukemia Signaling | 1.57E+00 |
| HMGB1 Signaling | 1.55E+00 |
| Guanosine Nucleotides Degradation III | 1.46E+00 |
| Prolactin Signaling | 1.46E+00 |
| Assembly of RNA Polymerase III Complex | 1.40E+00 |
| Role of IL-17A in Psoriasis | 1.40E+00 |
| Urate Biosynthesis/Inosine 5'-phosphate Degradation | 1.40E+00 |
| PDGF Signaling | 1.37E+00 |
| Thrombopoietin Signaling | 1.32E+00 |
| Lipoate Biosynthesis and Incorporation II | 1.31E+00 |
| Sulfate Activation for Sulfonation | 1.31E+00 |
| Cysteine Biosynthesis/Homocysteine Degradation | 1.31E+00 |

**Supplementary S1.** Molecular Pathways associated with 471 overlapping genes in human cell models (from Figure 1B); as calculated by Ingenuity Pathway Analysis.
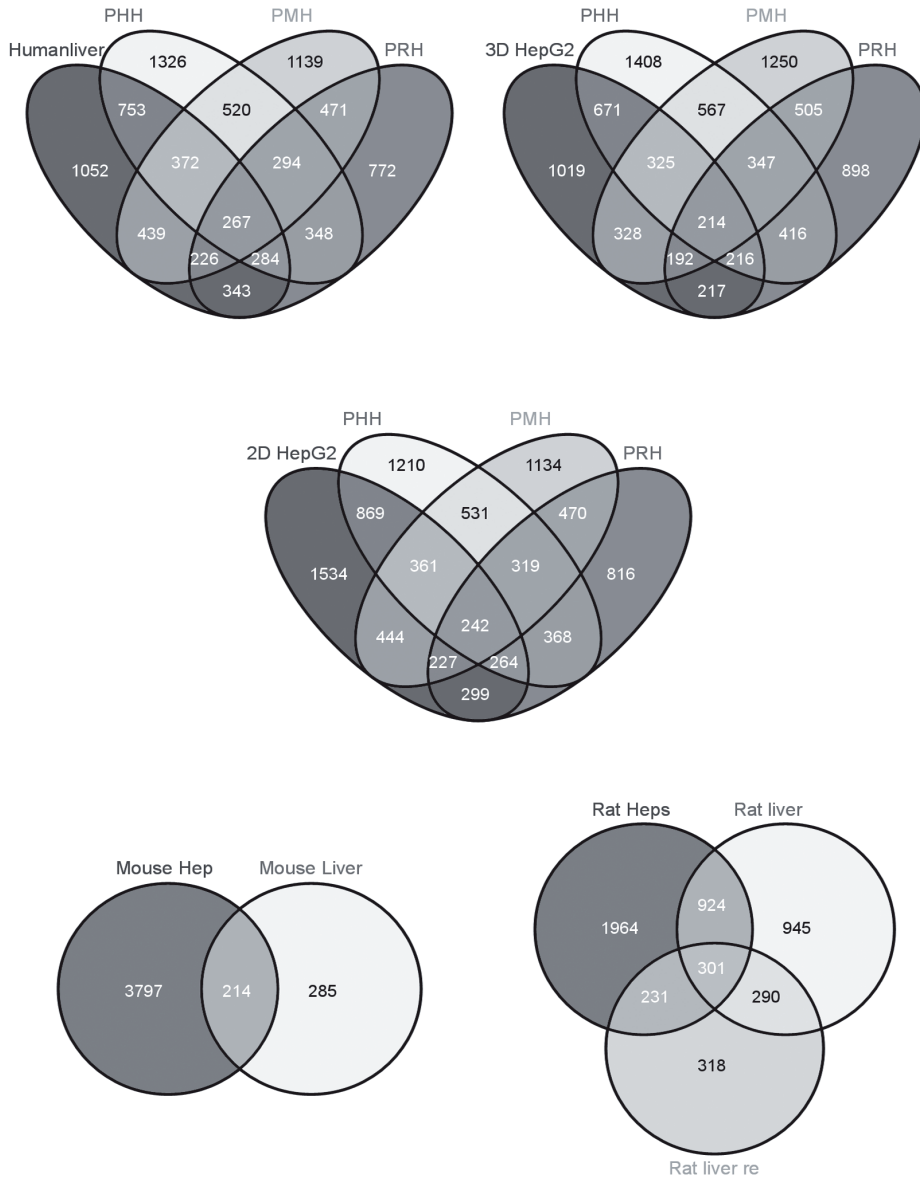
**Supplementary S2.** Venn diagrams of DEG's upon diclofenac treatment in human, mouse and rat model systems (PHH- primary human hepatocytes; PMH - primary mouse hepatocytes; PRH - primary rat hepatocytes).

**Supplementary S3.** Venn diagrams of significantly altered canonical pathways from human, mouse and rat DEG's upon diclofenac exposure.
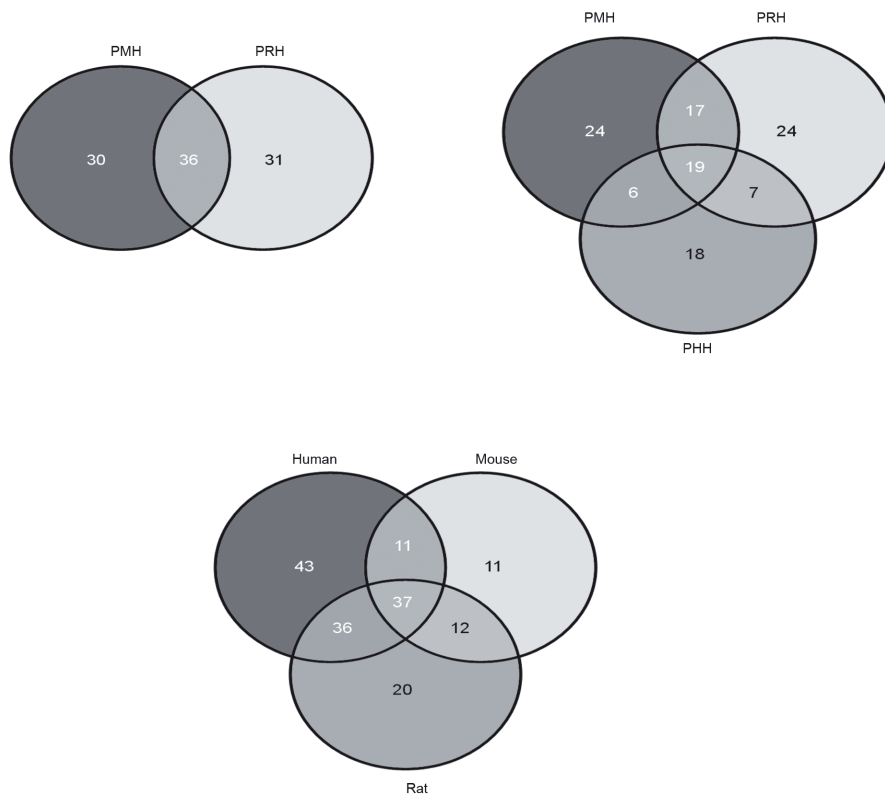


All human, all mouse and all rat models

**Supplementary S4.** List of pathways that overlap between human *in vitro* models and primary hepatocytes of human, mouse and rat. (PHH- primary human hepatocytes; PMH - primary mouse hepatocytes; PRH - primary rat hepatocytes).

| Molecular pathways that are common between 3D HepG2_PHH_PMH_PRH | |
|---|---|
| **Ingenuity Canonical Pathways** | **-log(p-value)** |
| Cell Cycle: G1/S Checkpoint Regulation | 4.01E+00 |
| NRF2-mediated Oxidative Stress Response | 3.59E+00 |
| Tryptophan Degradation X (Mammalian, via Tryptamine) | 3.09E+00 |
| Putrescine Degradation III | 3.09E+00 |
| tRNA Charging | 2.99E+00 |
| Tyrosine Degradation I | 2.87E+00 |
| Dopamine Degradation | 2.73E+00 |
| Hepatic Fibrosis / Hepatic Stellate Cell Activation | 2.24E+00 |
| Noradrenaline and Adrenaline Degradation | 2.20E+00 |
| Complement System | 2.20E+00 |
| PXR/RXR Activation | 2.18E+00 |

| | |
|---|---|
| Mevalonate Pathway I | 2.07E+00 |
| Histamine Degradation | 2.07E+00 |
| Choline Biosynthesis III | 2.00E+00 |
| Phenylalanine Degradation IV (Mammalian, via Side Chain) | 1.94E+00 |
| Colanic Acid Building Blocks Biosynthesis | 1.94E+00 |
| Asparagine Biosynthesis I | 1.93E+00 |
| Fatty Acid α-oxidation | 1.88E+00 |
| Oxidative Ethanol Degradation III | 1.88E+00 |
| RAN Signaling | 1.83E+00 |
| Superpathway of Geranylgeranyldiphosphate Biosynthesis I (via Mevalonate) | 1.83E+00 |
| Ethanol Degradation IV | 1.77E+00 |
| FXR/RXR Activation | 1.76E+00 |
| D-myo-inositol (1,4,5)-trisphosphate Degradation | 1.73E+00 |
| Aryl Hydrocarbon Receptor Signaling | 1.68E+00 |
| Serotonin Degradation | 1.63E+00 |
| Taurine Biosynthesis | 1.63E+00 |
| Glycine Biosynthesis I | 1.63E+00 |
| Antioxidant Action of Vitamin C | 1.60E+00 |
| Phospholipases | 1.57E+00 |
| Polyamine Regulation in Colon Cancer | 1.56E+00 |
| Tumoricidal Function of Hepatic Natural Killer Cells | 1.49E+00 |
| Superpathway of D-myo-inositol (1,4,5)-trisphosphate Metabolism | 1.49E+00 |
| Xenobiotic Metabolism Signaling | 1.49E+00 |
| Pancreatic Adenocarcinoma Signaling | 1.43E+00 |
| Superpathway of Cholesterol Biosynthesis | 1.40E+00 |
| Heme Degradation | 1.33E+00 |
| Phenylethylamine Degradation I | 1.33E+00 |
| Melatonin Degradation II | 1.33E+00 |
| Arginine Degradation I (Arginase Pathway) | 1.33E+00 |
| NAD Biosynthesis III | 1.33E+00 |
| L-cysteine Degradation I | 1.33E+00 |
| Ethanol Degradation II | 1.31E+00 |
| p38 MAPK Signaling | 1.31E+00 |

| Molecular pathways that are common between 2D HepG2_PHH_PMH_PRH | |
|---|---|
| **Ingenuity Canonical Pathways** | **-log(p-value)** |
| 4-hydroxyproline Degradation I | 3.76E+00 |
| tRNA Charging | 2.82E+00 |
| Superpathway of Serine and Glycine Biosynthesis I | 2.60E+00 |
| Tumoricidal Function of Hepatic Natural Killer Cells | 2.43E+00 |
| Complement System | 2.07E+00 |
| NRF2-mediated Oxidative Stress Response | 2.04E+00 |
| Cell Cycle: G1/S Checkpoint Regulation | 2.02E+00 |

| | |
|---|---|
| Hepatic Fibrosis / Hepatic Stellate Cell Activation | 2.02E+00 |
| Asparagine Biosynthesis I | 1.88E+00 |
| Tryptophan Degradation X (Mammalian, via Tryptamine) | 1.74E+00 |
| Putrescine Degradation III | 1.74E+00 |
| FXR/RXR Activation | 1.60E+00 |
| Lipoate Biosynthesis and Incorporation II | 1.58E+00 |
| Proline Degradation | 1.58E+00 |
| Taurine Biosynthesis | 1.58E+00 |
| Thiosulfate Disproportionation III (Rhodanese) | 1.58E+00 |
| Glycerol-3-phosphate Shuttle | 1.58E+00 |
| Glycine Biosynthesis I | 1.58E+00 |
| Apoptosis Signaling | 1.54E+00 |
| VEGF Signaling | 1.52E+00 |
| Dopamine Degradation | 1.51E+00 |
| Induction of Apoptosis by HIV1 | 1.37E+00 |
| Aldosterone Signaling in Epithelial Cells | 1.31E+00 |

| Molecular pathways that are common between human precision cut liver slices_PHH_PMH_PRH | |
|---|---|
| **Ingenuity Canonical Pathways** | **-log(p-value)** |
| Putrescine Degradation III | 4.16E+00 |
| Polyamine Regulation in Colon Cancer | 3.59E+00 |
| PXR/RXR Activation | 3.53E+00 |
| Histamine Degradation | 3.22E+00 |
| NRF2-mediated Oxidative Stress Response | 2.95E+00 |
| Fatty Acid α-oxidation | 2.92E+00 |
| Oxidative Ethanol Degradation III | 2.92E+00 |
| Arginine Degradation I (Arginase Pathway) | 2.91E+00 |
| Tryptophan Degradation X (Mammalian, via Tryptamine) | 2.83E+00 |
| Ethanol Degradation IV | 2.75E+00 |
| Cell Cycle: G1/S Checkpoint Regulation | 2.66E+00 |
| Acute Phase Response Signaling | 2.50E+00 |
| Dopamine Degradation | 2.48E+00 |
| Hepatic Fibrosis / Hepatic Stellate Cell Activation | 2.41E+00 |
| Sucrose Degradation V (Mammalian) | 2.38E+00 |
| Tumoricidal Function of Hepatic Natural Killer Cells | 2.31E+00 |
| Retinoate Biosynthesis I | 2.08E+00 |
| LXR/RXR Activation | 2.07E+00 |
| Ethanol Degradation II | 2.04E+00 |
| Noradrenaline and Adrenaline Degradation | 1.96E+00 |
| Complement System | 1.96E+00 |
| Protein Ubiquitination Pathway | 1.92E+00 |
| Guanosine Nucleotides Degradation III | 1.90E+00 |
| Aryl Hydrocarbon Receptor Signaling | 1.88E+00 |

| | |
|---|---|
| Acetyl-CoA Biosynthesis III (from Citrate) | 1.84E+00 |
| Asparagine Biosynthesis I | 1.84E+00 |
| ILK Signaling | 1.78E+00 |
| The Visual Cycle | 1.71E+00 |
| Small Cell Lung Cancer Signaling | 1.71E+00 |
| p38 MAPK Signaling | 1.57E+00 |
| Purine Nucleotides Degradation II (Aerobic) | 1.56E+00 |
| D-myo-inositol (1,4,5)-trisphosphate Degradation | 1.56E+00 |
| Lipoate Biosynthesis and Incorporation II | 1.54E+00 |
| Proline Degradation | 1.54E+00 |
| 4-hydroxyproline Degradation I | 1.54E+00 |
| Atherosclerosis Signaling | 1.51E+00 |
| Xenobiotic Metabolism Signaling | 1.47E+00 |
| LPS/IL-1 Mediated Inhibition of RXR Function | 1.47E+00 |
| FXR/RXR Activation | 1.47E+00 |
| Apoptosis Signaling | 1.41E+00 |
| Serotonin Degradation | 1.40E+00 |
| Gluconeogenesis I | 1.40E+00 |
| Methionine Salvage II (Mammalian) | 1.37E+00 |
| Phospholipases | 1.34E+00 |
| HMGB1 Signaling | 1.33E+00 |
| Superpathway of D-myo-inositol (1,4,5)-trisphosphate Metabolism | 1.33E+00 |

**Common elements in "2D HepG2" and "Human liver":**
4-hydroxyproline Degradation I
Cell Cycle: G1/S Checkpoint Regulation
Lipoate Biosynthesis and Incorporation II
Proline Degradation
Apoptosis Signaling

**Common elements in "3D HepG2" and "Human liver":**
Noradrenaline and Adrenaline Degradation
PXR/RXR Activation
Histamine Degradation
Fatty Acid α-oxidation
Oxidative Ethanol Degradation III
Ethanol Degradation IV
D-myo-inositol (1,4,5)-trisphosphate Degradation
Aryl Hydrocarbon Receptor Signaling
Serotonin Degradation
Phospholipases
Polyamine Regulation in Colon Cancer
Superpathway of D-myo-inositol (1,4,5)-trisphosphate Metabolism
Xenobiotic Metabolism Signaling
Arginine Degradation I (Arginase Pathway)
Ethanol Degradation II
p38 MAPK Signaling

**Common elements in "3D HepG2", "2D HepG2" and "Human PCLS":**
NRF2-mediated Oxidative Stress Response
Tryptophan Degradation X (Mammalian, via Tryptamine)
Putrescine Degradation III
Dopamine Degradation
Hepatic Fibrosis / Hepatic Stellate Cell Activation
Complement System
Asparagine Biosynthesis I
FXR/RXR Activation
Tumoricidal Function of Hepatic Natural Killer cells

3D HepG2_PHH_PMH_PRH

2D HepG2_PHH_PMH_PRH

15

3

6

9

16

5

16

hPCLS_PHH_PMH_PRH

105
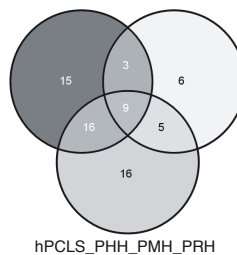
**Supplementary S5.** Genes associated with liver diseases from models systems in which the disease state is positively predicted from ingenuity pathway analysis.

## Liver inflammation

**Human liver slices**

| | | | | | |
|---|---|---|---|---|---|
| ABCB4 | ABCC2 | ADIPOR2 | APOB | CAMLG | CCL2 |
| CCL8 | CD274 | COL3A1 | CXCL1 | | |
| CXCL10 | CXCL2 | CYP2E1 | DDX5 | FKBP1A | GSTP1 |
| IFNAR1 | IFNAR2 | IL10 | RBIL8 | INSR | MMP9 |
| MTOR | NAGLU | PEMT | POR | PPARA | PPARG |
| PPP3CA | PPP3CBP | PP3CC | RASSF1 | SOD2 | THOP1 |
| TIMP1 | | | | | |

**Primary human hepatocytes**

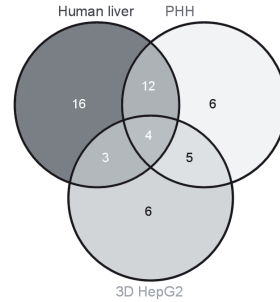| | | | | | |
|---|---|---|---|---|---|
| ABCB4 | ABCC2 | ADIPOR2 | AGTR1 | APOB | CAMLG |
| CSF1 | CXCL1 | CXCL10 | CXCL2 | CYP2E1 | EPO |
| GSTP1 | IL8 | NR3C1 | PDE3B | POLA1 | POLB |
| POLD1 | POR | PPARA | PPP3R1 | RASSF1 | |
| SLC10A1 | SLCO1B1 | SOD2 | THOP1 | | |

**3D HepG2**

| | | | | | |
|---|---|---|---|---|---|
| ADIPOR2 | ADK | AGTR1 | AMY2B | CAMLG | EPO |
| IFNGR1 | IL8 | IMPDH2 | NR3C1 | PEMT | POLA1 |
| POR | PPARG | PPP3CA | PPP3R1 | SLC6A4 | TNFRS- |
| F1A | | | | | |



## Liver Hyperplasia

**Human liver slices**

| | | | | | |
|---|---|---|---|---|---|
| A1BG | ABCC2 | ABCC3 | ADAM17 | ADAM9 | ADH1C |
| AKR1B10 | AKR1D1 | ALDOB | ANXA2 | APOA5 | ARPC5 |
| ATF5 | ATP1B3 | AXIN1 | C1S | C7 | CA2 |
| CASD1 | CASP8 | CDC25B | CDK14 | CDK5 | CD- |
| KN1B | CHUK | CKS2 | CP | CSE1L | CTNNB1 |
| CTSD | CYP1A1 | DGAT2 | DPP3 | DSE | DYNLL1 |
| EIF2AK2 | EIF4E | ELMO1 | EPHA2 | ERBB3 | FAIM |
| FAM83D | FCN3 | FOS | FRK | FUCA1 | GOLM1 |
| GOT1 | GPAA1 | H2AFY | HABP2 | HGS | HNRNP- |
| DL | HPD | HSD17B6 | HSP90AA1 | HSP90AB1 | HSPA8 |
| HTATIP2 | IFNAR1 | IFNAR2 | IL8 | ING4 | ISG15 |
| JUN | KAT5 | KDR | KIT | KNG1 | KRAS |
| LBP | MAPRE1 | MDM2 | MED30 | MMP9 | MTOR |
| NFE2L2 | NQO1 | NUPR1 | OSMR | PDGFRB | PDK4 |
| PFN1 | PGK1 | PHGDH | PLAUR | PNRC1 | POLE4 |
| POR | PPARG | PPP1R3C | PRDX1 | PRDX3 | PTEN |
| PTGS2 | RAD50 | RASSF1 | RASSF5 | RB1 | RDH16 |
| RELA | RELB | RIOK1 | RNMT | RPL4 | RRM1 |
| S100A4 | SERPINE1 | SLC22A9 | SLC35C1 | SLC47A1 | SL- |
| CO1B3 | SPARC | SRRT | SULF2 | TMX2 | TOP2B |
| TPI1 | TRIM8 | TUBB4B | TXN | TYMS | USP9X |
| VEGFA | VPS37A | VTN | WBSCR22 | YWHAG | |

**Primary human hepatocytes**

| | | | | | |
|---|---|---|---|---|---|
| A1BG | AADAC | ABCB1 | ABCC2 | ABCC3 | ABCC6 |
| ADAM17 | ADH1B | AKR1B10 | AKR1C1/AKR1C2 | | ALDOB |
| ANXA1 | ARID2 | ARSE | ASF1B | ATP1B3 | AURKA |
| BAG2 | BCL2L1 | BSG | C4BPA | C9 | CA2 |
| CA9 | CAP2 | CASD1 | CCNB1 | CCND1 | CD44 |
| CDK5 | CDK5RAP3 | CDKN1A | CENPH | CKS2 | COPG1 |
| CP | CREB3L3 | CRELD2 | CSF1 | CSPP1 | CY- |
| P1A1 | DGAT2 | DLC1 | DSE | DYNLL1 | E2F5 |
| ECT2 | EIF1AX | ELMO1 | ENPP2 | EPCAM | EPHA2 |
| ERBB2 | ERBB3 | FAIM | FAM83D | FGL1 | FOXQ1 |
| FUCA1 | GC | H2AFY | HABP2 | HAMP | HGS |
| HMGB1 | HNRNPDL | HPD | HPX | HSD17B6 | HSPA5 |
| HSPA8 | IL8 | IPO7 | ISG15 | ITIH4 | JUN |
| KEAP1 | LBP | LRG1 | MAP3K4 | MAT2A | MDM2 |
| MED30 | MET | MLF1IP | MT2A | MYO6 | NCAPG |
| NNMT | NPC1 | NR1H4 | NUPR1 | NUSAP1 | ORC6 |
| PAQR4 | PDK4 | PGLYRP2 | PHGDH | PKM | PLG |
| POLD3 | POLE | POLE2 | POLE3 | POLE4 | POR |
| PPP1R3C | PSEN1 | RAD50 | RASAL2 | RASSF1 | RB1 |

| | | | | | | | | | |
|---|---|---|---|---|---|---|---|---|---|
| RDH16 | RELA | RIOK1 | RNMT | RRM1 | RRM2 | S100A4 | SCP2 | SERPINE1 | SLC10A1 |
| SLC15A1 | SLC22A1 | SLCO1B1 | SMO | SMYD5 | SOX4 | SQLE | SRRT | SULF2 | TACSTD2 |
| TBP | TDO2 | TFCP2 | TM4SF1 | TMX2 | TOP2A | TPX2 | TRIM8 | TUBB4B | TYMP |
| TYMS | UBE2C | UBE2T | UCHL1 | UGT1A6 | VEGFA | VTN | WHSC1 | | |
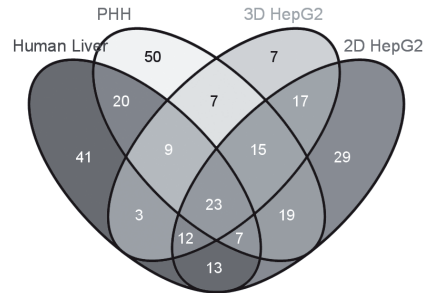
**3D HepG2**

| | | | | | | | | | |
|---|---|---|---|---|---|---|---|---|---|
| ABL1 | ADAM17 | AKR1D1 | ANLN | APOA5 | ARPC5 | ASRGL1 | ATAD5 | ATP1B3 | AURKA |
| AXIN2 | BIRC5 | CASD1 | CASP2 | CASP8 | CCDC138 | CCNB1 | CDC25B | CDK5 | CDKN3 |
| CKS2 | CSE1L | CTNNB1 | CYP1A1 | DGAT2 | DKK1 | DSE | E2F5 | ECT2 | EIF1AX |
| ENPP2 | EPHA2 | ERBB3 | FAM83D | FOS | GLUD1 | GOT1 | GSTT1 | H2AFY | HAMP |
| HEATR6 | HGS | HPD | IGFBP3 | IL8 | ISG15 | JUN | MAP3K4 | MAVS | MDM2 |
| MED30 | MLF1IP | MT2A | NCAPG | NPC1 | NQO1 | NUPR1 | NUSAP1 | ORC6 | OSMR |
| PGK1 | PKM | PLK4 | POLE2 | POLE4 | POR | PPARG | RIOK1 | RNMT | RPL13A |
| RRM1 | RRM2 | S100A4 | SCP2 | SERF2 | SERPINE1 | SLC2A1 | SOAT2 | SOCS1 | SQSTM1 |
| SRRT | STAT3 | SULF2 | TM4SF1 | TOP2A | TP53 | TPI1 | TPX2 | TUBB4B | TYMS |
| UBE2C | VEGFA | VPS37A | | | | | | | |

**2D HepG2**

| | | | | | | | | | |
|---|---|---|---|---|---|---|---|---|---|
| AADAC | ABCB1 | ABCC1 | ABCC2 | ABCC5 | ABCC6 | ADAM17 | AKR1B10 | AKR1C1/AKR1C2 | |
| AKR1D1 | APOA5 | ARL2 | ASF1B | ASRGL1 | ATAD5 | ATF5 | ATP1B3 | AXIN2 | B4GALT1 |
| BIRC5 | BRAF | C7 | CASP2 | CASP8 | CCDC138 | CCNB1 | CDC25B | CDK5 | CDKN1B |
| CDKN3 | CRELD2 | CSE1L | CST3 | CTNNB1 | CTSD | DGAT2 | DKK1 | DLC1 | E2F5 |
| E2F8 | EIF1AX | EIF3H | ENPP2 | EPHA2 | GDPD1 | GOT1 | GPAA1 | GSTT1 | HAMP | HEATR6 |
| FGFR1 | FOS | FOXQ1 | FRK | GDPD1 | GOT1 | GPAA1 | GSTT1 | HAMP | HEATR6 |
| HMGB1 | HP | HPD | HPX | HSPA5 | IFT81 | IGFBP3 | IL8 | ING4 | ISG15 |
| JUN | KCTD2 | LETM1 | LMCD1 | LRG1 | MAP3K4 | MCRS1 | MDM2 | MED30 | MMP2 |
| MYO6 | N4BP2L2 | NCAPG | NFE2L2 | NKD1 | NPC1 | NRAS | NUPR1 | ORC6 | OSMR |
| PAQR4 | PFN1 | PGK1 | PIK3CA | PIK3IP1 | PKM | PLK4 | PNRC1 | POLD3 | POLE |
| POLE2 | POLG | POR | PPARG | PPP1R3C | PRPF6 | RAD50 | RASSF1 | RIOK1 | RNMT |
| RRM1 | RRM2 | S100A4 | SERPINA6 | SERPINC1 | SERPINE1 | SLC2A1 | SLC35C1 | SMO | SOAT2 |
| SOX4 | SPARC | SQSTM1 | STAT3 | TGFB1 | TM4SF1 | TOP2A | TP53 | TRIM8 | TUBB4B |
| TYMS | UBE2C | UBE2T | USP9X | VEGFA | VPS37A | | | | |

## Liver Steatosis

**Human liver slices**

| | | | | | |
|---|---|---|---|---|---|
| ACACA | ACOX1 | ACOX2 | ADIPOR2 | APOB | AR |
| CAT | CCL2 | CYP2E1 | FABP4 | GNMT | GSTP1 |
| NPHP3 | PEMT | PLIN2 | PPARA | PPARG | PPARG- |
| C1A | SOD2 | UCP2 | | | |

**Primary human hepatocytes**

| | | | | | |
|---|---|---|---|---|---|
| ACADL | ACOX1 | ACOX2 | ADIPOR2 | APOB | CD44 |
| CYP2E1 | CYP4A11 | GSTP1 | HMGCR | MOGAT2 | |
| MOGAT3 | PDE3B | PLIN2 | PPARA | PPARGC1A | SOD2 |
| SPP1 | SREBF1 | | | | |

**2D HepG2**

| | | | | | |
|---|---|---|---|---|---|
| ACOX2 | CAT | CPT1A | DGAT1 | FASN | |
| MOGAT3 | PDE8A | PEMT | PLIN2 | PPARA | PPARG |
| PPARGC1A | TNFRSF1A | UCP2 | | | |

Human Liver — PHH — 2D HepG2 Venn diagram: Human Liver 6, overlap Human Liver/PHH 6, PHH 8, center 4, Human Liver/2D HepG2 4, PHH/2D HepG2 1, 2D HepG2 5
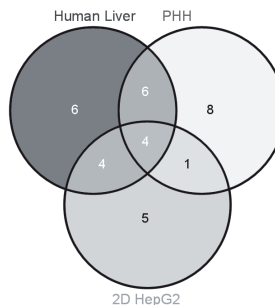
## Liver Cholestasis

**Human liver slices**

| | | | | | |
|---|---|---|---|---|---|
| ABCB4 | ABCB6 | ABCB7 | ABCC2 | ABCC3 | ABCG1 |
| ABCG2 | ADH1C | ADH4 | AKR1C3 | AKR1D1 | BAAT |
| CAT | CYP27A1 | CYP7B1 | GPX2 | IL8 | LBP |
| LIPA | MGST2 | NR0B2 | RDH16 | SCD | |
| SLC12A2 | SLC25A13 | SULT1A2 | UGP2 | UGT2B15 | |

**Primary human hepatocytes**

| | | | | | |
|---|---|---|---|---|---|
| ABCB4 | ABCB6 | ABCC2 | ABCC3 | ABCG2 | ACSL1 |
| ADH4 | ADH6 | APOA1 | ATP8B1 | BAAT | CY- |
| P27A1 | HDLBP | HMGCR | HPX | IL8 | LBP |
| LIPC | MGST2 | MGST3 | NR0B2 | NR1H4 | PAH |
| RDH16 | SCD | SCP2 | SLC10A1 | SLC22A1 | SL- |
| C35B1 | SLCO1B1 | SREBF1 | SULT1A1 | SULT1A2 | UGP2 |
| UGT2B15 | | | | | |

**3D HepG2**

| | | | | | |
|---|---|---|---|---|---|
| ABCG2 | ACSL1 | ADH6 | AKR1D1 | BLVRA | CYP7A1 |
| GK | GPX2 | HMGCR | HNF1B | IL8 | LIPA |
| MGST2 | MTTP | NR0B2 | SCP2 | SLC25A6 | UGP2 |

Human liver — PHH — 3D HepG2 Venn diagram: Human liver 8, overlap Human liver/PHH 12, PHH 14, center 5, Human liver/3D HepG2 3, PHH/3D HepG2 4, 3D HepG2 6
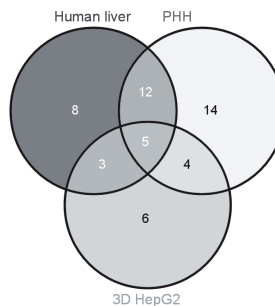
# CHAPTER 5

# A SCREEN FOR APOPTOTIC SYNERGISM BETWEEN CLINICAL RELEVANT NEPHROTOXICANT AND THE CYTOKINE TNF-α

Giulia Benedetti[1],*, Sreenivasa C. Ramaiahgari[1],*, Bram Herpers[1], Bob van de Water[1], Leo S. Price[1], Marjo de Graauw[1]

[1]Division of Toxicology, Leiden Academic Centre for Drug Research, Leiden University, Leiden, The Netherlands.

# ABSTRACT

Nephrotoxicity remains one of the main reasons for post-market drug withdrawal. Tumour necrosis factor α (TNF-α) secretion has been shown to underlie the nephrotoxicity induced by some of these drugs. Yet, there is currently no reliable and sensitive *in vitro* assay available to screen for nephrotoxicants of which toxicity largely depends on TNF-α secretion. Therefore, we developed and applied a sensitive fluorescence-based *in vitro* assay for TNF-α-mediated nephrotoxicity screening using mouse immortalized proximal tubular epithelial cells (IM-PTECs). Our assay allows rapid evaluation of TNF-α-mediated toxicant-induced apoptosis and necrosis using fixed endpoint and live cell measurements. To evaluate our assay, sixteen nephrotoxicants and two control non-nephrotoxicants were used. Out of the sixteen nephrotoxicants, eight induced cell death, of which five induced apoptosis as well as necrosis. Moreover, TNF-α significantly enhanced apoptotic cell death induced by cisplatin, cyclosporine A, tacrolimus and azidothymidine. These nephrotoxicants are known to induce inflammation *in vivo* which has been linked to an enhancement of nephrotoxicity for cisplatin, cyclosporine A and tacrolimus, confirming the functionality of our assay. Overall, our assay allows rapid and sensitive measurement of apoptosis and necrosis induced by a combination of nephrotoxicants and inflammatory components such as TNF-α and can be used as an alternative assay for nephrotoxicity prediction *in vitro*.

# INTRODUCTION

Nephrotoxicity is a significant cause of post-market drug withdrawal. This is partly due to inadequate and non-sensitive pre-clinical tests to detect the nephrotoxic potential of new drugs. Acute toxicity testing in animals is traditionally used to evaluate the potential toxicity of new chemicals. However, the increase in the number of new chemicals tested and the lack of sensitivity of the traditional animal tests have prompted pharmaceutical companies to explore *in vitro* cell culture screening systems for toxicity prediction. Several *in vitro* screening systems using different cell lines, such as primary cells, LLC-PK1 (swine), NRK-52E (rat), MDCK (canine), OK (opossum), HK-2 (human) and RPTEC/hTERT1 (human) have been developed to assess the nephrotoxic potential of compounds [1-10]. However, these assays do not take into account the factors contributing to the pathophysiology of nephrotoxicant-induced acute renal failure (ARF) in patients such as mediators of inflammation. Moreover, mostly only one cytotoxicity parameter was taken into account and fixed time-points were used.

It is known that upon a nephrotoxic insult, the proximal tubule is considered the major target. Nephrotoxic injury of proximal tubular epithelial cells (PTECs) is characterized by mitochondrial dysfunction, adenosine triphosphate (ATP) depletion, activation of stress signalling pathways, impaired solute and ion transport, loss of brush border morphology, loss of cell polarity and cytoskeletal disruption [11,12]. Loss of cell adhesion also correlates with loss of cell function, pro-apoptotic signalling and cell death [13]. During nephrotoxicant-induced ARF, inflammation plays a major role. Several nephrotoxicants have been shown to induce an inflammatory response and attenuation of the inflammation can result in renal-protective effects [14-18]. It is believed that during nephrotoxicity, the initial insult by the nephrotoxicant results in changes in vascular endothelial cells and/or in tubular epithelial cells leading to the generation of inflammatory mediators (cytokines and chemokines) by these cells. These inflammatory mediators induce migration and infiltration of leukocytes into the injured kidneys and, importantly, aggravate the primary injury induced by the nephrotoxicant [19].

One the main inflammatory mediators secreted by PTECs [20,21] as well as by the infiltrating immune cells [22] is the pro-inflammatory cytokine tumour necrosis factor α (TNF-α). TNF-α was shown to be up-regulated and directly involved in the pathophysiology of cisplatin- and acetaminophen-induced renal injury [23-25]. In addition, other nephrotoxicants were shown to up-regulate TNF-α levels in the kidneys, in serum or in macrophages, including adefovir [26], methotrexate [27], carmustine [28] and mitomycin C [29], but a functional role for TNF-α in the toxicity induced by these compounds remains unknown. Contradictory results were obtained for the

two immunosuppressive drugs cyclosporine A and tacrolimus. Both cyclosporine A and tacrolimus were shown to inhibit TNF-α production *in vitro* in macrophages [30] and cultured PTECs [31] as well as in murine models [32,33]. However, studies performed on renal transplant recipients treated with cyclosporine A or tacrolimus showed that cyclosporine A did not affect TNF-α production by peripheral blood mononuclear cells [34] and tacrolimus increased TNF-α production by monocytes [35]. Despite these contradictory results in the effects of these immunosuppressive drugs on TNF-α production, both are known to induce inflammation after renal transplantation [36-38].

In addition to upregulation of TNF-α, some nephrotoxicants clearly inhibit TNF-α production. Gentamicin was shown to inhibit lipopolysaccharide (LPS)-induced TNF-α production in human and mouse PTECs [39] even though it induced inflammation *in vivo* [40]. The antiviral azidothymidine reduced TNF-α levels in HIV-infected patients [41,42] and the analgesic diclofenac decreased mRNA levels of TNF-α in obese men [43].

Given the importance of the immune system in nephrotoxicity we set-out to develop an alternative *in vitro* assay for prediction of TNF-α-mediated drug-induced nephrotoxicity. Using immortalized proximal tubular epithelial cells (IM-PTECs) we developed and characterized a fluorescence-based *in vitro* assay for nephrotoxicity screening, which allows apoptosis and necrosis measurements at both at a fixed time point as well as live over a 24-48 hour time-course in the presence of the cytokine TNF-α. IM-PTECs were exposed to 16 different nephrotoxicants and two control non-nephrotoxicants in the presence or absence of TNF-α. In total, 8 nephrotoxicants induced apoptosis of which cisplatin, cyclosporine A, tacrolimus and azidothymidine-induced cell death was enhanced by TNF-α. Overall, our cell model for inflammation-related nephrotoxicity combined with semi high-throughput fluorescence-based measurements allows rapid and sensitive measurement of cell death and can be used as an alternative assay for nephrotoxicity prediction *in vitro*.

# MATERIALS AND METHODS

### Reagents

Cisplatin (Cis-PtCL2(NH3)2)) was provided by the pharmacy unit of University Hospital in Leiden (The Netherlands). Adefovir was acquired from Shanghai PI chemicals (Shanghai, China). All the other nephrotoxic and non-nephrotoxic compounds were acquired from Sigma-Aldrich (Zwijndrecht, The Netherlands). Mouse recombinant TNF-α was acquired from R&D Systems (Abingdon, UK). AnnexinV-Alexa488 was made as previously described [44]. Propidium iodide was provided by Sigma-Aldrich.

## Cell culture

Mouse immortalized proximal tubular cells (IM-PTECs) [45] were cultured at 33°C in DMEM/F12 medium (Invitrogen, Breda, The Netherlands) with 10% fetal bovine serum (Invitrogen, Breda, The Netherlands), 5 μg/ml insulin and transferrin, 5 ng/ml sodium selenite (Roche, Almere, The Netherlands), 20 ng/ml triiodo-thyronine (Sigma-Aldrich), 50 ng/ml hydrocortisone (Sigma-Aldrich), and 5 ng/ml prostaglandin E1 (Sigma-Aldrich) with L-glutamine and antibiotics (both from Invitrogen) and mouse interferon-γ (IFN-γ) (1 ng/ml; R&D Systems) in 5% CO2 and 95% air between passage 3 and 20. Prior to each experiment, the cells were differentiated into proximal tubular cells by culturing them for 4 days in restrictive conditions (at 37°C in the absence of IFN-γ). The cells were then plated in 96-well plates and cultured for 2 more days. In total, IMPTECs were cultured in restrictive conditions for 6 days, allowing the disappearance of SV40 activity and completion of differentiation [45].

## Exposure of the cells

Compound concentrations used in the study were based on previously published *in vitro* studies or were extrapolated from the plasma levels in patients. Compound stock solutions were prepared freshly in DMSO, water, NaCl or NaOH depending on the compounds. Stock solutions were diluted with complete medium to obtain 100X the final testing concentration. The final concentration of DMSO was maximum 0.1% IM-PTECs were exposed to 16 different nephrotoxic compounds and 2 control non-nephrotoxic compounds at two different concentrations in combination or not with TNF-α (8 ng/ml). Cisplatin was used as a positive control and the two non-nephrotoxic compounds valacyclovir and bisphenol A were used as negative controls. Proper vehicle controls were used (DMSO, water, NaCl or NaOH) according to the compounds. After 24 hours, the cells were re-exposed only to the compounds that are known to be administered in patients daily. The compound concentrations and exposure schedules are indicated in Table 1.

## Cell death measurement

Apoptosis and necrosis were measured simultaneously as described in Fig. 1. Apoptosis was measured using a live cell apoptosis assay previously described [44]. Briefly, binding of annexin V-Alexa488 conjugate to phosphatidyl serine present on the membranes of apoptotic cells was measured at 24 and 48 hours or was followed over time by imaging the cells every hour after drug ±TNF-α exposure with BD Pathway 855 imager (Becton Dickinson, Erembodegem, Belgium). The total area of annexin V-Alexa488 fluorescence per image was quantified using Image Pro (Media Cybernetics, Bethesda, MD). Necrosis was measured by incubating the cells with propidium iodide followed by imaging at 24 and 48 hours with a BD Pathway 855

imager (Becton Dickinson, Erembodegem, Belgium). The number of cells stained by propidium iodide was quantified using Image Pro (Media Cybernetics, Bethesda, MD).

## Statistical procedures

All data are expressed as mean ± standard error of the mean (S.E.M.). Statistical significance was determined by GraphPad Prism using an unpaired two-tailed t-test. The level of confidence is represented by p-values indicated in the figures. The apoptotic synergism between nephrotoxicant and TNF-α was quantified with the Chou-Talalay method [46] for the live cell death measurements.

| Compounds | Concentrations | Exposure times |
|:---:|:---:|:---:|
| Valacyclovir | 300 $\mu$M | 0 and 24 h |
| Bisphenol A | 5 $\mu$M | 0 and 24 h |
| Cyclosporine A | 10 and 20 $\mu$M | 0 and 24 h |
| Tacrolimus | 10 and 20 $\mu$M | 0 and 24 h |
| Cephaloridin | 200 and 500 $\mu$M | 0 and 24 h |
| Cephalothin | 200 and 500 $\mu$M | 0 and 24 h |
| Gentamicin | 200 and 1000 $\mu$M | 0 and 24 h |
| Neomycin | 40 and 400 $\mu$M | 0 and 24 h |
| Methotrexate | 30 and 300 $\mu$M | 0 h |
| Carmustine | 100 and 300 $\mu$M | 0 h |
| Mitomycin C | 100 and 150 $\mu$M | 0 h |
| Cisplatin | 10 $\mu$M | 0 h |
| Azidothymidine | 200 and 400 $\mu$M | 0 and 24 h |
| Adefovir | 4 and 5 $\mu$M | 0 and 24 h |
| Foscarnet | 250 and 1000 $\mu$M | 0 h |
| Phenacetin | 30 and 100 $\mu$M | 0 and 24 h |
| Acetaminophen | 750 and 1000 $\mu$M | 0 and 24 h |
| Diclofenac | 500 and 1000 $\mu$M | 0 and 24 h |

**Table 1.** Compound concentrations and exposure schedules

# RESULTS

**TNF-α enhanced the apoptotic response of renal cells exposed to cyclosporine A, tacrolimus, cisplatin and azidothymidine**

To identify nephrotoxic compounds of which nephrotoxicity was enhanced by the cytokine TNF-α we set-up a sensitive fluorescence-based *in vitro* assay for nephrotoxicity screening using immortalized proximal tubular epithelial cells (IM-PTECs). To test the predictive value of this assay, we used a panel of nephrotoxicants, including 2 immuno-suppressants, 4 antibiotics, 4 chemotherapeutics, 3 antivirals and 3 analgesics. None of the compounds significantly affected endogenous TNF-α secretion as determined by ELISA (data not shown), indicating that endogenous TNF-α secretion did not influence the assessment of the tested compounds. To determine whether TNF-α potentiated an apoptotic response as has been observed *in vivo* for cisplatin [24,25], we exposed the IM-PTECS to the panel of nephrotoxicants in combination with exogenous TNF-α. Apoptosis was measured on BD Pathway 855 imager using annexin V-alexa 488 at 24 and 48 hours. While no apoptosis was measured in the two control compounds valacyclovir and bisphenol A, 8 out of 16 nephrotoxic compounds induced apoptosis at 24 or 48 hours after treatment. These compounds included the two immunosuppressants cyclosporine A and tacrolimus, the four chemotherapeutics methotrexate, carmustine, mitomycin C and cisplatin, the antiviral azidothymidine and the analgesic diclofenac (Fig. 2). None of the antibiotics resulted in detectable apoptosis at the high concentrations tested - even after 48 hours exposure (Fig. 2). These findings were confirmed using a commercially available ATP-lite assay (data not shown). Of importance, the presence of serum in the exposure medium did not have an effect on drug-induced cell death as no significant difference was observed between cells exposed under low or high serum conditions, suggesting that drug-protein interactions were not an issue for the compounds tested (data not shown).

TNF-α enhanced the apoptotic response of 4 out of these 8 apoptosis-inducing compounds (Fig. 2). These included cisplatin, the two immunosuppressants cyclosporine A and tacrolimus, as well as the antiviral azidothymidine at the highest concentration. Cyclosporine A-induced apoptosis was more strongly enhanced by TNF-α at 24 hours in comparison to the response to tacrolimus and azidothymidine at 48 hours.

Intriguingly, while cisplatin showed a strong synergy with TNF-α, none of the other DNA damaging nephrotoxicant mimicked this response, despite their pro-apoptotic activities. In contrast, methotrexate showed the opposite effect with TNF-α at the highest concentration:  a significant decrease in apoptosis was observed when IM-PTECS were exposed to the compound in combination with TNF-α in comparison
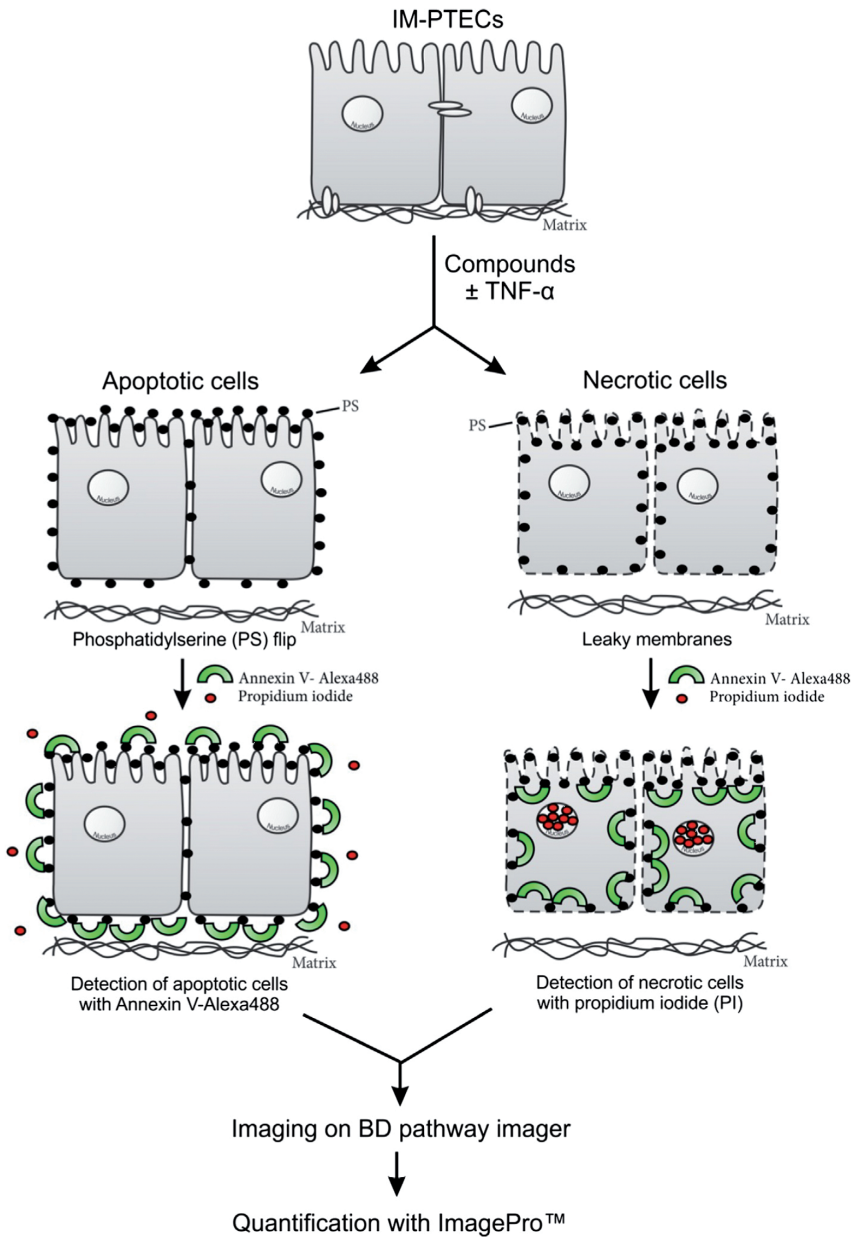
**Figure 1**. *Flowchart of the in vitro screen procedure.* Following exposure of the IM-PTECs to the compounds in the presence or not of TNF-α, the amount of apoptotic and necrotic cell death was determined in a fluorescent-based manner at 24 and 48 hours or followed over time. Apoptosis was measured with Annexin-V-Alexa488 conjugate, which binds the phosphatidyl serine that flips on the outer membrane in apoptotic cells, and necrosis was measured with propidium iodide, which binds to the nucleus only when the membrane of the cells is partly disrupted. The amount of apoptotic and necrotic cells was then quantified using ImagePro.
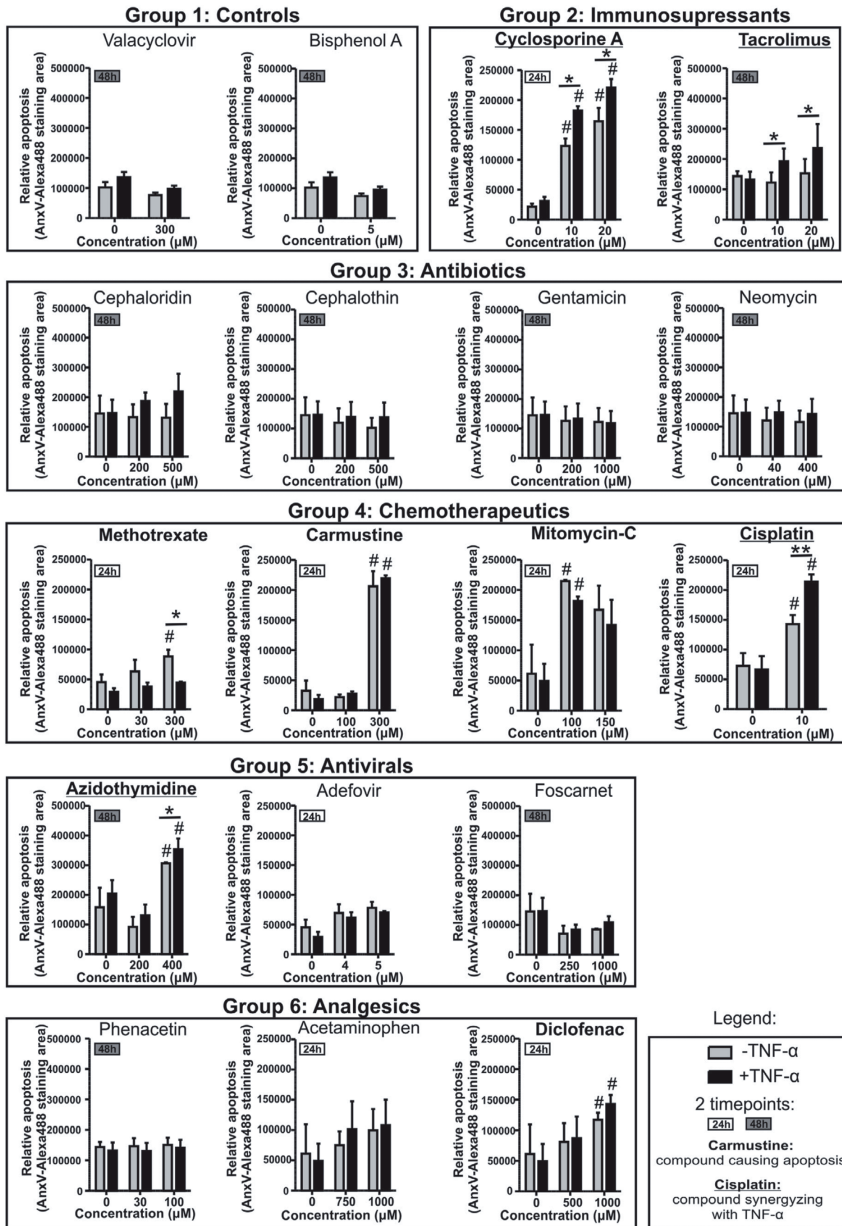
**Figure 2.** *TNF-α enhanced the apoptotic response of renal cells exposed to cyclosporine A, tacrolimus, cisplatin and azidothymidine.* IM-PTECs were exposed to two different concentrations of 16 different nephrotoxicants and two non-nephrotoxicants in combination or not of TNF-α (8 ng/ml) and apoptosis of the cells was measured at 24 and 48 hours. The compounds are grouped by pharmacological properties. The compounds inducing apoptosis are highlighted in bold and the compounds inducing synergistic apoptosis with TNF-α are highlighted in bold and are underlined. The data are represented as means of three independent experiments ± S.E.M. * P ≤ 0.05, ** P ≤ 0.01 and # P ≤ 0 .05 compared to vehicle-treated cells.

to exposure to the compound alone (Fig. 2).

## TNF-α enhanced the necrotic response of renal cells exposed to cyclosporine A and cisplatin

In addition to apoptosis, necrosis was measured in our IM-PTECs after exposure to the 16 different nephrotoxicants and 2 control non-nephrotoxicants in the presence or absence of TNF-α. Five out of the 16 nephrotoxicants showed staining for the necrosis maker propidium iodide. These compounds included the immunosuppressant cyclosporine A, the three chemotherapeutics carmustine, mitomycin C and cisplatin and the analgesic diclofenac (Fig. 3). The other three nephrotoxic compounds shown to induce apoptosis (Fig. 2) did not induce any necrosis - even after 48 hours (Fig. 3). As expected, the two negative controls also did not induce any necrotic response (Fig. 3).

Out of the 5 compounds inducing necrosis, TNF-α enhanced the response of two: cyclosporine A and cisplatin (Fig. 3). Although apoptosis induced by these compounds could result in secondary necrosis, the strong necrotic response observed after cyclosporine A treatment, suggests that the necrosis observed for this compound was not secondary necrosis.

## The TNF-α-mediated enhancement of apoptosis was confirmed with live apoptosis

To confirm the hits obtained in our primary compound screen, IM-PTECs were exposed to the four synergistic apoptosis-inducing compounds cisplatin, cyclosporine A, tacrolimus, and azidothymidine. For all of these four compounds, the enhanced apoptotic response towards TNF-α addition was confirmed (Fig. 4A and Fig. 5). Using the Chou-Talalay statistical test for synergy we could confirm confirmed the synergistic effect of TNF-α with cisplatin (CI of 0.99) and cyclosporine A (CI of 0.74 for 10$\mu$M and CI of 0.84 for 20$\mu$M).

More importantly, while cyclosporine A and cisplatin exposure alone resulted in an increase in apoptosis, a significant increase in apoptosis after tacrolimus and azidothymidine exposure was only observed in combination with TNF-α, indicating a synergistic response for combined treatment of TNF-α with tacrolimus and azidothymidine. These data indicate that our assay could identify nephrotoxic compounds that would not have been identified by current assays that do not incorporate the immune component.

Finally, to obtain more detailed information on the time of onset of apoptosis for the four synergistic apoptosis-inducing compounds cyclosporine A, tacrolimus, azidothymidine and cisplatin, a real time fluorescence-based apoptosis assay was used as was developed previously in our laboratory [44]. IM-PTECs were exposed to
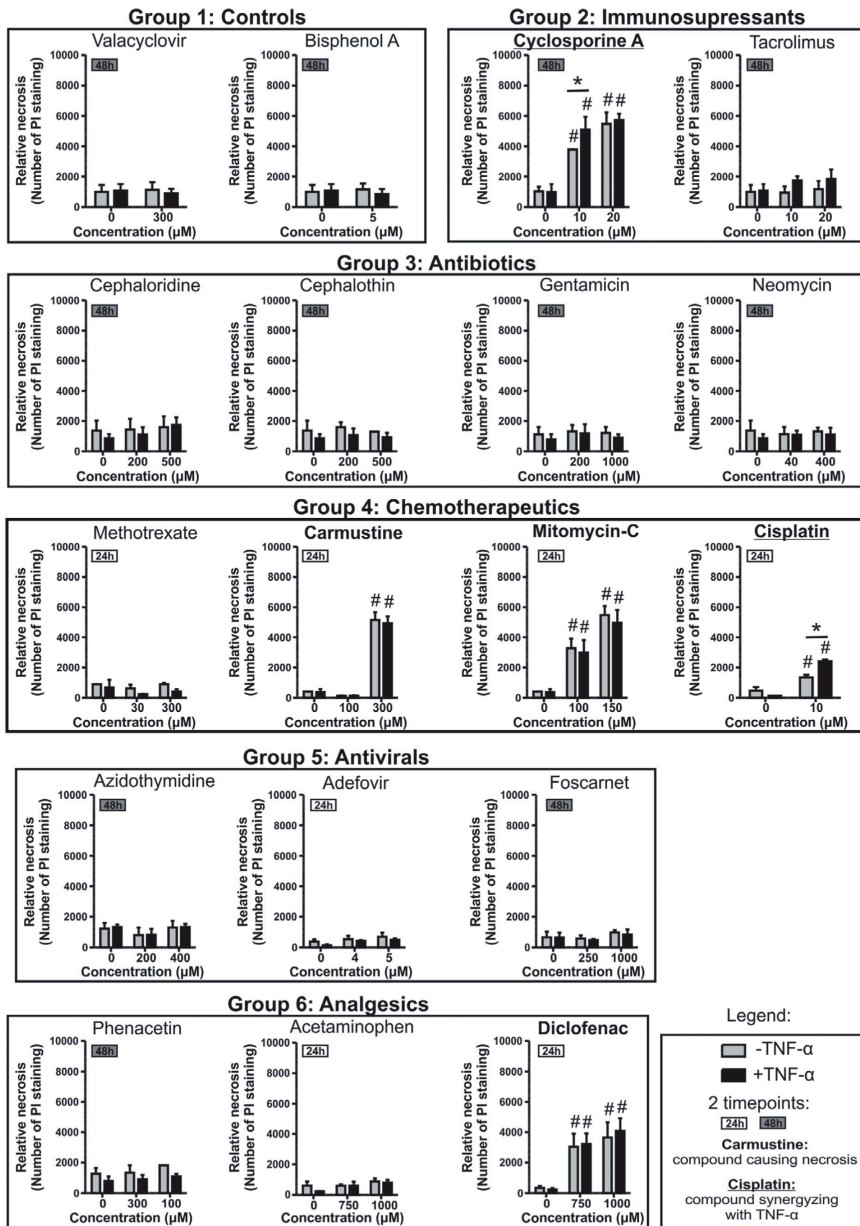
**Figure 3.** *TNF-α enhanced the necrotic response of renal cells exposed to cyclosporine and cisplatin.* IM-PTECs were exposed to two different concentrations of 16 different nephrotoxicants and two non-nephrotoxicants in combination or not of TNF-α (8 ng/ml) and necrosis of the cells was measured at 24 and 48 hours. The compounds are grouped by pharmacological properties. The compounds inducing necrosis are highlighted in bold and the compounds inducing synergistic necrosis with TNF-α are highlighted in bold and are underlined. The data are represented as means of three independent experiments ± S.E.M. * P ≤ 0.05, and # P ≤ 0 .05 compared to vehicle-treated cells.

the four compounds in the presence or absence of TNF-α and the onset of apoptosis was followed over time. While cisplatin and cyclosporine A gave a strong TNF-α-me-diated apoptotic response at 24 hours, as predicted, hardly any effect was observed after tacrolimus or azidothymidine treatment at 24 hours (Fig. 4B). Yet, TNF-α significantly enhanced apoptosis of the IM-PTEC cells over a 24-48 hour time-course. Using this live apoptosis assay, we could clearly observe that TNF-α enhanced the onset of apoptosis induced by both cisplatin and cyclosporine A.
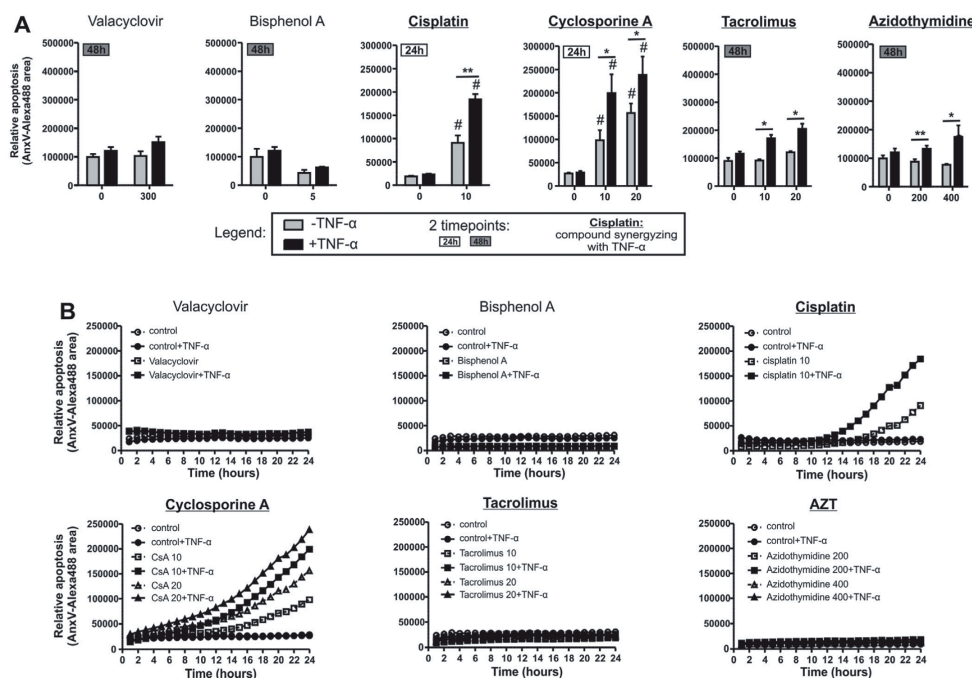


**Figure 4.** *The synergistic apoptotic response of renal cells exposed to the four compounds in combination with TNF-α was confirmed with live apoptosis.* IM-PTECs were exposed to two different concentrations of the 4 synergistic nephrotoxicants and the two non-nephrotoxicants in combination or not of TNF-α (8 ng/ml) and apoptosis of the cells was measured at 24h and 48h (A) or was followed over time until 24 hours (B). The compounds inducing synergistic apoptosis with TNF-α are highlighted in bold and are underlined. The data are represented as means of three independent experiments ± S.E.M. * $P \leq 0.05$, ** $P \leq 0.01$ and # $P \leq 0.05$ compared to vehicle-treated cells.

# DISCUSSION

Recent efforts have been made to develop new *in vitro* screening tests for the pre-diction of nephrotoxicity of new chemicals. Although, these *in vitro* systems cannot reproduce the complex behaviour of animal cells *in vivo*, they allow toxicity testing
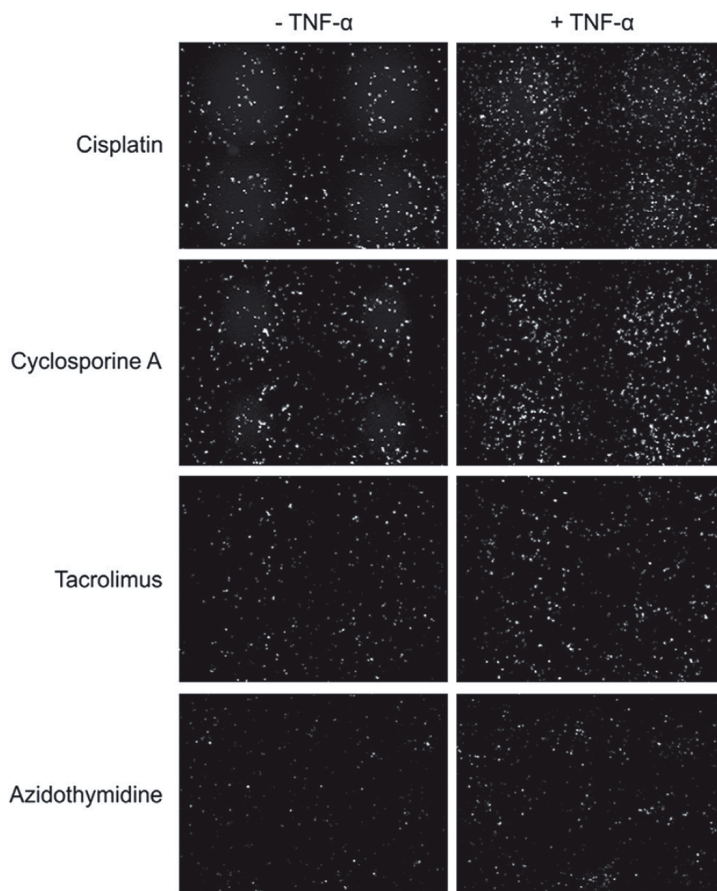
**Figure 5.** *Annexin-V staining of apoptotic cells after exposure to the drugs synergizing with TNF-α.* Annexin-V staining of the apoptotic cells was visualized by a BD Pathway 855 imager for IM-PTECS exposed to compounds in combination of not with TNF-α. Increased annexin-V stained cells was demonstrated for all 4 compounds inducing a synergistic apoptosis of the cells with TNF-α. The images represented here were obtained with the highest concentration for each compound at 24 hours for cisplatin and cyclosporine A and 48 hours for tacrolimus and azidothymidine and are representative of three independent experiments.

in a high throughput manner and provide important predictive and mechanistic information. Yet, nephrotoxicity remains a critical cause of drug withdrawal. Here we set-out to extend beyond these current *in vitro* tests by incorporating one of the most important contributors of nephrotoxicity and main secreted pro-inflammatory cytokine TNF-α. To evaluate the predictive potential of our assay a small screen was performed using 16 different nephrotoxicants. Cell death induced by the compounds in the presence or absence of TNF-α was assessed by a semi-high throughput fluorescence-based method. This innovative method allowed the measurement of both apoptosis and necrosis in real-time, which is a clear advantage over current com-

mercially available assays. In total we identified 8 out of 16 compounds that induced cell death, of which 5 induced apoptosis as well as necrosis. Moreover, TNF-α significantly enhanced the nephrotoxic response of cisplatin, cyclosporine A, tacrolimus and azidothymidine.

We recently examined the mechanisms underlying the synergistic response between cisplatin and TNF-α. This synergistic apoptotic response was due to inhibition of the NF-κB pathway and consequently increased c-Jun N-terminal kinase (JNK) activation [47]. A similar mechanism may be involved in the response between TNF-α and the three other nephrotoxicants identified in our screen. Indeed, Du *et al*. showed that both cyclosporine A and tacrolimus inhibited TNF-α-induced NF-κB activation in renal cells [48]. Moreover, cyclosporine A was shown to induce JNK activation in primary human PTECs [49] and tacrolimus induced JNK activation in Madin Darby canine kidney cells [50]. Thus far, it remains unknown whether the inhibition of NF-κB is directly associated with the changes in JNK activation as we observed for cisplatin and TNF-α co-exposure. Also, azidothymidine was reported to inhibit NF-κB, but studies were performed in Epstein-Barr virus-positive Burkitt lymphoma lines [51]. Moreover, to the best of our knowledge, no studies showed that azidothymidine treatment results in activation of JNK.

In contrast to the aforementioned compounds, co-exposure of the chemotherapeutic methotrexate with TNF-α led to a reduction in methotrexate-induced apoptosis. Protective effects of TNF-α on methotrexate-induced apoptosis were previously observed in macrophages *in vitro* and was shown to be due to enhanced activation of the NF-κB pathway [52]. Whether TNF-α reduce methotrexate-induced apoptosis in IM-PTECs via enhanced activation of the NF-κB pathway has also yet to be determined.

Since cell death was used as a read-out for renal cell injury, 50% of the compounds could not be identified as a nephrotoxicant in our assay, despite the fact that all of the compounds used in our screen induce nephrotoxicity in the clinic. One explanation may be that despite being nephrotoxic, many of the compounds are not reported to induce cell death *in vivo*. Indeed, in contemporary pre-clinical assays it is difficult to identify compounds that are nephrotoxic but do not induce cell death [4,5,39,53]. Even so, the lack of acetaminophen- and phenacetin-induced cytotoxicity in our assay could be explained by lack of bioactivation to reactive intermediates [5,54]. The lack of cell death response for neomycin and gentamicin is most likely due to the lack of the membrane binding site in the brush border and basolateral membrane [55] and for cephaloridine, cephalothin, and adefovir could be due to low expression of the transporter organic anion-transporting polypeptide 1 (OAT1) responsible for the uptake of the compounds [56-58]. Alternatively, our IM-PTEC cells, like any other proximal tubular cell line cultured *in vitro* depend on glycolysis com-

pared to oxidative phosphorylation for PTEC in the *in vivo* situation. These issues require further investigation.

Despite the fact that the nephrotoxicity of some compounds was not identified with our assay, the real-time, dynamic measurement of cell death in combination with the addition of the immune component TNF-α allowed identification of compounds that were mainly toxic in the presence of TNF-α, such as tacrolimus. This observation correlated well with patient data where cyclosporine A induced more nephrotoxicity and inflammation after kidney transplantation than tacrolimus [37,59]. Furthermore, some of the compounds that failed to induce cytotoxicity in our assays were shown to affect the NF-κB pathway in renal cells or other cell lines and organs, including acetaminophen [60], gentamycin [61,62] and neomycin [63,64]. Incorporating NF-κB reporter IM-PTECs in our current fluorescence-based cytotoxicity assay may enhance assay sensitivity and identify compounds like gentamycin and neomycin as nephrotoxicants in an *in vitro* pre-clinical setting.

In conclusion, real-time measurements of apoptosis and necrosis in IM-PTECs in the presence of TNF-α, represents a novel method to detect nephrotoxicants that may go undetected in conventional *in vitro* nephrotoxicity screening assays.

# REFERENCES

1       Li, W. et al. Use of cultured cells of kidney origin to assess specific cytotoxic effects of neph-rotoxins. Toxicology in vitro : an international journal published in association with BIBRA 17, 107-113 (2003).

2       Li, W. et al. Human primary renal cells as a model for toxicity assessment of chemo-therapeutic drugs. Toxicology in vitro : an international journal published in association with BIBRA 20, 669-676, doi:10.1016/j.tiv.2005.09.016 (2006).

3       Weber, F., Freudinger, R., Schwerdt, G. & Gekle, M. A rapid screening method to test apoptotic synergisms of ochratoxin A with other nephrotoxic substances. Toxicology in vitro : an interna-tional journal published in association with BIBRA 19, 135-143, doi:10.1016/j.tiv.2004.08.002 (2005).

4       Wu, Y. et al. Multiplexed assay panel of cytotoxicity in HK-2 cells for detection of renal proximal tubule injury potential of compounds. Toxicology in vitro : an international journal published in association with BIBRA 23, 1170-1178, doi:10.1016/j.tiv.2009.06.003 (2009).

5       Zhang, L., Mu, X., Fu, J. & Zhou, Z. In vitro cytotoxicity assay with selected chemicals using hu-man cells to predict target-organ toxicity of liver and kidney. Toxicology in vitro : an international journal published in association with BIBRA 21, 734-740, doi:10.1016/j.tiv.2007.01.013 (2007).

6       Duff, T. et al. Transepithelial resistance and inulin permeability as endpoints in in vitro nephro-toxicity testing. Altern Lab Anim 30 Suppl 2, 53-59 (2002).

7       Wieser, M. et al. hTERT alone immortalizes epithelial cells of renal proximal tubules with-out changing their functional characteristics. Am J Physiol Renal Physiol 295, F1365-1375, doi:10.1152/ajprenal.90405.2008 (2008).

8       Pfaller, W. & Gstraunthaler, G. Nephrotoxicity testing in vitro--what we know and what we need to know. Environ Health Perspect 106 Suppl 2, 559-569 (1998).

9       Limonciel, A. et al. Lactate is an ideal non-invasive marker for evaluating temporal alterations in cell stress and toxicity in repeat dose testing regimes. Toxicology in vitro : an international jour-nal published in association with BIBRA 25, 1855-1862, doi:10.1016/j.tiv.2011.05.018 (2011).

10      Jang, K. J. et al. Human kidney proximal tubule-on-a-chip for drug transport and nephrotoxicity assessment. Integr Biol (Camb), doi:10.1039/c3ib40049b (2013).

11      Bush, K. T., Keller, S. H. & Nigam, S. K. Genesis and reversal of the ischemic phenotype in epithelial cells. J Clin Invest 106, 621-626, doi:10.1172/JCI10968 (2000).

12      Kays, S. E. & Schnellmann, R. G. Regeneration of renal proximal tubule cells in primary culture following toxicant injury: response to growth factors. Toxicol Appl Pharmacol 132, 273-280, doi:S0041-008X(85)71108-8 [pii]10.1006/taap.1995.1108 (1995).

13      Cordes, N. Integrin-mediated cell-matrix interactions for prosurvival and antiapoptotic signaling after genotoxic injury. Cancer Lett 242, 11-19, doi:10.1016/j.canlet.2005.12.004 (2006).

14      Yalavarthy, R. & Edelstein, C. L. Therapeutic and predictive targets of AKI. Clin Nephrol 70, 453-463 (2008).

15      Araujo, L. P. et al. Annexin A1 protein attenuates cyclosporine-induced renal hemodynamics changes and macrophage infiltration in rats. Inflamm Res 61, 189-196, doi:10.1007/s00011-011-0400-z (2012).

16      Pabla, N. & Dong, Z. Cisplatin nephrotoxicity: mechanisms and renoprotective strategies. Kid-ney international 73, 994-1007, doi:10.1038/sj.ki.5002786 (2008).

17      Quiros, Y., Vicente-Vicente, L., Morales, A. I., Lopez-Novoa, J. M. & Lopez-Hernandez, F. J. An integrative overview on the mechanisms underlying the renal tubular cytotoxicity of gentamicin. Toxicol Sci 119, 245-256, doi:kfq267 [pii]10.1093/toxsci/kfq267 (2011).

18      Naughton, C. A. Drug-induced nephrotoxicity. Am Fam Physician 78, 743-750 (2008).

19      Akcay, A., Nguyen, Q. & Edelstein, C. L. Mediators of inflammation in acute kidney injury. Me-diators Inflamm 2009, 137072, doi:10.1155/2009/137072 (2009).

20      Ramesh, G. & Brian Reeves, W. Cisplatin increases TNF-alpha mRNA stability in kidney prox-imal tubule cells. Ren Fail 28, 583-592, doi:10.1080/08860220600843839 (2006).

21      Ramesh, G., Kimball, S. R., Jefferson, L. S. & Reeves, W. B. Endotoxin and cisplatin synergis-tically stimulate TNF-alpha production by renal epithelial cells. Am J Physiol Renal Physiol 292, F812-819, doi:10.1152/ajprenal.00277.2006 (2007).

22    Liu, M. et al. A pathophysiologic role for T lymphocytes in murine acute cisplatin nephrotoxicity. J Am Soc Nephrol 17, 765-774, doi:10.1681/ASN.2005010102 (2006).

23    Ghosh, J., Das, J., Manna, P. & Sil, P. C. Acetaminophen induced renal injury via oxidative stress and TNF-alpha production: therapeutic potential of arjunolic acid. Toxicology 268, 8-18, doi:10.1016/j.tox.2009.11.011 (2010).

24    Ramesh, G. & Reeves, W. B. TNF-alpha mediates chemokine and cytokine expression and renal injury in cisplatin nephrotoxicity. J Clin Invest 110, 835-842, doi:10.1172/JCI15606 (2002).

25    Ramesh, G. & Reeves, W. B. TNFR2-mediated apoptosis and necrosis in cisplatin-induced acute renal failure. Am J Physiol Renal Physiol 285, F610-618, doi:10.1152/ajprenal.00101.2003 (2003).

26    Piao, R. L. et al. Adefovir dipivoxil modulates cytokine expression in Th1/Th2 cells in patients with chronic hepatitis B. Mol Med Report 5, 184-189, doi:10.3892/mmr.2011.627 (2012).

27    Asvadi, I. et al. Protective effect of pentoxyfilline in renal toxicity after methotrexate administration. Eur Rev Med Pharmacol Sci 15, 1003-1009 (2011).

28    Helal, G. K. et al. Metallothionein induction reduces caspase-3 activity and TNFalpha levels with preservation of cognitive function and intact hippocampal neurons in carmustine-treated rats. Oxid Med Cell Longev 2, 26-35 (2009).

29    Pogrebniak, H. W., Matthews, W. & Pass, H. I. Chemotherapy amplifies production of tumor necrosis factor. Surgery 110, 231-237 (1991).

30    Remick, D. G., Nguyen, D. T., Eskandari, M. K., Strieter, R. M. & Kunkel, S. L. Cyclosporine A inhibits TNF production without decreasing TNF mRNA levels. Biochemical and biophysical research communications 161, 551-555 (1989).

31    Yard, B. A. et al. CsA, FK506, corticosteroids and rapamycin inhibit TNF alpha production by cultured PTEC. Kidney Int 44, 352-358 (1993).

32    Cicora, F. et al. [Immunosuppression in kidney donors with rapamycin and tacrolimus. Proinflammatory cytokine expression]. Medicina (B Aires) 72, 3-9 (2012).

33    Nguyen, D. T. et al. Cyclosporin a modulation of tumor necrosis factor gene expression and effects in vitro and in vivo. J Immunol 144, 3822-3828 (1990).

34    Peces, R. & Urra, J. M. Effect of calcium-channel blocker on tumour necrosis factor alpha (TNF alpha) production in cyclosporin-treated renal transplant recipients. Nephrol Dial Transplant 10, 871-873 (1995).

35    Weimer, R. et al. Switch from cyclosporine A to tacrolimus in renal transplant recipients: impact on Th1, Th2, and monokine responses. Hum Immunol 61, 884-897 (2000).

36    Araujo, L. P. et al. Interaction of the anti-inflammatory annexin A1 protein and tacrolimus immunosuppressant in the renal function of rats. Am J Nephrol 31, 527-533, doi:10.1159/000309756 (2010).

37    Lauzurica, R. et al. Subclinical inflammation in renal transplant recipients: impact of cyclosporine microemulsion versus tacrolimus. Transplant Proc 39, 2170-2172, doi:10.1016/j.transproceed.2007.06.023 (2007).

38    Pichler, R. H. et al. Pathogenesis of cyclosporine nephropathy: roles of angiotensin II and osteopontin. J Am Soc Nephrol 6, 1186-1196 (1995).

39    Zager, R. A., Johnson, A. C. & Geballe, A. Gentamicin suppresses endotoxin-driven TNF-alpha production in human and mouse proximal tubule cells. Am J Physiol Renal Physiol 293, F1373-1380, doi:10.1152/ajprenal.00333.2007 (2007).

40    Geleilete, T. J. et al. Role of myofibroblasts, macrophages, transforming growth factor-beta endothelin, angiotensin-II, and fibronectin in the progression of tubulointerstitial nephritis induced by gentamicin. J Nephrol 15, 633-642 (2002).

41    De Simone, C. et al. Clinical and immunologic effects of combination therapy with intravenous immunoglobulins and AZT in HIV-infected patients. Immunopharmacol Immunotoxicol 13, 447-458, doi:10.3109/08923979109019716 (1991).

42    Morlat, P. et al. Evolution of tumor necrosis factor-alpha serum concentrations in HIV infected individuals treated with zidovudine. Pathol Biol (Paris) 44, 716-719 (1996).

43    van Erk, M. J. et al. Insight in modulation of inflammation in response to diclofenac intervention: a human intervention study. BMC Med Genomics 3, 5, doi:10.1186/1755-8794-3-5 (2010).

44    Puigvert, J. C., de Bont, H., van de Water, B. & Danen, E. H. High-throughput live cell imaging of apoptosis. Current protocols in cell biology / editorial board, Juan S. Bonifacino ... [et al.] Chapter 18, Unit 18 10 11-13, doi:10.1002/0471143030.cb1810s47 (2010).

45    Stokman, G. et al. Epac-Rap signaling reduces cellular stress and ischemia-induced kidney failure. J Am Soc Nephrol 22, 859-872, doi:ASN.2010040423 [pii]10.1681/ASN.2010040423 (2011).

46    Chou, T. C. Drug combination studies and their synergy quantification using the Chou-Talalay method. Cancer Res 70, 440-446, doi:10.1158/0008-5472.CAN-09-1947 (2010).

47    Benedetti, G. et al. TNF-α-mediated NF-κB Survival Signaling Impairment by Cisplatin Enhances JNK Activation Allowing Synergistic Apoptosis of Renal Proximal Tubular Cells. Biochem Pharmacol, doi:doi:10.1016/j.bcp.2012.10.012 (2012).

48    Du, S. et al. Suppression of NF-kappaB by cyclosporin a and tacrolimus (FK506) via induction of the C/EBP family: implication for unfolded protein response. J Immunol 182, 7201-7211, doi:10.4049/jimmunol.0801772 (2009).

49    Pallet, N., Thervet, E. & Anglicheau, D. c-Jun-N-Terminal Kinase Signaling Is Involved in Cyclosporine-Induced Epithelial Phenotypic Changes. J Transplant 2012, 348604, doi:10.1155/2012/348604 (2012).

50    Jeon, S. H. et al. Taurine reduces FK506-induced generation of ROS and activation of JNK and Bax in Madin Darby canine kidney cells. Hum Exp Toxicol 29, 627-633, doi:10.1177/0960327109359019 (2010).

51    Kurokawa, M. et al. Azidothymidine inhibits NF-kappaB and induces Epstein-Barr virus gene expression in Burkitt lymphoma. Blood 106, 235-240, doi:10.1182/blood-2004-09-3748 (2005).

52    Lo, S. Z., Steer, J. H. & Joyce, D. A. Tumor necrosis factor-alpha promotes survival in methotrexate-exposed macrophages by an NF-kappaB-dependent pathway. Arthritis Res Ther 13, R24, doi:10.1186/ar3248 (2011).

53    Schwertz, D. W., Kreisberg, J. I. & Venkatachalam, M. A. Gentamicin-induced alterations in pig kidney epithelial (LLC-PK1) cells in culture. The Journal of pharmacology and experimental therapeutics 236, 254-262 (1986).

54    Hu, J. J. et al. Sex-related differences in mouse renal metabolism and toxicity of acetaminophen. Toxicology and applied pharmacology 122, 16-26, doi:10.1006/taap.1993.1167 (1993).

55    Williams, P. D., Bennett, D. B., Gleason, C. R. & Hottendorf, G. H. Correlation between renal membrane binding and nephrotoxicity of aminoglycosides. Antimicrob Agents Chemother 31, 570-574 (1987).

56    Uwai, Y., Ida, H., Tsuji, Y., Katsura, T. & Inui, K. Renal transport of adefovir, cidofovir, and tenofovir by SLC22A family members (hOAT1, hOAT3, and hOCT2). Pharm Res 24, 811-815, doi:10.1007/s11095-006-9196-x (2007).

57    Ho, E. S., Lin, D. C., Mendel, D. B. & Cihlar, T. Cytotoxicity of antiviral nucleotides adefovir and cidofovir is induced by the expression of human renal organic anion transporter 1. J Am Soc Nephrol 11, 383-393 (2000).

58    Tune, B. M. Nephrotoxicity of beta-lactam antibiotics: mechanisms and strategies for prevention. Pediatr Nephrol 11, 768-772 (1997).

59    Martins, L. et al. Cyclosporine versus tacrolimus in kidney transplantation: are there differences in nephrotoxicity? Transplant Proc 36, 877-879, doi:10.1016/j.transproceed.2004.03.083 (2004).

60    Boulares, A. H., Giardina, C., Inan, M. S., Khairallah, E. A. & Cohen, S. D. Acetaminophen inhibits NF-kappaB activation by interfering with the oxidant signal in murine Hepa 1-6 cells. Toxicological sciences : an official journal of the Society of Toxicology 55, 370-375 (2000).

61    Juan, S. H. et al. Tetramethylpyrazine protects rat renal tubular cell apoptosis induced by gentamicin. Nephrol Dial Transplant 22, 732-739, doi:10.1093/ndt/gfl699 (2007).

62    Volpini, R. A., Costa, R. S., da Silva, C. G. & Coimbra, T. M. Inhibition of nuclear factor-kappaB activation attenuates tubulointerstitial nephritis induced by gentamicin. Nephron Physiol 98, p97-106, doi:10.1159/000081558 (2004).

63    Garcia-Trapero, J., Carceller, F., Dujovny, M. & Cuevas, P. Perivascular delivery of neomycin inhibits the activation of NF-kappaB and MAPK pathways, and prevents neointimal hyperplasia and stenosis after arterial injury. Neurol Res 26, 816-824 (2004).

64    Cuevas, P., Diaz-Gonzalez, D. & Dujovny, M. Glioma cell-associated sustained activation of the transcription factor, nuclear factor-kappa B, was inhibited by neomycin. Neurol Res 25, 271-274 (2003).

# CHAPTER 6

## DISCUSSION AND CONCLUSION

Sreenivasa C. Ramaiahgari,
Bob van de Water and Leo S. Price

With an estimated cost of $1.8 billion and 10 -15 years development time for a single drug [1-3], drug attrition at late stage development or withdrawal from the market is a serious concern for both industry and society. Recent technical advances have revolutionized pharmaceutical research, giving rise to new methodologies and systems biology approaches to interpret the mechanistic biological response. Application of these technologies in the drug development pipeline is expected to have a major positive impact on the discovery of novel drug targets and the development of safe medicines.

Drug attrition due to toxicity and efficacy have increased in recent years [4]. Though there were several scientific advances that helped in discovering new therapeutic targets, the methods used to test toxicity had little improvements. A principal reason for this is lack of physiologically relevant test systems that can be used for pre-clinical screening. We mainly rely on animal models to predict human specific responses. Though animal models will give biological responses involving a whole organism, often the drug metabolism, pharmacokinetics and pharmacodynamics are quite different to humans, for example nifedipine, a calcium channel blocker is metabolized by CYP3A4 in humans but not in rats [5]. Also CYP isoforms are different in each species making it difficult and dangerous to extrapolate animal data to humans [6]. To overcome this, human cell based *in vitro* models could be used. However, the current gold standards – primary human cells - are difficult to obtain and rapidly lose tissue specific functions. Assays using immortalized cell lines have also been developed, but these poorly represent human tissue due to loss of tissue specific functions in a non-physiological environment. Often, the cells used are of cancer origin and host extensive genomic alterations. Though several models have been proposed for long-term culture of differentiated cells, a thorough validation of these models is required to assess their efficiency and practical applicability in high-throughput screening assays. A combination of human cell-based organotypic systems with mechanism-based toxicity profiling and high content screening methods to study dynamic cellular perturbations will be promising future tools in reducing drug attrition rates and developing safer drugs.

In this thesis we discuss a novel high-throughput screening (HTS) compatible organotypic *in vitro* model that was developed to study drug induced liver injury (DILI). This simple static 3D-cell culture model induces morphological and functional differentiation of hepatocytes into polarized epithelial spheroids. An in-depth analysis of these spheroids was performed to assess the functional similarity to *in vivo* hepatocytes. Microarray gene expression analysis was performed in time during hepatocyte differentiation to study various elements involved in the formation of polarized spheroids. A comparative transcriptomic study showed similarities in the

mechanistic responses between this model and higher *in vivo* models. In this thesis I also describe a high content screening assay that was developed to study dynamic cell stress responses to toxicants.

Overall, the main focus of this thesis it to address current problems in the pre-clinical drug safety assessment in areas related to advancing current *in vitro* models, methodologies used to study toxicity and application of advanced 'omics approaches to predict drug induced toxicity.

## 3D cell culture systems in pre-clinical drug development

Ever since the invention of 2D cell culture systems there has been little progress in developing *in vitro* models that mimic the tissue-like microenvironment. Cells in our body reside in a three-dimensional space surrounded by extracellular matrix. This facilitates cell-cell and cell-matrix interactions that regulate gene and protein expression essential for proper tissue function [7]. Several models have been developed to simulate a 3D environment, but to successfully implement them in a drug development pipeline, the model should be suitable for high-throughput testing, retain a tissue like architecture and polarity for an extended period to allow chronic drug exposures and most importantly is sensitive in identifying toxic compounds. In chapter 2 we described a hydrogel-based static 3D cell culture model for inducing and maintaining differentiated spheroids from liver hepatoma cell line HepG2. Spheroids are also formed from HepG2 cells grown on peptide gels [8] and scaffold-free hanging drops [9]. However, due to the presence of native extracellular matrix ligands, the morphological complexity and functional similarity to *in vivo* hepatocytes is much more pronounced in our model. HepG2 spheroids in our hydrogel system show well-defined apical and baso-lateral domains resembling polarized hepatocytes. In chapter 2 transcriptomic changes in time during 3D culture were analysed. This gave us an overview of the genes associated with differentiation and regulation of functional pathways in HepG2 spheroid culture. A recent study showed formation of liver buds with co-cultures of iPSC's with mesenchymal stem cells and endothelial cells (HUVEC's); when these liver buds are transplanted into mice they vascularized and showed functional properties of a liver [10]. 83 genes involved in development of liver were analyzed and shown to increase in these liver buds; these 83 genes were also serially upregulated in HepG2 spheroids (Chapter 2) indicating a degree of restoration of the complex ontogenic profile of human liver in HepG2 spheroids.

The metabolism of drugs to toxic intermediates frequently underlies hepatotoxicity [11]. The rapid loss of specific CYP450 enzymes in primary human hepatocytes [12, 13] or overall low levels in immortalized cell lines including HepG2 cells [14] compromise accurate prediction of metabolite induced toxicity. Stable metabolic

competence that can enable chronic drug exposures is an ultimate goal for toxicity screening assays. Microarray transcript analysis showed serial upregulation of several phase I, II, and III drug metabolic enzymes in 3D cultured HepG2 spheroids up to 28 days with stable higher expression between day 21 and day 28 (Chapter 3), some of these genes were also validated by qPCR analysis which complemented the microarray analysis (Chapter 2). HPLC/LC-MS analysis showed higher metabolite levels of phase I, phase II metabolites (glucuronidation, sulphation) in 3D HepG2 spheroids from midazolam (CYP3A4), diclofenac (CYP2C9 and glucuronidation), bufuralol (CYP2D6), testosterone (substrate for multiple CYP's) and paracetamol (sulphation) substrates indicating increased metabolic competence compared to monolayer HepG2 cells. With increased metabolic competence and the ability to sustain functional stability for longer periods in microplates, HepG2 spheroids may be attractive tools in pre-clinical drug safety testing.

Current *in vitro* models used in conventional screening assays are not compatible for repeated drug exposure studies. This is mainly due to their continued growth in tissue culture plates requiring more space with time. HepG2 spheroids overcome this limitation as spheroid differentiation leads to a pronounced reduction of proliferation, such that spheroid size remains stable after day 14. Indeed, protein and mRNA levels of Ki-67, a marker for cell proliferation were undetectable in differentiated HepG2 spheroids (Chapter 2). HepG2 cultured on synthetic hydrogel in combination with integrin binding peptide domains did not result in inhibition of cell proliferation (in house observations) highlighting the importance of ECM with native tissue composition. Microarray analysis also showed strong inhibition of the cell cycle pathway in HepG2 spheroids (Chapter 2). Low levels of cell proliferation were also observed in differentiated HepaRG spheroids and in hanging drops [15] enabling long-term drug exposure studies. The sensitivity to known DILI compounds [16, 17] was also significantly higher in HepG2 spheroids with repeated dosing regimens (Chapter 2). Previous studies applying high-content imaging approaches to primary human hepatocyte cultures measuring mitochondrial function, oxidative stress and GSH content could differentiate toxic and non-toxic compounds at a dose range of 100-fold cMax [17]. Similarly, scoring based on mitochondrial membrane potential, DNA content, intracellular calcium levels and plasma membrane permeability on HepG2 cells identified DILI compounds with 93% sensitivity at 30-fold cMax concentrations [18]. In our study the repeated dosing of HepG2 spheroids showed sensitivity in identifying all the DILI compounds tested (8). For example, the withdrawn drug trovafloxacin mesylate was toxic at its maximum plasma concentration (cMax) with TC50 5.6 µM, whereas the TC50 of trovafloxacin mesylate was around 23.7 µM and 35.7 µM in a study on micro-patterned primary human hepatocytes from 2 different donors [19]. In the same study another withdrawn drug, troglitazone was toxic in

one donor and negative in other donor, underscoring the problem of donor variability with primary human hepatocytes. Troglitazone was toxic in our study with a TC50 of 100 µM (Chapter 2). Though we used a small set of compounds to test in this study (4 negative and 8 DILI compounds), we emphasized that the repeated dosing is critical to accurately predict compound toxicity. Repeated (lower concentration) dosing might actually represent a more accurate representation of the mechanism of toxicity in humans compared to single high dose exposures on 2D *in vitro* models, which have a high incidence of false positives due to parent compound accumulation or other off-target effects. Further validation with a large set of compounds is required to more comprehensively and accurately assess the sensitivity of HepG2 spheroids in identifying DILI.

**Toxicogenomics in drug development**

Toxicogenomics could play a major role in lead discovery and reducing attrition of compounds at later stages of drug development. Mechanistic understanding of how molecules are involved in toxic injury could lead to identification of biomarkers that could serve as a reference to test new chemical entities. Reliable human *in vitro* models would be ideal for predictive toxicogenomic studies, allowing increased throughput, reduced animal testing and reduced costs. Though primary human hepatocytes are considered as 'gold standards' in *in vitro* screening assays [20], large inter-individual variability has also been seen in toxicogenomic-transcript profiling [21, 22]. Transcriptomic profiling has shown that HepG2 cells are better in discriminating genotoxic and non-genotoxic compounds compared to HepaRG cells [23]. With its stable non-proliferating phenotype HepG2 spheroids could be ideal for toxicogenomic studies. We have seen significant upregulation of many pathways associated with functional hepatocytes in HepG2 spheroids (Chapter 3). Xenobiotic metabolism pathways such as PXR/RXR, PPARα/RXRα are significantly activated in HepG2 spheroids. PXR induces the expression of CYP3A4, which is involved in metabolism of an estimated 60% of xenobiotics [24] other target genes include phase I enzymes CYP - 2B6, 2B9, SC8, 2C9, 2C19 and drug transporters MRP2, OATP2 [25]. PPARα involve in activation CYP4A family and CYP 1A, 2A, 2C, 2E sub families.  Thus presence of active xenobiotic metabolism pathways may help in identifying genes associated with mechanistic toxic response in predictive toxicogenomic studies. Chapter 4 describes microarray gene expression profiles of HepG2 spheroids treated with diclofenac compared with *in vivo* mouse and rat models, 2D HepG2 cells, primary human hepatocytes and human liver slices. Molecular pathways associated with diclofenac induced hepatocyte injury such as mitochondrial dysfunction were activated in HepG2 spheroids, human liver slices and rat liver models, but not in other models. Previous studies have shown that the Nrf2 signaling pathway plays

an important role in diclofenac injury. Genes such as HO-1 in the Nrf2 pathway are important markers for hepatocellular injury. HO-1 gene up regulation was seen in *in vivo* models and HepG2 spheroids but not in HepG2 cells grown in monolayer cultures (Chapter 4) indicating enhanced functional activities of HepG2 spheroids similar to higher models. Cholestasis is observed in patients taking diclofenac [26]. Genes related to cholestatic liver disease were also significantly activated in HepG2 spheroids. In this study we have investigated transcript profiles from HepG2 spheroids exposed to a single dose of diclofenac. A detailed investigation with increasing dose and time points would likely provide further insight into the mechanisms leading to diclofenac-induced hepatocellular injury. The transcriptomic responses observed with a single dose of diclofenac indicate that, in many aspects, HepG2 spheroids show similarities in the stress response compared to human liver slices, primary human hepatocytes and *in vivo* models than its 2D counterpart.

Identification of key events and stress pathways involved in response to a toxic injury will provide information about important genes and proteins that could be used as indicators of a cytotoxic cascade. Early screening assays to identify these stress reporters would be valuable in drug discovery. Imaging based approaches such as High Content Screening (HCS) assays may complement compound prioritization strategies in pre-clinical drug screening.

**High Content Screening (HCS) methods in preclinical drug development**

Current *in vitro* assays measure cell death as an endpoint to assess the safety of compounds. Cell death may provide an estimation of a lethal dose, but it cannot represent complex molecular perturbations that occur during cell stress and injury. High content screening will allow us to visualize dynamic cellular responses upon xenobiotic stress and may provide an efficient evaluation of the compound's safety profile. With the advancement in automated imaging systems, HCS is now becoming compatible with HTS. Imaging systems are integrated with robotics and automated live cell imaging can be performed. In chapter 5, we describe the use of such an imaging platform to study the dynamic apoptotic and necrotic responses of mouse kidney proximal tubular epithelial cells (PTEC's) in real time after exposure to toxicants. PTEC's are susceptible to drug induced injury due to their re-absorption and secretory functions. Pro-inflammatory cytokine such as TNFα are induced as a result of nephrotoxicant insult to the kidney, which in turn aggravates the toxic injury [27, 28]. In this study, the dynamic role of TNFα in increasing apoptosis (Annexin-V) and necrosis (Propidium iodide) in mouse PTEC's was studied in real time. Cisplatin, cyclosporine A, tacrolimus and azidothymidine showed a synergistic apoptotic response to TNFα (Chapter 5). Though we could identify nephrotoxic compounds, 50% of the tested drugs did not show any signs of toxicity in this study. This may

largely be attributed to the lack of organotypic physiology in monolayer cultures, as most nephrotoxic drugs cause kidney injury by complex pathogenic mechanisms such as changes in intraglomerular hemodynamics, inflammation and crystalline nephropathy caused by pro-urine concentration [29], which will demand complex organotypic models for their detection at the very least. Additionally, lack of metabolic competence and species differences in these monolayer-cultured mouse PTEC's could also be a reason for decreased sensitivity. Utilization of complex human cell based 3D cell culture models, simulating physiological structure and function together with immune components are expected to improve the prediction of nephrotoxicity, but given the complexity of this organ, there is a long way to go before animal models can be completely replaced.

HCS is a new tool that was introduced to toxicology in recent years and none of the drugs that are currently on the market have passed through this type of screening assay. The pharmaceutical industry is now utilizing these assays at pre-clinical screening assays [30] and analyzing its potential to overcome current limitations in drug screening. With current improvements in integrating HCS with HTS, and feasibility to analyze multiple indicators of cell stress simultaneously, HCS would be a valuable tool in prioritizing new chemical entities.

## CONCLUSION AND FUTURE PERSPECTIVES

To address the need for an *in vitro* model with improved functionality and stability for a longer period, we have developed a hydrogel based static 3D *in vitro* model using HepG2 cells. This model induces robust morphological and functional differentiation, with a strong induction of metabolic enzymes and transporters, many of which are poorly expressed in monolayer cultures. Functional bile canaliculi are formed in 3D HepG2 spheroid cultures. Comparative microarray gene expression analysis of our 3D HepG2 model with primary human hepatocytes, HepaRG and human liver revealed its close resemblance to human liver at the pathway level. The metabolic competence of HepG2 spheroids in hydrogels could be retained for up to 4 weeks, making repeated drug exposures feasible and repeated dosing on these spheroids was sensitive in identifying DILI compounds. Comparative transcriptomic profiling of diclofenac induced stress response mechanisms were similar in higher *in vivo* models and *in vitro* HepG2 spheroids. The assay we have developed is implemented in a 384 well format for low cost and increased throughput. This assay represents a novel and more physiologically relevant method for studying drug-induced liver injury.

In this model we used Matrigel, for re-differentiation of HepG2 cells into mature hepatocytes acquiring many specialized functions. Matrigel is a basement membrane matrix containing laminin (~60%), type IV collagen (~30%), entactin (~8%) and various quantities of decorin, transforming growth factor β1 and other

growth factors that help in cell attachment and differentiation [31]. Collagen type IV and laminin are present in developing and adult liver and are known to promote hepatocyte differentiation [32]. The exact mechanism involved in differentiation of HepG2 cells in Matrigel has to be further investigated. Cell surface integrins bind to laminins and collagens and induce differentiation [33] and we think this may be the first step in the differentiation of HepG2 cells in 3D culture. In this study we have seen a strong expression of β1-integrin on the basal surface of the polarized HepG2 spheroids. β1 integrin plays a crucial role in the early phases of development, [34] adhesion of β1 inegrin to Matrigel is evident in our observations. Further investigation on expression and role of other integrin binding sites on HepG2 spheroids might help in designing synthetic gels with tailored integrin binding domains for hepatocyte adhesion, growth and differentiation. If successful, this may circumvent the need of animal-derived Matrigel that has an undefined composition. Several studies have reported batch-to-batch experimental variation with Matrigel, but in our studies we did not see a significant difference in the spheroid morphology, gene expression (qPCR validation) or cytotoxic readouts with different batches.

With a defined cell density we were able to achieve a spheroid size of ~100 µm, which is important for proper gaseous exchange as spheroids above >200 µm cause hypoxia [35]. H&E staining of HepG2 spheroids (Chapter 2) show a cavity in the center of the spheroid. Though we did not investigate the presence of apoptotic or necrotic cells, histological examination suggests that the cavity may have some debris from extracellular matrix or apoptotic cells. Apoptosis is an intrinsic part of tissue remodeling. In 3D cultures of mammary epithelial cells, cavitation was shown to occur by apoptosis of cells in the interior of the spheroid [36]. Normally, apoptotic cells are cleared by macrophages, which are not present in our *in vitro* model. Necrosis can be induced by a lack of oxygen or nutrients. However, we believe that this is unlikely in HepG2 spheroids with optimal spheroid size.

The functional unit of the liver, the acinus is divided into 3 zones based on the distance from the arterial blood supply [37]. Zone 1, which is closest to the portal vein, receives the most oxygenated blood and hepatocytes in this region have functions that include gluconeogenesis, β-oxidation, amino acid catabolism and cholesterol synthesis. CYP450 metabolism, glycolysis, lipogenesis are mainly carried by zone 3 hepatocytes [37-39]. The increased expression of drug metabolism enzymes and genes involved in glycolysis, cholesterol synthesis etc. may indicate the presence of zonal gradients and functions in HepG2 spheroids. Oxygen levels in cell culture incubators have a significant impact on the functional activity of hepatocytes [40]. Normal monolayer cell cultures are exposed to 21% oxygen, whereas hepatocytes *in vivo* have oxygen levels of 8-9% in zone 1 and 3-5% in zone 3 [41]. Though we

did not measure the oxygen levels in HepG2 spheroids, the presence of ECM gel may have resulted in physiological oxygen concentrations and thereby increased functionality.

The successful application of an organotypic *in vitro* model in an industrial setup depends on its simplicity and compatibility to HTS assays. This HepG2 spheroid model stands out with several advantages compared to other spheroid models. The advantages include compatibility with regular microplates, use of easily available well-characterized HepG2 cells, which differentiate into a non-proliferating spheroid with a stable phenotype for longer periods. Spheroids from bioreactors or hanging drops need to be transferred to plates before performing an assay and they are no longer in an environment that induced the formation of spheroids, whereas in our model HepG2 spheroids are stably attached to the hydrogel for any downstream applications.

With a stable non-proliferating phenotype of HepG2 spheroids may answer the need for an *in vitro* model for sub-chronic toxicity studies. Our repeated dosing study for 7-days was sensitive in identifying all the hepatotoxic compounds tested, highlighting the importance of repeated dosing in toxicity screening assays. The increased sensitivity could be due to mechanistic toxic injury, for example bosentan, which induces cholestatic liver injury, was not toxic in a single exposure study in spheroids, but upon repeated dosing the toxicity was observed. Further studies with cholestatic endpoints are required to confirm our hypothesis. We have observed that the spheroids are viable with a polarized phenotype at least until 45 days (data not shown), which provides an opportunity for further long-term toxicity studies. The synthetic fluorescent bile acid uptake assay (chapter 2) that we have developed to assess inhibition of OATP1B3 transporter activity may also be used to screen drugs that obstruct bile flow leading to cholestatic liver injury. HepG2 spheroids could have a multitude of applications, which needs to be further explored.

Co-culturing HepG2 spheroids with other liver cell types may further improve its physiological relevance and identification of chemical entities where immune mediators or other factors secreted by non-parenchymal cells play a key role in aggravating liver injury. Co-culture of iPSC's (with human MSC's/HUVEC's) on Matrigel led to formation of liver buds *in vitro* [10]; it would be interesting to investigate if a similar level of differentiation and phenotypic characteristics could be achieved with HepG2 cells. iPSC derived hepatocytes were recently tested for safety assessment studies. iPSC's on 3D (nanopillar plate) were shown to perform better than 2D iPSC's and HepG2 cells in identifying hepatotoxic compounds [42], but the metabolic competence and sensitivity to hepatotoxic compounds was still significantly lower than PHH. iPSC's cells require special differentiation and selection methods, their ease of use and strengths are yet to be evaluated for successful application in the

pharmaceutical industry. The use of simple culture methods (10% FBS in DMEM) for HepG2 spheroid culture without the need of a proprietary or special media formulations as required for HepaRG and iPSC's culture will inevitably increase reliability and reproducibility and reduce cost of this model. In our experience, complex media formulations that included several growth factors to induce differentiation showed poor assay reproducibility (Kidney proximal tubule 3D Cell cultures, data not shown). DMSO a key factor in differentiation of HepaRG cells was also shown to induce 3-4 fold higher LDH and AST levels, reduction in proliferation and decreased hepatic functions [43]. Though this is a limitation for drug screening assays, previous studies and our observations have shown that HepaRG cell gene expression is more similar to PHH than HepG2 cells which may increase its predictive power in drug screening assays. But, it has to be also noted that HepG2 cells performed better in discriminating genotoxic compounds than HepaRG cells [21, 23].

Dis-advantages of our HepG2 spheroid model may include the use of animal origin ECM product, with undefined growth factors and batch-to-batch variability. The levels of CYP450 enzymes though higher are still significantly lower to those of PHH. There is an increased susceptibility to contamination during long-term maintenance of spheroids, which demands a careful attention in maintaining sterile conditions. Contamination during late stages of differentiation would cost significant amount of time in a scientific study. Future studies with improved synthetic biomaterials that could mediate cellular differentiation and serve as better 3D matrices have to be tested. Co-culturing HepG2 cells with other hepatic cells and studying their role in improving physiological characteristics would be interesting to analyze.

With several advantages and dis-advantages in each model a large validation screen on these models would help in identifying a better model in pre-clinical safety testing assays, which may help to decreasing drug attrition rates.

The pressure to develop predictive *in vitro* models not only comes from the pharmaceutical industry to decrease drug attrition but also from legislative pressure to ban animal testing. Recently, in March 2013, animal testing to evaluate human safety of cosmetic products and their ingredients was banned in the EU [44]. HepG2 spheroid model and other organotypic models could be used as an alternative to animal models after a thorough validation of their performance in various fields. Combination of –omic approaches (protein, miRNA, metabolomic) together with transcriptomic study would provide more insights into mode of action of a drug and discovering biomarkers. New assays that we have developed for testing ADME properties of new chemical entities and high-content screening methods to evaluate dynamic cellular stress responses are promising new tools for assessment of toxicity.

# REFERENCES

1    DiMasi, J. a., Hansen, R. W. & Grabowski, H. G. The price of innovation: new estimates of drug development costs. Journal of health economics 22, 151-185, doi:10.1016/s0167-6296(02)00126-1 (2003).

2    Morgan, S., Grootendorst, P., Lexchin, J., Cunningham, C. & Greyson, D. The cost of drug development: a systematic review. Health Policy 100, 4-17, doi:10.1016/j.healthpol.2010.12.002 (2011).

3    Paul, S. M. et al. How to improve R&D productivity: the pharmaceutical industry's grand challenge. Nat Rev Drug Discov 9, 203-214, doi:10.1038/nrd3078 (2010).

4    Roberts, R. A. et al. Reducing attrition in drug development: smart loading preclinical safety assessment. Drug Discov Today, doi:10.1016/j.drudis.2013.11.014 (2013).

5    Zuber, R., Anzenbacherova, E. & Anzenbacher, P. Cytochromes P450 and experimental models of drug metabolism. Journal of cellular and molecular medicine 6, 189-198 (2002).

6    Martignoni, M., Groothuis, G. M. & de Kanter, R. Species differences between mouse, rat, dog, monkey and human CYP-mediated drug metabolism, inhibition and induction. Expert opinion on drug metabolism & toxicology 2, 875-894, doi:10.1517/17425255.2.6.875 (2006).

7    Ben-Ze'ev, A. Animal cell shape changes and gene expression. BioEssays : news and reviews in molecular, cellular and developmental biology 13, 207-212, doi:10.1002/bies.950130502 (1991).

8    Malinen, M. M., Palokangas, H., Ylipertula, M. & Urtti, A. Peptide Nanofiber Hydrogel Induces Formation of Bile Canaliculi Structures in Three-Dimensional Hepatic Cell Culture. Tissue Eng Part A, doi:10.1089/ten.TEA.2012.0046 (2012).

9    Fozia, N. Organotypic Cultures of Hepg2 Cells for In Vitro Toxicity Studies. Journal of Bioengineering and Biomedical Sciences (2011).

10    Takebe, T. et al. Vascularized and functional human liver from an iPSC-derived organ bud transplant. Nature 499, 481-484, doi:10.1038/nature12271 (2013).

11    Guengerich, F. P. Cytochrome P450s and other enzymes in drug metabolism and toxicity. The AAPS journal 8, E101-111, doi:10.1208/aapsj080112 (2006).

12    Westerink, W. M. a. & Schoonen, W. G. E. J. Cytochrome P450 enzyme levels in HepG2 cells and cryopreserved primary human hepatocytes and their induction in HepG2 cells. Toxicology in vitro : an international journal published in association with BIBRA 21, 1581-1591, doi:10.1016/j.tiv.2007.05.014 (2007).

13    Hart, S. N. et al. A comparison of whole genome gene expression profiles of HepaRG cells and HepG2 cells to primary human hepatocytes and human liver tissues. Drug metabolism and disposition: the biological fate of chemicals 38, 988-994, doi:10.1124/dmd.109.031831 (2010).

14    Wilkening, S., Stahl, F. & Bader, A. Comparison of primary human hepatocytes and hepatoma cell line Hepg2 with regard to their biotransformation properties. Drug metabolism and disposition: the biological fate of chemicals 31, 1035-1042, doi:10.1124/dmd.31.8.1035 (2003).

15    Gunness, P. et al. 3D organotypic cultures of human HepaRG cells: a tool for in vitro toxicity studies. Toxicol Sci 133, 67-78, doi:10.1093/toxsci/kft021 (2013).

16    Chen, M. et al. FDA-approved drug labeling for the study of drug-induced liver injury. Drug Discov Today 16, 697-703, doi:10.1016/j.drudis.2011.05.007 (2011).

17    Xu, J. J. et al. Cellular imaging predictions of clinical drug-induced liver injury. Toxicol Sci 105, 97-105, doi:10.1093/toxsci/kfn109 (2008).

18    O'Brien, P. J. et al. High concordance of drug-induced human hepatotoxicity with in vitro cytotoxicity measured in a novel cell-based model using high content screening. Archives of toxicology 80, 580-604, doi:10.1007/s00204-006-0091-3 (2006).

19    Khetani, S. R. et al. Use of micropatterned cocultures to detect compounds that cause drug-induced liver injury in humans. Toxicol Sci 132, 107-117, doi:10.1093/toxsci/kfs326 (2013).

20    LeCluyse, E. et al. Expression and regulation of cytochrome P450 enzymes in primary cultures of human hepatocytes. Journal of biochemical and molecular toxicology 14, 177-188 (2000).

21    Jetten, M. J., Kleinjans, J. C., Claessen, S. M., Chesne, C. & van Delft, J. H. Baseline and genotoxic compound induced gene expression profiles in HepG2 and HepaRG compared to primary human hepatocytes. Toxicol In Vitro 27, 2031-2040, doi:10.1016/j.tiv.2013.07.010 (2013).

22    Gerets, H. H. J. et al. Characterization of primary human hepatocytes, HepG2 cells, and HepaRG cells at the mRNA level and CYP activity in response to inducers and their predictivity

for the detection of human hepatotoxins. Cell biology and toxicology, doi:10.1007/s10565-011-9208-4 (2012).

23  Jennen, D. G. et al. Comparison of HepG2 and HepaRG by whole-genome gene expression analysis for the purpose of chemical hazard identification. Toxicol Sci 115, 66-79, doi:10.1093/toxsci/kfq026 (2010).

24  Lehmann, J. M. et al. The human orphan nuclear receptor PXR is activated by compounds that regulate CYP3A4 gene expression and cause drug interactions. The Journal of clinical investigation 102, 1016-1023, doi:10.1172/JCI3703 (1998).

25  Kliewer, S. A., Goodwin, B. & Willson, T. M. The nuclear pregnane X receptor: a key regulator of xenobiotic metabolism. Endocrine reviews 23, 687-702, doi:10.1210/er.2001-0038 (2002).

26  Banks, A. T., Zimmerman, H. J., Ishak, K. G. & Harter, J. G. Diclofenac-associated hepatotoxicity: analysis of 180 cases reported to the Food and Drug Administration as adverse reactions. Hepatology 22, 820-827 (1995).

27  Benedetti, G. et al. TNF-alpha-mediated NF-kappaB survival signaling impairment by cisplatin enhances JNK activation allowing synergistic apoptosis of renal proximal tubular cells. Biochemical pharmacology 85, 274-286, doi:10.1016/j.bcp.2012.10.012 (2013).

28  Ramesh, G. & Reeves, W. B. TNF-alpha mediates chemokine and cytokine expression and renal injury in cisplatin nephrotoxicity. The Journal of clinical investigation 110, 835-842, doi:10.1172/JCI15606 (2002).

29  Naughton, C. A. Drug-induced nephrotoxicity. American family physician 78, 743-750 (2008).

30  Bickle, M. The beautiful cell: high-content screening in drug discovery. Analytical and bioanalytical chemistry 398, 219-226, doi:10.1007/s00216-010-3788-3 (2010).

31  Kleinman, H. K. & Martin, G. R. Matrigel: basement membrane matrix with biological activity. Seminars in cancer biology 15, 378-386, doi:10.1016/j.semcancer.2005.05.004 (2005).

32  Lora, J. M., Rowader, K. E., Soares, L., Giancotti, F. & Zaret, K. S. Alpha3beta1-integrin as a critical mediator of the hepatic differentiation response to the extracellular matrix. Hepatology 28, 1095-1104, doi:10.1002/hep.510280426 (1998).

33  Streuli, C. H. et al. Laminin mediates tissue-specific gene expression in mammary epithelia. J Cell Biol 129, 591-603 (1995).

34  Fassler, R. et al. Lack of beta 1 integrin gene in embryonic stem cells affects morphology, adhesion, and migration but not integration into the inner cell mass of blastocysts. J Cell Biol 128, 979-988 (1995).

35  Asthana, A. & Kisaalita, W. S. Microtissue size and hypoxia in HTS with 3D cultures. Drug Discov Today 17, 810-817, doi:10.1016/j.drudis.2012.03.004 (2012).

36  Debnath, J. & Brugge, J. S. Modelling glandular epithelial cancers in three-dimensional cultures. Nature reviews. Cancer 5, 675-688, doi:10.1038/nrc1695 (2005).

37  Jungermann, K. & Katz, N. Functional hepatocellular heterogeneity. Hepatology 2, 385-395 (1982).

38  Lindros, K. O. Zonation of cytochrome P450 expression, drug metabolism and toxicity in liver. General pharmacology 28, 191-196 (1997).

39  Gebhardt, R. Metabolic zonation of the liver: regulation and implications for liver function. Pharmacology & therapeutics 53, 275-354 (1992).

40  Yan, H. M., Ramachandran, A., Bajt, M. L., Lemasters, J. J. & Jaeschke, H. The oxygen tension modulates acetaminophen-induced mitochondrial oxidant stress and cell injury in cultured hepatocytes. Toxicol Sci 117, 515-523, doi:10.1093/toxsci/kfq208 (2010).

41  Kietzmann, T. & Jungermann, K. Modulation by oxygen of zonal gene expression in liver studied in primary rat hepatocyte cultures. Cell Biol Toxicol 13, 243-255 (1997).

42  Takayama, K. et al. 3D spheroid culture of hESC/hiPSC-derived hepatocyte-like cells for drug toxicity testing. Biomaterials 34, 1781-1789, doi:10.1016/j.biomaterials.2012.11.029 (2013).

43  Hoekstra, R. et al. The HepaRG cell line is suitable for bioartificial liver application. Int J Biochem Cell Biol 43, 1483-1489, doi:10.1016/j.biocel.2011.06.011 (2011).

44  EU: final ban on animal experiments for cosmetic ingredients implemented. Altex 30, 268-269 (2013).

# APPENDIX

**NEDERALANDSE SAMENVATTING**
**ENGLISH SUMMARY**
**LIST OF ABBREVIATIONS**
**CURRICULUM VITAE**
**LIST OF PUBLICATIONS**

# NEDERLANDSE SAMENVATTING

Medicijn-geïnduceerde orgaantoxiciteit is een groot probleem bij de ontwikkeling van medicijnen en voor de veiligheid van patiënten die een behandeling ondergaan. Een medicijn bestempelen als veilig is een ingewikkelde uitdaging en de tijd heeft bewezen dat huidige methodes niet altijd betrouwbaar zijn. Hierdoor heeft de wetenschappelijke gemeenschap een impuls gekregen om het ontwikkelingsproces van medicijnen te verbeteren. Het bepalen van toxiciteit wordt vandaag de dag gedaan door onderzoek op knaag- of andere zoogdieren. Dit soort onderzoek is op dit moment de enige manier om toxiciteit op lange termijn te bepalen – ondanks dat de voorspellende waarde van dierstudies soms wordt betwijfeld.

Toxiciteit is vaak idiosyncratisch, wat betekent dat slechts enkele personen van de groep die het medicijn neemt toxische reacties vertonen. Deze personen reageren anders op de medicijnen vanwege hun specifieke genetische achtergrond of een achterliggende ziekte. Hierdoor is het nog moeilijker om het type toxiciteit van een geneesmiddel te voorspellen voordat het middel op de markt komt. Het is daarom belangrijk om het precieze mechanisme van toxiciteit te onderzoeken en mensen op de hoogte te stellen van de mogelijke bijwerkingen van een geneesmiddel. Dankzij de technologische ontwikkelingen van de afgelopen jaren kunnen we op dit moment zelfs kleine veranderingen in de expressie van duizenden genen tegelijk associëren met medicijngebruik. Desondanks is kennis over het mechanisme van toxiciteit van veel geneesmiddelen slechts minimaal aanwezig of zelfs afwezig. Een van de redenen is het gebrek aan juiste modellen om toxiciteit in mensen te voorspellen. Cellen, geïsoleerd uit humaan weefsel, vormen een beter modelsysteem dan de huidige modellen, maar deze cellen kunnen niet een lange tijd buiten het lichaam overleven. Daarentegen kunnen geimmortaliseerde humane cellijnen zoals HepG2 levercellen onbeperkt groeien en zijn ze dus een geschikte bron van cellen voor in vitro onderzoek. Het nadeel van deze cellen is dat zij hun weefselspecifieke functies niet kunnen vasthouden in standaard celkweek, waardoor de voorspellende waarde voor toxiciteit-onderzoek sterk afneemt. Het behouden van weefselspecifieke functies gedurende celkweek is essentieel voor de betrouwbaarheid van in vitro modellen. Sinds de ontwikkeling van de weefselkweekflessen rond 1920 zijn er geen grote veranderingen meer geweest in de standaard kweekmethoden. Op dit moment zijn driedimensionale kweekmethoden in ontwikkeling, maar zij hebben nog geen plaats in de standaard kweekmethoden gebruikt voor in vitro toxiciteits-testen. Dit proefschrift beschrijft de ontwikkeling van een drie dimensioneel (3D) model waarin meercellige weefsels gekweekt worden in een hydrogel, waarbij de weefselspecifieke functies behouden blijven. Aangezien de lever een grote rol speelt in detoxificatie van medicatie en vaak de meeste schade oploopt gedurende medici-

jn-geïnduceerde toxiciteit, hebben we ons het meest gericht op de ontwikkeling van een robuust in vitro model voor levertoxiciteit. Verder beschrijft dit proefschrift ook ons onderzoek naar hoe het immuunsysteem niertoxiciteit kan verergeren en introduceren we een geavanceerde screeningsmethode die gebruikt kan worden om celtoxiciteit te meten.

Lichaamscellen leven in een drie-dimensionele ruimte omgeven door extracellulaire matrix. Deze matrix speelt ook een rol in signaleringsprocessen en regeling van weefselspecifieke functies. De hydrogel Matrigel en de extracellulaire matrix hebben vergelijkbare eigenschappen en deze gel is dus geschikt om levercellen op te laten groeien. Zoals beschreven in **hoofdstuk 2**, stoppen HepG2 levercellen gekweekt op een 3D hydrogel met delen, differentiëren ze en behouden de weefselspecifieke functies van primaire levercellen beter dan dezelfde HepG2 cellen gekweekt op standaard plastic 2D kweekschaaltjes. Zo vertonen in 3D gekweekte HepG2 cellen bijvoorbeeld een hogere expressie en functie van genen betrokken bij het metabolisme van geneesmiddelen. Door dit herstelde metabolisme kan het oorspronkelijke medicijn worden gemetaboliseerd tot een toxische tussenvorm, en herkend worden als een mogelijke toxische stof. De verhoogde gevoeligheid van dit model maakt ook het onderzoek naar het onderliggende mechanisme van toxiciteit mogelijk. In **hoofdstuk 3** wordt een microarray analyse beschreven waarin de genexpressie van in 3D gekweekte HepG2 sferoïden een significante verandering laat zien van moleculaire signaleringsroutes die betrokken zijn bij het metabolisme van geneesmiddelen. Verscheidene andere signaleringsroutes geassocieerd met het behoud van lever-specifieke functies waren ook sterker aanwezig in 3D HepG2 sferoïden dan in de 2D HepG2 celkweken. Analyse van het hele genoom van levercellen, gekweekt in verschillende in vitro modellen, laat grote verschillen en overeenkomsten zien vergeleken met primaire levercellen. Expressie van genen betrokken bij de celcyclus was sterk onderdrukt in 3D gekweekte HepG2 cellen en daardoor vergelijkbaar met cellen uit de menselijke lever. Dit bevestigt onze observaties in **hoofdstuk 2**. Continue proliferatie in 2D celkweken beperkt blootstelling aan stoffen voor langere periodes, omdat de cellen dan alle beschikbare groeiruimte bezetten en uiteindelijk doodgaan door gebrek aan ruimte. Als de cellen georganiseerd worden in een gepolariseerde 3D sferoïde stopt de proliferatie. Het fenotype wordt behouden voor vele dagen, waardoor het model geschikt is om de effecten van geneesmiddelen gedurende langere periodes te onderzoeken. Herhaalde stimulaties maakten cellen gevoeliger voor toxische effecten en verbeterde identificering van toxische stoffen in ons onderzoek (**hoofdstuk 2**). In 3D gekweekte HepG2 sferoïden zijn gemakkelijk in gebruik en ontwikkelen een gedifferentieerd fenotype vergelijkbaar met primaire levercellen. Dit maakt deze kweekmethode een veelbelovend model voor het routinematig screenen van nieuwe geneesmiddelen.

In **hoofdstuk 4** hebben we een systematische vergelijking gemaakt van veranderingen in genexpressie in verscheidene in vitro en in vivo modellen na bloot-stelling aan diclofenac, een bekend hepatotoxisch middel. Dit heeft geleid tot een beter begrip van de onderliggende stresssignaleringsroutes in humane- en diermod-ellen. In 3D gekweekte HepG2 sferoïden reageerden sterker op diclofenac en de diclofenac-geïnduceerde stressresponsen waren vergelijkbaar met die in humane levercoupes. Moleculaire mechanismen geassocieerd met diclofenac-geïnduceerde leverschade zoals de Nrf2 signaalcascade en mitochondriële dysfunctie, waren ver-hoogd. Dit impliceert dat in 3D gekweekte HepG2 sferoïden een goed model vormen voor toekomstig toxicogenomisch onderzoek.

In **hoofdstuk 5** hebben we de rol van TNFα, een pro-inflammatoir cytokine in medicijn-geïnduceerde niertoxiciteit onderzocht. Pro-inflammatoire signaalstoffen spelen een belangrijke rol in het verergeren van de toxiciteit van sommige medici-jnen. Voor deze studie gebruikten we een zogeheten 'high-content assay' , waarin over tijd apoptose en necrose als gevolg van een gecombineerde stimulatie van TNFα en niertoxische stoffen werd bepaald. Voor cisplatine, cyclosporine A, tacro-limus en aiodothymidine werd een synergistisch effect waargenomen in combinatie met TNFα. Voor de andere niertoxische stoffen konden we geen synergistisch effect waarnemen in dit experiment, alhoewel dit misschien wel het geval is in een ver-beterd model zoals in een 3D cell culturen en/of het gebruik van andere reporters gedurende het experiment. Ondanks deze tekortkomingen kan deze 'high-content assay' een nieuwe screening-techniek op industriële schaal vormen, speciaal voor het screenen van chemische stoffen.

Kort samengevat hebben onze studies aangetoond dat met 3D celkweek een fysiologisch relevante niche ontstaat waarin cellen worden gestimuleerd om geïntegreerde weefsels met weefselspecifieke eigenschappen te vormen. Grote voordelen van deze 3D kweken zijn de aanwezigheid van een actief metabolisme van medicijnen en de stabiliteit van de celeigenschappen over een langere tijd. Dit maakt dit type celkweek uitermate geschikt voor het testen van geneesmiddelen op grote schaal. Het incorporeren van fluorescente reporter eiwitten uit stress signaler-ingsroutes zou dit model bijvoorbeeld kunnen uitbreiden en verbeteren en zal leiden tot nieuwe mogelijkheden in de reguliere testen voor toxiciteit in de toekomst.

# ENGLISH SUMMARY

Drug induced organ toxicity has remained a major challenge in drug development and for the safety of patients undergoing treatment. Classifying a drug as safe is a complex challenge and history has shown that the current methods are not always reliable, driving innovation in the scientific community to improve the drug discovery pipeline. Toxicity assessment using rodent and other mammalian species as surrogate models is a common practice as they are the only available alternative for studying long-term effects of the drug – although the reliability of other species in predicting human toxicity is under question.

Toxicity is often idiosyncratic affecting only few individuals due to their genetic background or underlying disease conditions which makes it even more complicated to predict a type of toxicity before a drug is released into the market. Therefore it is important to study the detailed mechanism of toxicity associated with a drug and alert people to potential side effects. Though the technology has advanced in recent years allowing us to study changes in thousands of genes upon drug exposure using microarray or sequencing technologies, current knowledge on the mechanisms associated with drug-induced toxicity is either minimal or absent for the majority of drugs. This is partly due to the absence of test models that would respond in a similar way to humans when exposed to a drug. Freshly isolated cells from human tissues can serve as better test models but they cannot survive for long periods outside the body in a non-physiological environment. With their unlimited growth, immortalized human cells obtained either by genetic manipulation or from a cancer tissue represent a convenient source of cells for *in vitro* studies, but they are unable to maintain tissue specific functions in a culture dish limiting their value in understanding human toxicity. Improvements in current culture methods to preserve organ specific functions are essential for reliable *in vitro* models. Since the development of the tissue culture flask in the early 1920's there haven't been major advances in standard in vitro tissue culture practices. Methods to culture three-dimensional tissues are developing rapidly, but have not yet entered mainstream use for in vitro testing. This thesis describes the development of a hydrogel based three-dimensional (3D) model for culturing multicellular tissues that retain their specialized functions. Since liver plays a major role in drug detoxification and is a prime target for drug induced liver injury, we mainly focused on developing a robust *in vitro* model for assessing liver toxicity as a first step. This thesis also describes our investigation to understand the role of immune mediators in aggravating kidney injury and introduces an advanced high-content screening approach that we used to measure cytotoxicity.

Cells in our body reside in a three-dimensional space surrounded by extracellular matrix, which mediates cellular signaling and regulation of tissue specific

functions. We used Matrigel, a hydrogel that has similar properties to extracellular matrix and supports the growth of hepatocytes. As shown in **chapter 2**, HepG2 cells cultured on a 3D hydrogel stop proliferating, differentiate and maintain specialized functions of hepatocytes to a higher degree than cells cultured as monolayer cultures on a two-dimensional (2D) plastic dish. Gene expression and function of several important drug metabolising enzymes are significantly increased when HepG2 cells are placed in 3D culture. This increased functionality can enable drugs to be metabolized into their toxic intermediates and manifest their toxic effects. The resulting increase in sensitivity to toxic compounds also facilitates investigation of the underlying mechanisms involved in onset of toxicity. In **chapter 3**, microarray gene expression analysis demonstrated significant upregulation of molecular pathways associated with drug metabolism in 3D HepG2 spheroid cultures. Several other molecular pathways that are associated with physiological maintenance of liver-specific functions were also enriched in 3D HepG2 spheroids compared to 2D monolayer cultures. Whole genome gene expression comparison of in vitro cellular models to human liver gene expression showed the similarities and differences associated with cellular models. Cell cycle pathway was strongly suppressed in 3D HepG2 cultures and the gene expression was similar to human liver supporting our observations in **chapter 2**. Continuous cell proliferation in 2D cultures is a major limitation for long-term drug exposures, as cells occupy the available space and die due to overcrowding. Once the cells organize into a polarized spheroid in 3D cultures they stop proliferating and maintain this stable phenotype for several days presenting opportunities to study long-term effects of drugs *in vitro*. Repeated exposures were indeed more sensitive in identifying toxic compounds in our study (**Chapter 2**). With its ease of use, availability and a differentiated phenotype showing many hallmarks of liver tissue 3D HepG2 spheroid cultures are promising for routine drug screening assays. In **chapter 4**, we made a systematic comparison of gene expression changes in various in vitro and in vivo models upon exposure to the hepatotoxicant, diclofenac. This allowed us to understand the cellular stress responses associated with the toxicant and their expression in human and animal model systems. We have seen that 3D HepG2 spheroids were more responsive to diclofenac induced stress responses resembling human precision cut liver slices. Molecular mechanisms that are known to be associated with diclofenac injury such as Nrf2 signaling pathway and mitochondrial dysfunction were enriched indicating that this model may be useful for future toxicogenomic studies.

In **chapter 5**, we investigated the role of the pro-inflammatory cytokine, TNFα, in drug-induced nephrotoxicity. Inflammatory mediators are known to play a major role in aggravating toxicity induced by some drugs. In this study we set up a high-content screening approach to measure apoptosis and necrosis in real time

upon exposure to nephrotoxicants in the presence of TNFα. The assay was sensitive in identifying a synergistic effect of TNFα in enhancing nephrotoxicity caused by cisplatin, cyclosporineA, tacrolimus and aziodothymidine. We were unable to detect toxicity induced by other nephrotoxicants, which may be improved by using three-dimensional cell cultures and/or including other reporters for live cell imaging. Nonetheless, our automated real time imaging represents a novel high-content screening approach to screen for chemical entities on an industrial scale.

In summary, our studies have shown that 3D cultures provide a physiological niche to cells allowing them to form integrated tissues with associated tissue specific functions. The presence of active drug metabolism pathways and their ability to maintain a stable phenotype for long periods in microplates offers a great advantage for large scale screening for compound toxicity. Further development of this model, for example by incorporating fluorescent reporters of specific cell stress pathways offers additional scope for improving toxicity testing in the future.

# LIST OF ABBREVIATIONS

| | |
|---|---|
| 2D | Two-dimensional |
| 3D | Three-dimensional |
| ADME | Absorption, distribution, metabolism and excretion |
| AhR | Aryl hydrocarbon receptor |
| ARE | Antioxidant responsive elements |
| ATP | Adenosine triphosphate |
| CAR | Constitutive androstane receptor |
| CLF | Cholyl-lysyl-fluorescein |
| CYP450 | Cytochrome P-450 |
| DEG | Differentially expressed genes |
| DILI | Drug induced liver injury |
| DMEM | Dulbecco's modified eagle's medium |
| DMSO | Dimethyl sulfoxide |
| ECM | Extracellular matrix |
| FMO5 | Flavin Containing Monooxygenase 5 |
| FXR | Farnesoid X receptor |
| G6PC | Glucose-6-Phosphatase |
| GADD45A | Growth arrest and DNA-damage-inducible protein 45 alpha |
| GAPDH | Glyceraldehyde-3-phosphate dehydrogenase |
| HNF4A | Hepatocyte Nuclear Factor 4 |
| HO-1 | Heme oxygenase 1 |
| HSP40 | Heat shock protein 40 |
| iPSC | induced pluripotent stem cells |
| LC-MS | Liquid chromatography – mass spectrometry |
| LPS | Lipopolysaccharide |
| LXR | Liver X receptor |
| MDM2 | Mouse double minute 2 homolog |
| NF-κB | Nuclear factor kappa B |
| Nrf2 | Nuclear factor (erythroid-derived 2)-like 2 |
| PAS | Periodic acid Schiff's reaction |
| PBS | Phosphate buffered saline |
| PCLS | Precision cut liver slices |
| PTEC | Proximal tubular epithelial cells |
| PXR | Pregnane X receptor |
| ROS | Reactive oxygen species |
| RXR | Retinoid X receptor |
| TNFα | Tumor necrosis factor α |

# CURRICULUM VITAE

Sreenivasa Chakravarthy Ramaiahgari was born on 19th November 1981 in Pulivendula, India. Fascinated by the discoveries in biotechnology, he chose to pursue a Bachelor's degree in Biotechnology at Bangalore University, Bangalore, India. During this time he also attended a practical training course in Genetic Engineering at Jain University, Bangalore, India. His first tissue culture experience comes from his Bachelor's internship at University of Agricultural Sciences, Bangalore where he gained practical hands on experience with plant tissue culture methods. His enthusiasm further drove him to pursue Master's degree in Biotechnology at University of Abertay Dundee, Scotland, UK. He did his masters internship at Roslin Institute, Edinburgh, UK - the lab famously known for first mammalian cloning. He worked in the Department of Genetics and Genomics investigating molecular mechanisms associated with PRRS viral infection in pigs under the supervision of Dr. Ait-Ali and Prof. Archibald. His work at Roslin Institute assisted a publication; inspired by the project he continued working with the same group for another 6 months after his Masters degree. Later, he joined BioReliance, Glasgow, UK; where he was actively involved in testing various biological products for viral clearance in compliance with the requirements of the UK and German GLP Regulations, the US FDA Good Laboratory Practice Regulations (21 CFR 58), the Japanese GLP standard and the OECD principles of Good Laboratory Practice. After nearly 3 years at BioReliance, he started his PhD research at Division of Toxicology, Leiden Academic Center for Drug Research (LACDR)/ Leiden University under the supervision of Dr. Leo Price and Prof. Bob van de Water. His PhD research involved developing advanced *in vitro* models for studying drug-induced toxicity. He received prestigious Bo Holmstedt Memorial Foundation (BHMF) award at Eurotox 2013 meeting in Switzerland for his research work describing a feasible method for the solution of a toxicological problem under maximum respect to the 3R-principle (Reduce, Refine, Replace animal testing). He is quite interested in improved *in vitro* methodologies and the promise it holds for the future of *in vitro* studies. He started a information website - 3DCELL-BIO.COM – which brings together current research on advanced *in vitro* methods; and creates open forums for scientific discussions- mainly focusing on Toxicology.

## LIST OF PUBLICATIONS

**A 3D in vitro model of differentiated HepG2 cell spheroids with improved liver-like properties for repeated dose high-throughput toxicity studies**
**Ramaiahgari SC**, den Braver MW, Herpers B, Terpstra V, Commandeur JN, van de Water B, Price LS.
Archives of Toxicology 2014; 88(5): 1083-95.

**A screen for apoptotic synergism between clinical relevant nephrotoxicant and the cytokine TNF-alpha**
Benedetti G*, **Ramaiahgari SC**\*, Herpers B, van de Water B, Price LS, de Graauw M.
Toxicology In Vitro 2013; 27(8): 2264-72.

**Epac-Rap Signaling Reduces Oxidative Stress in the Tubular Epithelium**
Stokman G, Qin Y, Booij TH, **Ramaiahgari SC**, Lacombe M, Dolman ME, van Dorenmalen KM, Teske GJ, Florquin S, Schwede F, van de Water B, Kok RJ, Price LS.
Journal of American Society of Nephrology (In Press).

**cAMP signalling protects proximal tubular epithelial cells from cisplatin-induced apoptosis via activation of Epac**
Qin Y, Stokman G, Yan K, **Ramaiahgari SC**, Verbeek F, de Graauw M, van de Water B, Price LS.
British journal of pharmacology 2012; 165-4b: 1137-50.

**Elevated insulin-like growth factor 1 receptor signaling induces antiestrogen resistance through the MAPK/ERK and PI3K/Akt signaling routes**
Zhang Y, Moerkens M, **Ramaiahgari SC**, de Bont H, Price L, Meerman J, van de Water B.
Breast cancer research 2011; 13(3): R52.

**Functional analysis of the porcine USP18 and its role during porcine arterivirus replication**
Ait-Ali T, Wilson AW, Finlayson H, Carre W, **Ramaiahgari SC**, Westcott DG, Waterfall M, Frossard JP, Baek KH, Drew TW, Bishop SC, Archibald AL.
Gene 2009; 439(1-2): 35-42.

**3D cell models** (Hepatotoxicity screening on in vitro models and role of 'Omics) Book chapter in Toxicogenomics – based cellular models – Alternatives to animal testing for safety assessment (Edited by Jos Kleinjans) (2014)
**Ramaiahgari SC** and Price LS.

**3D cell culture improves liver-specific characteristics of HepG2 cells: a gene expression analysis-based comparison of different in vitro hepatocyte models**
**Ramaiahgari SC**, Coonen M, Meerman JHN, Jennen D, van de Water B, van Delft JH and Price  LS.
Manuscript in preparation

**Systemic comparison of diclofenac induced gene expression changes in diverse in vitro and in vivo models and species**
**Ramaiahgari SC**, Wink S, Hadi M, John Meerman, Luijten M, Groothuis GM, van de Water B and Price LS.
Manuscript in preparation

* These authors contributed equally to the study.